Università degli Studi di Napoli Federico II

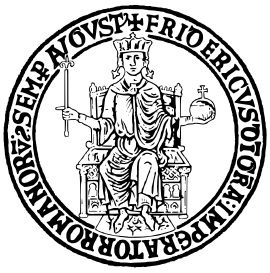

Scuola Politecnica e delle Scienze di Base

Dipartimento di Ingegneria Chimica dei Materiali e della Produzione Industriale

a dissertation submitted in partial fulfillment of

the requirements for the degree of

doctor of philosophy

Rheological Determination of Polyolefin Architecture

Tutor
Prof. Nino Grizzuti
Prof. Theo A Tervoort

Cotutor
Prof. Rossana Pasquino
Prof. Salvatore Costanzo
Prof. Giovanni Ianniruberto

Candidate
Vincenzo Ianniello

2019 - 2023

Candidate's declaration

I hereby declare that this thesis submitted to obtain the academic degree of Philosophiæ Doctor (Ph.D.) in Industrial Products and Processes Engineering is my own unaided work, that I have not used other than the sources indicated, and that all direct and indirect sources are acknowledged as references.
Parts of this dissertation have been published in international journals and/or conference articles (see list of the author's publications at the end of the thesis).

This work is part of the research project #834, which was financed by DPI, P.O. Box 902, 5600 AX Eindhoven, the Netherlands.

Napoli, March 22, 2023

_____

Vincenzo Ianniello

Abstract

The present work concerns the use of rheology to obtain quantitative information on the microstructure of polyolefin-based materials. Such properties have crucial implications along both directions of the chain-of-knowledge of polymeric materials. Moving backwards, in the direction of polymer synthesis, rheology is able to link the material response to the details of the molecular architecture. Moving forwards, in the direction of technological applications, rheology is able to provide a relevant link to the processing as well as to the final material properties. Determining the molecular structure of polyolefin-based materials is a relevant scientific and technological challenge. Molecular weight, its distribution, and structural details are fundamental parameters for materials design and processing, but often difficult to ascertain. The main objective of the present work is to study the molecular details of specific polyolefin-based systems through an innovative rheological approach. Linear rheology is measured in concentrated, entangled solutions, instead of melts, thus overcoming some intrinsic experimental difficulties encountered in measuring the latter. Molecular models and constitutive equations for entangled solutions are used to extract the quantitatively relevant microstructural information.

Keywords: Rheology, Polymer Solution, Molecular Weight Distribution

Sommario

Il presente lavoro si basa sull'uso della reologia per ottenere informazioni quantitative sulla microstruttura dei materiali poliolefinici. Queste ultime hanno implicazioni cruciali sulla conoscenza dei materiali polimerici. In particolare, dal punto di vista della sintesi dei polimeri, la reologia è in grado di collegare la risposta del materiale ai dettagli dell'architettura molecolare. Da un punto di vista delle applicazioni tecnologiche, la reologia è in grado di fornire un collegamento rilevante alla lavorazione e alle proprietà finali del materiale. La determinazione della struttura molecolare dei materiali poliolefinici è una sfida scientifica e tecnologica importante. Il peso molecolare, la sua distribuzione e i dettagli strutturali sono parametri fondamentali per la progettazione e la lavorazione dei materiali, ma spesso difficili da accertare. L'obiettivo principale del presente lavoro è studiare i dettagli molecolari dispecifici sistemi a base di poliolefine attraverso un approccio reologico innovativo. Vengono misurate le proprietà reologiche lineari di soluzioni concentrate ed entanglate, invece che nel stato di fuso puro, superando così alcune difficoltà sperimentali intrinseche incontrate nella misurazione di queste ultime. I modelli molecolari e le equazioni costitutive per le soluzioni entanglate sono utilizzati per estrarre le informazioni microstrutturali quantitativamente rilevanti.

Parole chiave: Reologia, Soluzioni Polimeriche, Distribuzione dei Pesi Molecolari

Contents

Chapter 1

Introduction

1.1 Preamble

Plastics materials have revolutionized our world, contributing to the tremendous technological progress of the last century. Their ease of processing through molding, extrusion, and casting, allows for different morphologies that influence the final properties of the product (mechanical, strength, durability) and provide great versatility in many application fields. These characteristics have led to an exponential increase in the worldwide plastics production and have contributed to a gradual substitution or, in some cases, integration with conventional materials such as metals, minerals, textile fibers, etc.

The synthesis of polymeric materials started with nitrocellulose in 1862 [1] and, since then, it underwent a rapid progress. In the early 1950s, Hogan and Bank found that ethylene can be polymerized under moderate conditions (3–4 MPa and 70–100 °C) with chromium oxide catalysts on silica support. This process was employed to produce *High Density Polyethylene (HDPE)* in 1956. In 1953, Ziegler and Natta independently developed a family of stereospecific transition-metal catalysts that led to the synthesis and commercialization, in 1957, of polypropylene (PP) [1]. Nowadays, PE and PP are the most produced plastic materials, with an expected yearly production of 230 millions of metric tons in 2023 [2].

In spite of the huge production volume and variety of applications, several aspects related to the link between synthesis, processing and mechanical properties of polyolefins are still matter of research. For example, it is difficult to relate the molecular weight and molecular weight distribution (MWD) of such materials to the final properties, especially when the average molar mass is very high. In the latter case, a major challenge comes from obtaining reliable measurements of the MWD with standard analytical methods.
The present work aims at establishing robust experimental protocols for obtaining the MWD of Polyolefins (POs) with ultrahigh molecular weight via rheological techniques and more generally, to establish a protocol to relate rheology and polymer architectures.

1.2 Polyolefins

Polyolefins (POs) are a class of polymers synthesized from olefins or alkenes. These are monomeric precursors characterized by at least one carbon-carbon double bond. The most common precursors are ethylene, propylene, 1-butene, and other α-olefins, whereas the most common POs are high density polyethylene *(HDPE)*, low density polyethylene *(LDPE)*, linear low density polyethylene *LLDPE*, ultra high molecular weight *(UHMW)* polyethylene or polypropylene (PP), as well as blends of these polymers. Polyethylene (PE) and isotactic polypropylene (i-PP) are utilized in a huge variety of applications such as packaging, cable insulations, pipes and valves, toys, housewares, etc. Due to their low toxicity compared to many other common plastics, PE and i-PP are also the least expensive polymers.
Polyethylene is largely used to replace traditional materials such as paper or metals. It is characterized by a simple chemical formula $(-CH_2-CH_2-)_n$. Depending on the synthetic route, it is possible to obtain PEs with different physical properties depending on the chain length, the degree of branching and the length of the branches. In this respect, PE can be classified in three categories: LDPE, LLDPE and HDPE.
LDPE has a highly branched molecular structure (see Figure 1.1) and the most common use for films in packaging, agricultural coverings, and carrying bags.

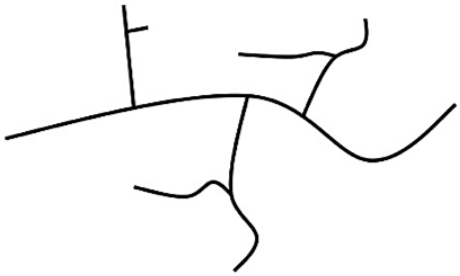

Figure 1.1. Schematic structure of LDPE

HDPE is characterized by a high crystallinity degree which makes it the most rigid material among the polyethylene categories. It has a linear molecular structure (see Figure 1.2) and can be syntesized with a broad or narrow molecular weight distribution (MWD). Depending on the MWD, HDPE can be used in different application fields: food packaging, bottles pipes

Figure 1.2. Schematic structure of HDPE

LLDPE is similar to HDPE but with a lower cristallinity due to the presence of short branches (see Figure 1.3). LLDPE is frequently mixed with one of the elements above mentioned to produce thin films. Due to its toughness and durability, it is used to produce larger items like lids.

Figure 1.3. Schematic structure of LLDPE

The formula of PP, instead, is characterized by a main $-CC-$ chain with a lateral methyl group (CH_3). The spatial arrangement of the methyl group around the main chain determines three types of PP: atactic PP (aPP) with a random distribution of CH_3, isotactic PP (iPP) with CH_3

groups distributed on one side of the main chain and syndiotactic PP (sPP) in which the lateral groups are distributed alternately around the main chain. In Figure 1.4, the different polypropylenes structure, according to its stereoregularity are reported. The higher the regularity of the methyl lateral group, the higher is the degree of crystallinity, melting temperature, tensile strength, rigidity and hardness [3].

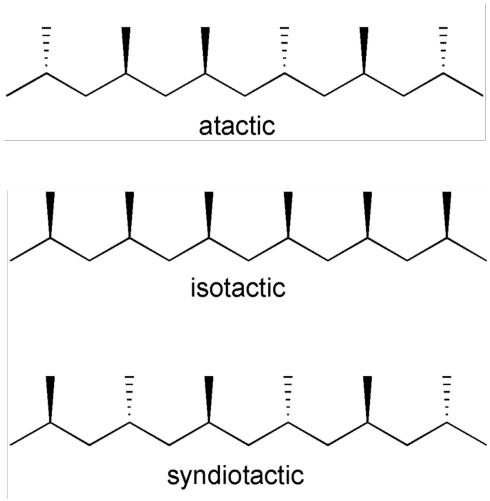

Figure 1.4. Stereoregularity of PP

With respect to PE, PP is a cheaper material, and for this reason it is currently of great industrial interest. However, PP has a higher crystallization temperature and it is less resistant to oxygen.
For both PE and PP, when the molar mass of the polymer exceeds 10^6 g/mol, UHMW materials are achieved.

1.3 Ultrahigh molecular weight materials

Molecular weight and macromolecular distribution are properties that strongly influence physical and mechanical properties such as drawability, and toughness. In recent years, the need for producing strong fibers promoted the synthesis of high molecular weight polymers.

Concerning polyolefins, the use of metallocene-based catalysists allowed to produce chains with $1 \times 10^5 - 2.5 \times 10^5$ monomers, a much larger number compared to approximately 2000 monomers of HDPE. Nowadays, UHMW POs are used in industry for the production of gears and sliding guides, medical industry for the manufacture of orthopedic joint replacements, defense applications such as ballistic protection. UHMWPE is the most common PO for medical applications. Due to its bio-compatibility, chemical inertia, resistance to abrasion and impact, and low surface friction coefficient, along with excellent fatigue resistance, it is used as joint insert, usually coupled with metal components. Regarding the application for wires or ballistic protection, experiments show that a rope made of UHMWPE performs 15 times better than a steel cable with 8 times less weight [4].
From a processing perspective, the molecular weight of such class of polymers, in particular for polyethylene, is inevitably associated with a large number of entanglements per chain, resulting in sustained elastic modulus and melt viscosity. The latter may represent a limit for the processability of the materials. Furthermore, the high viscoelasticity is a major issue for the rheological characterization of UHMW POs. On the other hand, it is of primary importance to develop characterization methods to assess the molecular weight and molecular weight distribution of these materials in order to control the properties of the resulting products.

1.4 Polymer dispersity and its effect on the rheological and mechanical properties of polymers

Polymeric materials consisting of equal chains are almost impossible to achieve in industrial processes, thus some dispersion degree is expected. For this reason, the molecular weight is generally defined in average terms. Different average quantities are useful to define the degree of dispersity. The *number average molecular weight* is defined as follows:

$$\bar{M}_n = \frac{\sum_i n_i * M_i}{\sum_i n_i} = \sum_i N_i * M_i \tag{1.1}$$

where n_i and N_i are the number and molar fraction of molecules with a molecular weight of M_i, respectively. Another possibility is to define a *weight average molecular weight*, M_w. The weight-average molecular weight is strongly influenced by the presence of large molecular weight fractions. The definition is the following:

$$\bar{M}_w = \frac{\sum_i w_i * M_i}{\sum_i w_i} = \sum_i W_i * M_i = \frac{\sum_i n_i * M_i^2}{\sum_i n_i * M_i} \tag{1.2}$$

where w_i and W_i are the weight and the weight fraction of molecules with a molecular weight M_i, respectively. M_w is always larger than M_n. An additional parameter used to characterize the molecular weight of a polymer is the viscosimetric molecular weight. This value, as will be shown later, is obtained from rheological measurements.
Figure 1.5 shows where the different molecular weights can be found in a typical molecular weight distribution.

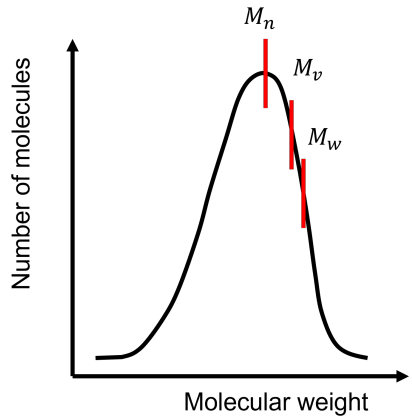

Figure 1.5. Schematic illustration of a molecular distribution and where the main parameters are located on the curve (the x-axis is reported in log-scale)

In Figure 1.5, the viscosity average molecular weight (M_v) is reported. It can be obtained from the viscosity of solutions in diluted regime. For a given polymeric system, the ratio between M_w and M_n, the so-called *polydispersity index* (PDI), is indicative of the breadth of the macromolecular distribution. For monodisperse polymers PDI is equal to 1.

Rheology is strongly affected by molecular weight and polydispersity index. For example, a larger PDI induces a lower shear rate where the shear thinning behavior occurs. Furthermore, a more polydysperse sample features a broader transition from the Newtonian plateau to the thinning regime, as shown in Figure 1.6.

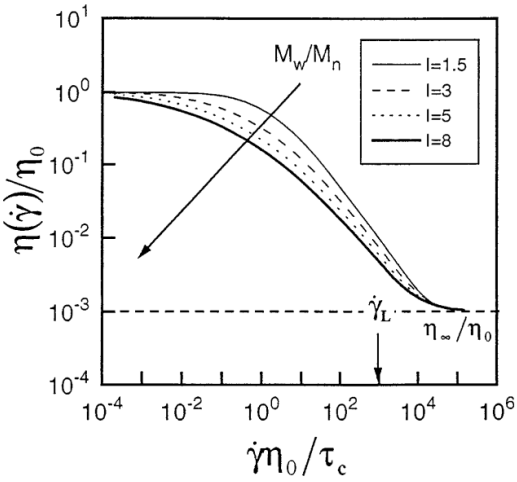

Figure 1.6. Effect of polydispersity on the shear viscosity (picture from [5])

Concerning the dynamic shear rheological response, a higher polydispersity index results in the impossibility to reach a well-defined plateau modulus (see Figure 1.7).

1.5 Experimental techniques for determining the average molecular weight of polymers

In this section, the most used techniques for the evaluation of the weight-average molecular weight and macromolecules distribution are presented. Most techniques require dissolution of the polymer in a solvent at low concentrations. In addition, in most cases, the knowledge of some parameters that depend on the polymer-solvent pair or instrument calibrations are required before proceeding with measurements. The last method is based on the viscoelastic response, which can be particularly sensitive to

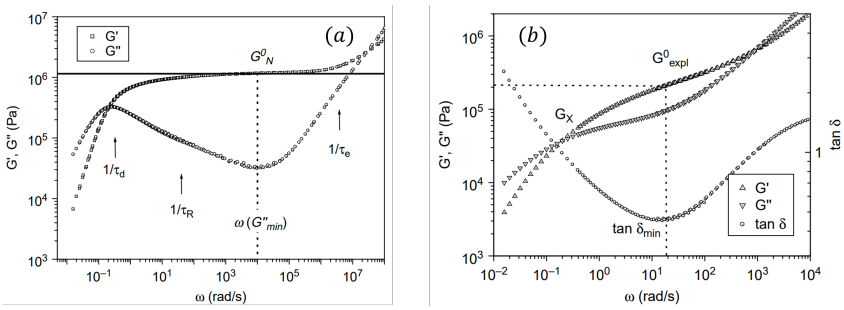

Figure 1.7. Effect of polydispersity on the dynamic moduli of (a) monodisperse and (b) polydisperse samples (pictures from [6])

the presence of high molecular weight chains compared to the more standard techniques. However, the application of rheological models is required in order to describe the relaxation dynamics of the polymer system.

1.5.1 Scattering techniques

Light scattering is one of the most common non-destructive techniques to investigate complex fluids. Through light scattering measurements, it is possible to evaluate the macromolecule size in terms of the gyration radius, and the weight-average molecular weight of a polymer.
The basic principle of this technique is that light passing through a polymer solution is partly absorbed by the molecules and partly scattered in all directions. The molecule that generates the light scatter must be large enough to give the scatter, but smaller than the wavelength of the light. Rayleigh theory is used to describe this phenomenon.

$$\frac{Kc}{R_\theta} = \left(\frac{1}{M_w} + 2A_2c\right)\frac{1}{P_\theta} \tag{1.3}$$

where c is the concentration, M_w is the weight-average molecular weight, θ is the scattering angle, A_2 is the second virial coefficient, R_θ is the Rayleigh ratio (defined as the ratio between scattered light intensity and incident light intensity), K is a constant, also known as the contrast, which depends on the wavelength and solvent-polymer system and P_θ is the form

factor defined as the ratio between the intensity scattered at angle θ and the intensity extrapolated to zero angle at low polymer concentration (typically $< 1\%v$), *i.e.* in absence of interferences. In Equation 1.3, the higher-order virial terms have been neglected by assuming low concentration.
The parameters K and P_θ are calculated as follows:

$$K = \frac{4\pi^2}{\lambda_0^4 N_A}\left(n_0 \frac{dn}{dc}\right)^2 \tag{1.4}$$

$$\frac{1}{P_\theta} = 1 + \frac{16\pi^2 n_0^2 R_g^2}{3\lambda_0^2}\sin^2\frac{\theta}{2} \tag{1.5}$$

In Equation 1.4 and 1.5, λ_0 is the wavelength, N_A is the Avogadro number, n_0 is the solvent refractive index, R_g the gyration radius and $\frac{dn}{dc}$ is the variation of the refractive index of the sample with concentration. Equation 1.3 states that the higher molecular weight and dimension of a molecule, the greater the scattered light.
Scattering techniques can be classified in two groups: SLS (static light scattering) and DLS (dynamic light scattering). In SLS experiments, the intensity amplitude of light statically scattered by the sample is measured, whereas in DLS tests the fluctuations of the scattered light at a given angle are measured.
Generally, the SLS technique is used to measure the molecular weight, whereas DLS is mainly performed to quantify the molecule dimension by evaluating the radius of gyration.

A further classification can be made according to the angle at which the measurement is performed. In particular, it is possible to distinguish:

- *SALS* (low angle light scattering). The preferred technique to measure the molecular weight at the lowest possible angle ($\theta \to 0$). LALS can be defined if $\theta < 10\,\text{deg}$. It results reliable for $R_g > \ 10 - 15nm$.

- *RALS* (right angle light scattering). A measurement is performed at $\theta = 90\,\text{deg}$ and it results reliable for $R_g < \ 15nm$.

- *MALS* (multi-angle light scattering). These are measurements at different angles. MALS is useful for measuring the radius of gyration of molecules.

1.5.2 Intrinsic viscosity

The molecular weight can be evaluated by measuring the intrinsic viscosity of the polymer dissolved in a solvent in the limit of diluted regime. Referring to η as the viscosity of solution, η_s as the viscosity of the pure solvent, and c as the solute concentration, the following parameters can be defined:

$$\eta_{sp} = \frac{\eta}{\eta_s} - 1 \tag{1.6}$$

$$\eta_{red} = \frac{\eta_{sp}}{c} \tag{1.7}$$

$$[\eta] = \lim_{c \to 0} \left(\frac{\eta_{sp}}{c} \right) \tag{1.8}$$

where η_{sp} is the *specific viscosity*, η_{red} is the *reduced viscosity*, and $[\eta]$ is the *intrinsic viscosity*. The intrinsic viscosity gives information about the average size of molecules in a diluted solution (chains do not interact each other). The evaluation of molecular weight is possible by applying the well-known *Mark – Houwink – Sakurada* equation, which correlates the intrinsic viscosity to the viscosimetric molecular weight [7].

$$[\eta] = kM^{\alpha} \tag{1.9}$$

in Equation 1.9, k and α are parameters which depend on the polymer-solvent system and the temperature. For a good solvent, α ranges between 0.5 and 0.8, whereas its value is 0.5 in case of θ-solvent (chain is in an unperturbed state, *i.e.* Gaussian coil).
Intrinsic viscosity measurements can be affected by errors due to high polydispersity or a high degree of branching. Over the years, various corrective methods have been proposed to refine the results from intrinsic viscosity measurements [8, 9, 10].
Typically, intrinsic viscosity measurements are performed in a glass capillary viscometer. The elution time of the diluted solution at various concentrations through the capillary is measured. A reduced viscosity is evaluated for each solution and, by extrapolation to zero concentration, the intrinsic viscosity can be determined.
From an experimental point of view, the evaluation of intrinsic viscosity involves easy measurements. For this reason, it is often coupled to a Gel

Permeation Chromatography to determine the distribution of molecular weights.

1.5.3 Gel permeation chromatography

Size exclusion chromatography (SEC), also called Gel permeation chromatography (GPC), is the most widely used physical separation technique for the evaluation of molecular weight distribution. In a chromatographic column, a mobile phase (polymer dissolved in a solvent) flows thorugh a stationary phase, *i.e.*, an inert support characterized by a distribution of pores of different sizes. Since there is no chemical interaction involved during the process, the mobile phase passes through the pores of the support. Large molecules will have a shorter elution time since they cannot penetrate the pores of the stationary phase. Smaller chains, on the other hand, passing through the pores, come out of the column with a higher elution time. It is important to highlight that the separation is by the size of macromolecules and not by molecular weight. However, the size of the macromolecule scales with the molecular weight, therefore it is possible to derive the molecular weight distribution via GPC.
SEC-GPC measurements can be coupled with additional detectors to evaluate the gyration radius and intrinsic viscosity.
To evaluate the distribution of molecular weights, it is necessary to calibrate the instrument by means of standards. The calibration can be conventional or universal. For a conventional calibration, standards of known molecular weight are used. The separation is carried out based on the size (hydrodynamic volume). The sample has an elution time that depends on its hydrodynamic volume and thus on molecular weight. Consequently, a *molecular weight vs elution volume* curve is built, which allows the measurement of an unknown sample.
For the universal calibration, a *hydrodynamic volume vs elution volume* plot is built. The measurement of intrinsic viscosity is directly related to hydrodynamic volume through a relation such as $M_w[\eta] = f(V_h)$. Accordingly, for an unknown sample, the calibration curve gives the hydrodynamic volume for a measured elution time. Further, from the online measurement of intrinsic viscosity, the molecular weight can be derived thanks to the MHS equation (see Equation 1.9).

1.5.4 Rheological Approach

The evaluation of molecular weight by means of GPC and intrinsic viscosity measurements can be unreliable, especially in the case of high molecular weight polymers. In fact, chains with very high molecular weights ($> 10^6 Da$) may have problems crossing the column. In particular, for UHMW polymers, the phenomenon of "*late elution*" may occur. In particular, longest chains are eluted with shorter chains.
Rheology can be a very reliable tool for assessing the molecular weight distribution of polymers. It is particularly sensitive to the presence of the high molecular weights that mostly influence the longest relaxation time of the system.
The evaluation of MWD can be inferred from linear viscoelastic data based on either the flow curve or the relaxation modulus. As shown in the next chapter, different methods for the evaluation of the molecular weight distribution from rheological measurements are available in the literature [11]. Some techniques are based on empirical correlations between rheological quantities, such as plateau modulus and zero shear viscosity, and MWD [12]. Polydispersity also correlates with the shape of Van-Gurp-Palmen plots [13]. Other methods are based on molecular models [14, 15, 16, 17, 18, 19]. These are divided in two general categories referred to as viscosity model and modulus model [14, 16]. In the viscosity models, it is assumed that the viscosity of the polydisperse melt depends on the viscosity and mass fraction of the single components according to a nonlinear mixing rule [20, 21]. The MWD can be determined from viscosity data combining both differential and integral approaches [22]. In the modulus model, the molecular weight distribution is related to the relaxation modulus of the melt. The modulus model is more sensitive to low concentration of high molecular weight fractions [12, 23].
One of the main advantages of the rheological approach with respect to GPC is the sensitivity to molecular architecture. As branched systems have different relaxation dynamics, two polymers with same M_w but different architectures, *i.e.* linear vs. branched, exhibit a different relaxation spectrum.

1.6 Research Motivation

In summary, to date, relevant challenges associated with the characterization and processing of POs are:

- determining the molecular topology of polymer chains, in particular the degree and distribution of branching;
- determining Molecular Weight (MW) and Molecular Weight Distribution (MWD) of both linear and branched ultra-high molecular weight polyolefins.
- determining the details of the chain architecture, such as the block distribution of polyolefin-based copolymers;

Rheology emerges as a valuable technique to address these challenges. However, the objectives above are difficult to achieve for several reasons. On the experimental side, performing linear and non-linear viscoelastic measurements on polymer melts may is non-trivial for UHMW polymers. For example:

- when dealing with very large MW melts, the measurements can be hindered by torque and normal force overload, elastic shear-induced fracture caused by normal stress differences, difficulties with sample loading due to very long relaxation times.
- for semi-crystalline polymers, as most polyolefins, crystallization actually forbids measurements at relatively low temperatures, strongly limiting the quantitative access to rheological features that are sensitive to molecular architecture;
- thermal stability is always an issue in polymer melt rheology, as high temperatures inevitably lead to polymer degradation.

The aim of this work is to study the molecular details of specific polyolefins by means of an innovative rheological approach. This will be achieved by measuring a polymer system in concentrated, entangled solutions, instead of melts, in order to overcome some of the intrinsic experimental difficulties listed above. After establishing the rheological response of the materials,

molecular models are used as a tool to quantitatively relate the macroscopic viscoelastic response of a polymer system to its molecular details. The choice of an appropriate solvent for diluting polyolefin melts is challenging. Solvents for polyolefins are toxic, flammable, difficult to find, and to handle. Therefore, the preparation and use of such solutions need particular care. Once a proper solvent is found, the optimization of the dissolution process, study of the stability and homogeneity of the prepared solutions, and determination of the best experimental conditions (temperature and concentration) must be performed in order to investigate the rheological properties and the macromolecular details of polyolefin melts. The use of polymer solutions instead of melts has advantages in that it reduces:

- temperatures during testing, avoiding degradation;
- crystallization phenomena, because of the plasticizing effect of the solvent;
- phenomena of instability, such as edge fracture;
- the torque and normal force required during tests, because of the decreasing of system viscoelasticity.

This means that, if phase separation phenomena are avoided, the window of viscoelastic characterization can be substantially widened.

Chapter 2

Background and state of the art

2.1 Synthesis and processing of UHMw POs

In industry, the synthesis of polyolefins is conducted in slurry or gas-phase reactors. The combination of type of reactor, polymerization process, initiators, and catalyst, results in materials with different properties including macromolecular architecture or degree of crystallinity. The latter is strongly related to the elasticity, strength and flexibility of the resulting polymer.
Regarding the catalysts, the synthesis of materials such as PE or PP is mainly performed through Ziegler-Natta catalysis in the heterogeneous phase. The presence of numerous active sites, however, leads to a broad macromolecular distribution. By using a single-site catalysts, the resulting molecular weight distribution can be better monitored. This type of catalysts are based on metallocenes, and their disadvantage is that, being in homogeneous phase, they can be used in solution polymerization.
The present work is mainly focused on ultra high molecular weight polyolefins, For this reason, a brief description of the most widely used synthesis techniques in industry are reported for UHMW PE and iPP. The most common method for the synthesis of UHMWPE is to conduct the polymerization in a slurry reactor in presence of a heterogeneous Ziegler-Natta catalyst. The temperature at which polymerization occurs is relatively

high (60 to 100 °C). Consequently, the chain growth is faster than the crystallization of chains, resulting in a high entanglements degree. The multitude of active sites, due to the type of catalyst, results in a broad molecular weight distribution. The development of reactor powder technology led to synthesize UHMWPE with a reduced degree of entanglements. In particular, the focus has shifted to the synthesis of disentangled UHMWPE. Polymerization takes place using catalysts with multiple active sites separated from each other, or with a metallocene catalyst with a single active center. The degree of entanglement is reduced by tuning the synthesis process conditions. In fact, as the temperature decreases, the kinetics of chain crystallization increases relative to the rate of polymerization [24, 25].

Less attention has been paid to UHMW iPP from a scientific point of view. The synthesis methods are essentially the same as those used for PE. In the past, iPP was produced in a slurry reactor with catalyst in solution. The synthesis led to the mixture of an isotactic and an atactic (amorphous phase, less interesting from an industrial point of view). Consequently, an extraction step of the amorphous phase was necessary. The most used technique to prepare UHMWPP is based on the use of metallocene catalysts, which require low process temperatures and consequently slow chain growth. In spite of the fact that Ziegler-Natta catalysts are the most common methods to produce iPP, the synthesis of UHMWPP was neglected for long time. A possible explanation could be that most of the catalysts used for the synthesis involve numerous chain transfer reactions, resulting in a decrease in the molecular weight of the polymer.

Chapter 1 briefly reports the applications fields of polyolefins and in particular of UHMW polymers. However, it is necessary to point out that, from an industrial point of view, one of the applications that has received most attention is the production of fibers with high strength and modulus. In order to obtain such fibers, chains must be oriented through the application of a large deformation in the solid state. UHMW polymers are good candidates for obtaining high-performance fibers, since it has been seen that as the molecular weight increases, the tensile strength increases. Technically, UHMWPE, because of its high entanglement number, would not be a good candidate for this process. However, as demonstrated in [26, 27], this problem can be solved by working in solution. In particu-

lar, UHMWPE can be dissolved in organic solvents like decalin[28, 29]. Dissolution, dramatically, reduces the number of entanglements, and ultra drawing can be achieved following crystallization and solvent removal.
Since UHMWPP is very similar to PE, the same technique for fiber drawing has also been proposed [30]. However, despite the addition of nucleating agents, the maximum tensile strength value achieved is $1GPa$ compared to the $3GPa$ obtained by drawing UHMWPE. Remaining in the field of application of UHMWPE, the development of processes to synthesize materials with a narrower molecular weight distribution is very important in the medical field. UHMWPE with a narrow MWD is demanded to the purpose of improving the life-time of artificial hip and knee replacements [31, 32, 33].

2.2 Rheology

2.2.1 Brief hystorical perspective and basic concepts

"Were one to speak of the science of matter as we speak of the science of electricity, no one would know what was being referred to". This sentence was reported by Eugene C. Bingham in a paper published in 1929 [34, 35], a date that marks the genesis of Rheology as a branch of fluid mechanics concerned with studying phenomena related to the deformation and flow of matter. Before the birth of rheology as a modern science, however, the flow of materials was already investigated by scientists.

For example, the definition of viscosity was established 300 years earlier by Newton. In 1687, he defined the resistance of an ideal fluid as "proportional to the velocity by which the parts of the fluid are being separated from each other" [36]. Newton's observations led to the following law:

$$\sigma = \eta \cdot \dot{\gamma} \tag{2.1}$$

where σ is the shear stress and $\dot{\gamma}$ is the shear rate. In Equation 2.1, the proportionality coefficient η is the viscosity.
Interestingly, in the same period, while Newton was formulating the paradigm of the purely viscous liquid, Robert Hooke was studying the antipodean material behaviour, namely the purely elastic solid. In 1675, Hooke published, *"ceiiinosssttuv"*. What he stated turned out to be the Latin anna-

gram of the famous phrase *"ut tensio, sic vis"* ("as the extension, so the force") [37]. The sentence stated the proportionality between strain and stress, expressed formulaically by the following law:

$$\sigma = G \cdot \gamma \tag{2.2}$$

in which γ is the shear strain and G is the elastic shear modulus.

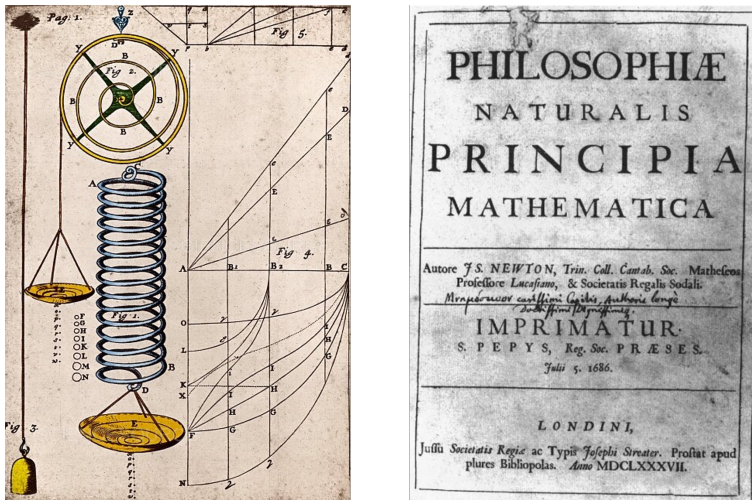

Figure 2.1. Picture of Hook's experiment (on the left) and Newton's book of 1687 (on the right)

Lord Kelvin recognized that both different behaviours could be manifested by a single metallic material [38]. This observations led to the so called Kelvin-Voigt model to describe the viscoelastic behavior of a solid material. In the 1867, Maxwell proposed a dual approach with respect to the Kelvin-Voigt model, the spring-dashpot model, to describe the behavior of such materials which act as viscous on long time scale [39].
Nowadays, rheology studies everything related to materials known as "complex fluids," that is, those that deviate from the behavior of ideal or Newtonian fluids. Viscoelastic materials have a timescale dependence on the applied deformation or stress. This can be rationalized by introducing a

dimensionless number, the so called *Deborah number (De)*:

$$De = \frac{characteristic\ time\ of\ material}{characteristic\ time\ of\ observation} \tag{2.3}$$

At low strain rates, or low deformations, a superposition principle, the so-called *Boltzmann superposition principle*, holds between stress and strain. Such a condition is referred to as linear regime. Microscopically, by applying a small deformation, molecules keep their equilibrium configuration. Increasing the deformation, the microstructure can be strongly perturbed.

2.2.2 Rheometric experiments and viscoelastic quantities

Stress Relaxation

In a Stress Relaxation experiment, a constant value of strain γ is applied and the resulting stress σ is measured.

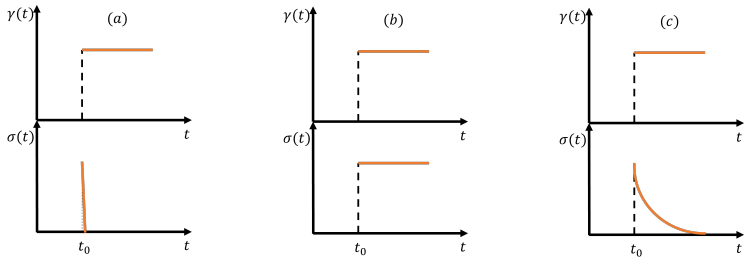

Figure 2.2. Stress Relaxation test for a Liquid (a), Solid (b) and viscoelastic material (c)

In Figure 2.2, the response of the different materials to a sudden deformation is reported:

- The behavior of a purely viscous liquid is expressed by Newton's law (Equation 2.1), therefore, an instantaneous deformation leads to an infinite shear rate. The resulting stress is infinite but it decays to zero as soon as the applied strain reaches a constant value (Figure 2.2a). Ideally, the stress is a Dirac function.

- Applying an instantaneous deformation to a purely elastic material (Figure 2.2b), it keeps a constant stress like a spring, as expressed by the Hooke's law (Equation 2.2).
- A viscoelastic material displays a solid-like response at short times (the higher is the strain, the higher is the stress), whereas the stress tends to zero for long time scales (Figure 2.2c).

The stress relaxation test can be analyzed by introducing the so called *relaxation modulus*. It results by the normalization of the stress with respect to the applied strain:

$$G(t) = \frac{\sigma(t)}{\gamma_0} \tag{2.4}$$

In the linear regime, as stress and strain are proportional, the resulting modulus does not depend on the applied deformation. One possibility to express the Boltzmann superposition principle is the following:

$$\sigma(t) = \int_{-\infty}^{t} G(t-t')\dot{\gamma}(t')dt' \tag{2.5}$$

where t is the present time, $\sigma(t)$ is the stress at present time, and t' is the past time.

Creep-Recovery

The dual test with respect to the stress relaxation is the creep experiment. A fixed stress is applied at a time t_0. At time $t > t_0$, the stress is released and the strain is measured during the entire time interval. In Figure 2.3 the response for viscous, elastic and viscoelastic materials is reported.

- For a purely viscous liquid the strain is linear in time with a slope equal to the Newtonian viscosity given by Newton's law. When the stress is removed, the strain remains constant, as the energy to deform the material is dissipated by viscous heating (Figure 2.3a).
- For an elastic material, Hooke's law applies (Equation 2.2). Therefore for a constant stress, the strain is constant. The energy supplied to the material is returned after the stress is released (Figure 2.3b).

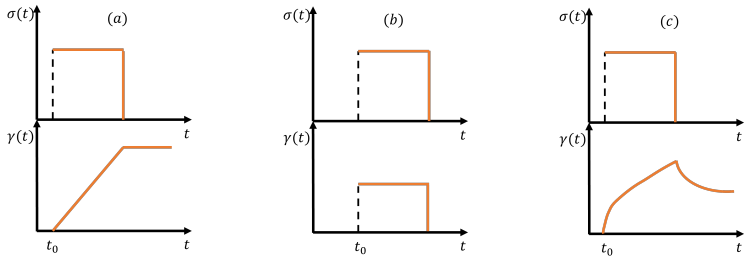

Figure 2.3. Creep-Recovery test for Liquid (a), Solid (b) and a viscoelastic material (c)

- A viscoelastic material has an intermediate behavior between solid and liquid. At short time scales, the deformation increases rapidly like a solid. Then it follows a linear regime like a liquid. When the stress is removed, the strain is partially recovered (Figure 2.3c).

For a creep test, it is possible to define a normalized strain, the so-called creep compliance:

$$J(t) = \frac{\gamma(t)}{\sigma_0} \tag{2.6}$$

A creep experiment can be performed in a linear regime if the applied stress is small enough such that the compliance is stress-independent. The Boltzmann superposition principle can be expressed in terms of compliance:

$$\gamma(t) = \int_{-\infty}^{t} J(t-t')\dot{\sigma}(t')dt' \tag{2.7}$$

Coupling Equation 2.5-2.7, one obtains the following relation between the relaxation modulus and the creep compliance:

$$\int_{0}^{t} G(s)J(t-s)ds = t \tag{2.8}$$

where $s = t - t'$. For large values of stress, the compliance becomes stress-dependent $J = J(t, \sigma)$.
Equation 2.8 suggests that $J(t)$ can be obtained if $G(t)$ is known and viceversa.

In order to understand the complete viscoelastic behavior of a material, it is necessary to obtain a relaxation spectrum over the widest possible time (or frequency) range.
From a practical point of view, the measure of stress after an instantaneous strain may not be a reliable method to explore the terminal regime of the material. In fact, a decreasing torque value read by the instrument is observed, leading to a lower sensitivity.
In case the time-temperature superposition principle can not be used, a creep measurement can be a reliable method to evaluate the terminal regime. However, this is an ill-posed problem and many solutions have been proposed in order to obtain a relaxation modulus or dynamic moduli from a creep experiment. Among the different methods, Honerkamp and Weese [40] proposed a method based on the evaluation of the retardation spectrum by means of Tikhonov regularization. A different procedure was proposed by Schwarzl [41]. In the latter, the evaluation of spectrum is avoided by fitting the compliance and transforming it directly into dynamic compliance.

Oscillatory response

The most common method to investigate the viscoelasticity of a material is the dynamic oscillatory response. In an oscillatory test it is possible to apply a sinusoidal shear strain or stress. In the case of a strain-controlled experiment, the strain is described by a sinusoidal expression, as reported in Equation 2.9.

$$\gamma(t) = \gamma_0 \sin(\omega t) \tag{2.9}$$

For small strains, the measured stress is still sinusoidal and shifted of a phase angle δ with respect to the strain.

$$\sigma(t) = \sigma_0 \sin(\omega t + \delta) \tag{2.10}$$

If the strain is small enough to remain in the linear regime, the frequency response test is referred to as Small-Amplitude Oscillatory Shear (SAOS) and can be analyzed in terms of two parameters: the amplitude ratio $G_d = \frac{\sigma_0}{\gamma_0}$, which is equal to the magnitude of the complex modulus, $|G^*|$, and the phase-shift angle δ. SAOS results are frequently reported in terms of dynamic moduli as functions of frequency: storage modulus $G'(\omega)$ and

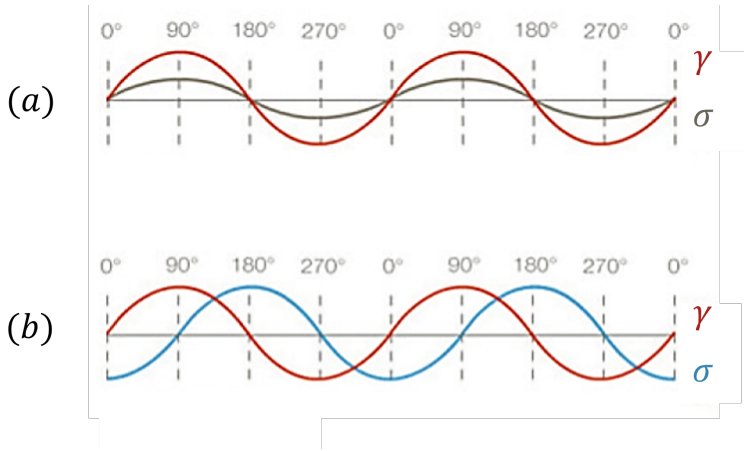

Figure 2.4. (a) stress and strain in purely elastic solid, (b) shift between stress and strain in a purely viscous liquid

loss modulus $G''(\omega)$.
The mathematical expression of the dynamic moduli comes from Equation 2.10, which can be rewritten as follows:

$$\sigma(t) = \sigma_0[\sin(\omega t)\cos(\delta) + \cos(\omega t)\sin(\delta)] \tag{2.11}$$

Dividing the right and left sides in Equation 2.11 by γ_0, one obtains:

$$\frac{\sigma(t)}{\gamma_0} = \frac{\sigma_0\cos(\delta)}{\gamma_0}\sin(\omega t) + \frac{\sigma_0\sin(\delta)}{\gamma_0}\cos(\omega t) \tag{2.12}$$

In Equation 2.12, $G' = \frac{\sigma_0\cos(\delta)}{\gamma_0}$ and $G'' = \frac{\sigma_0\sin(\delta)}{\gamma_0}$.
The dynamic moduli can be expressed in terms of amplitude ratio and phase-shift angle:

$$G' = G_d\cos(\delta) \tag{2.13}$$
$$G'' = G_d\sin(\delta) \tag{2.14}$$

In general, the storage modulus G' is linked to the elastic behavior and the loss modulus G'' to the viscous behavior. From the dynamic moduli is

possible to define the complex viscosity $|\eta^*(\omega)|$:

$$|\eta^*(\omega)| = \frac{\sqrt{G'^2 + G''^2}}{\omega} \tag{2.15}$$

where $\sqrt{G'^2 + G''^2}$ is defined as the complex modulus $|G^*|$.
From the linear viscoelasticity theory, it is possible to derive relations between the relaxation modulus and the dynamic moduli:

$$G'(\omega) = G_e + \omega \int_0^\infty [G(t) - G_e] \sin \omega t dt \tag{2.16}$$

$$G''(\omega) = \omega \int_0^\infty [G(t) - G_e] \cos \omega t dt \tag{2.17}$$

where G_e is the equilibrium modulus.

2.3 Polymer Dynamics

The study of polymer dynamics began in the '30s with the theory of rubber elasticity. In 1932, Meyer introduced the concept of the statistical conformation that macromolecules can assume [42]. Specifically, the different statistical conformations that a chain may assume depend on the thermal agitation of the constituent atoms of the chain. Thus, it was evident the analogy with the kinetic theory of gases, which had been consolidated a few years earlier with the understanding of Brownian motions of particles [43, 44]. In 1934, the concept of random coil was embraced in [45, 46]. In [45], the authors focused their attention on the entropic nature of the rubber elasticity from an experimental point of view. Other contributions to the the theory can be found in the works of Mooney [47] and Treolar [48]. Regarding the study of polymers, the first quantitative model was proposed by Rouse in 1953 [49], then adapted for solutions by Zimm in 1956 [50]. Many years later, in 1971, De Gennes proposed the diffusive motion of a polymer chain known as *reptation* [51] and Doi and Edwards (DE), in 1978, theorized the *tube-model* from the mean field theory [52, 53, 54]. Neglecting corrections and refinements made to the standard DE theory, a final theory on polymers was derived.

2.3.1 Polymer conformations

Polymers are long chains made of monomeric units. The chains can assume a variety of conformations as a result of Brownian motion. To characterize the size of such systems, a quantitative approach must be established. A polymer chain can be schematized as in Figure 2.5, *i.e.*, a sequence of $A_1, ..., A_n$ atoms linked by r_i bonding vectors.

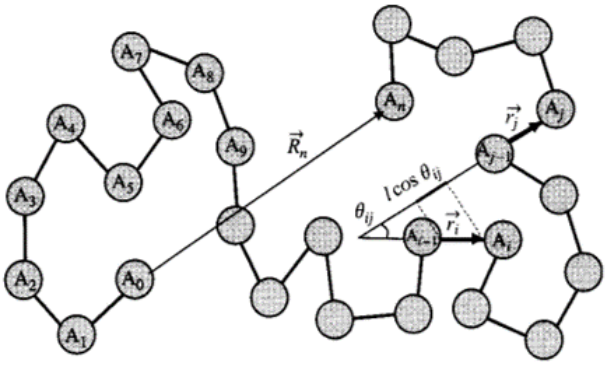

Figure 2.5. Schematic illustration of a polymer chain (from [55])

There is no preferred direction at equilibrium. A parameter may be defined to specify the size of the chain.

$$< \underline{R}_n > = \sum_{i=1}^{n} \underline{r}_i = 0 \tag{2.18}$$

The parameter defined in Equation 2.18 is called *end-to-end vector*. The symbol $< \cdot >$ indicates the average over all possible conformations that the chain may assume
The definition of the squared end-to-end vector may be an alternate method to determine the length of the chain because the average of the end-to-end vector is zero. As a result of the square operation, negative contributions are neglected and only positive contributions are included.

$$< \underline{R}^2_n > = \sum_{i,j=1}^{n} < \underline{r}_i \cdot \underline{r}_j > \tag{2.19}$$

In case of all bond vectors having the same length l, the right term in Equation 2.19 assumes the following expression:

$$< \underline{r}_i \cdot \underline{r}_j >= l^2 \cos(\theta_{ij}) \tag{2.20}$$

where θ_{ij} is the angle between two bonds. Depending on the assumptions made in Equation 2.20, it is possible to distinguish the different molecular models (*freely jointed chain, freely rotating chain, worm-like chain, etc.*, see Figure 2.6). The easiest model is represented by the *freely jointed chain*, in which there is no correlation between the direction of different bond vectors ($\cos(\theta_{ij}) = 0$ for $i \neq j$).

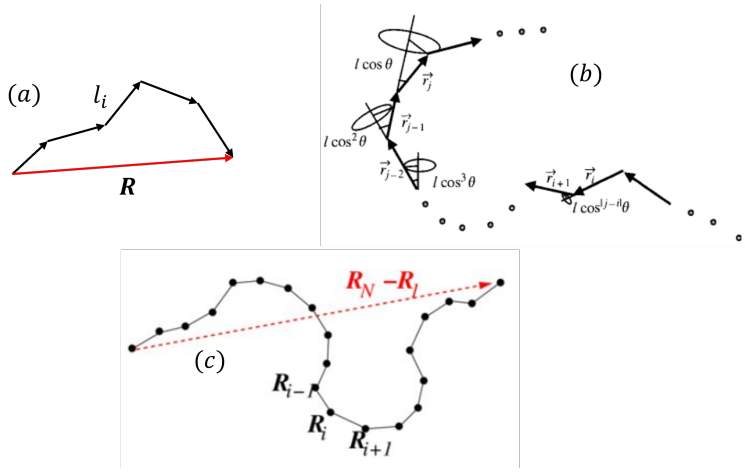

Figure 2.6. Representation of (a) freely jointed chain, (b) freely rotating chain, (c) worm-like chain

In this case the squared end-to-end vector assumes a simple expression:

$$< \underline{R}^2_n > = C_\infty n l^2 \tag{2.21}$$

where C_∞ is called characteristic ratio and it is independent on the number of monomers (for $n \to \infty$). The characteristic ratio measures the decrease in chain flexibility brought on by short-range interactions. A further simplification can be made by introducing the so-called Kuhn length, a length such that two consecutive chain segments do not interact with each other.

The resulting system can be schematized as showed in Figure 2.7. The

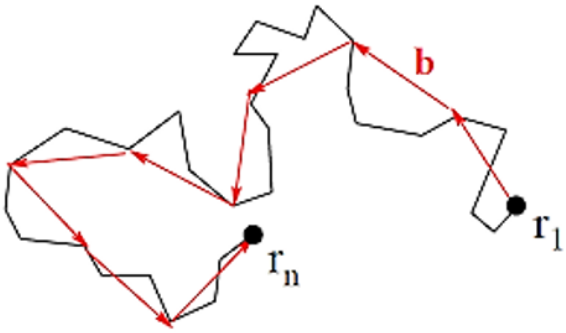

Figure 2.7. equivalent freely jointed chain

squared end-to-end vector can be expressed as follow:

$$< \underline{R}^2_n > = Nb^2 = C_\infty nl^2 \tag{2.22}$$

where $b = \frac{C_\infty nl^2}{R_{max}}$ is the Kuhn length, N is the number of Kuhn monomers and R_{max} is the maximum end-to-end distance. The Kuhn length is specific for each chemistry.
The squared end-to-end vector can be useful to quantify the dimension of the linear chain. However, if there are many or no ends (*e.g.* branched polymers), the *radius of gyration* is introduced. In the case of a branched polymers, Figure 2.8 depicts an illustration of the radius of gyration. The square gyration radius is determined by the average square distance between monomers in a certain conformation and the polymer's center of mass as reported in Equation 2.23.

$$R_g^2 = \frac{1}{N}\sum_{i=1}^{N}\left(\underline{R_i} - \underline{R_{cm}}\right)^2 \tag{2.23}$$

In the case of a linear chain, the expression of the radius of gyration is

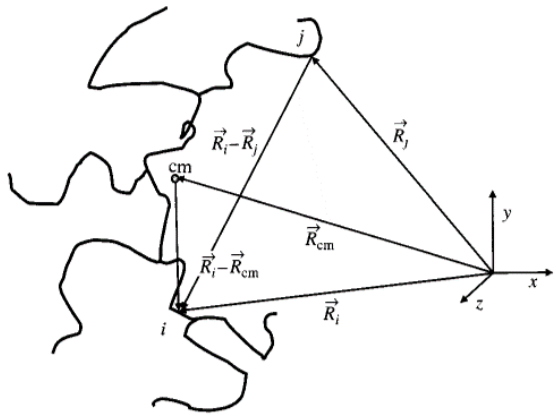

Figure 2.8. Illustration of the radius of gyration in the case of a branched polymers (from [55])

reported in Equation 2.24.

$$< R_g^2 > = \frac{Nb^2}{6} = \frac{< \underline{R}^2 >}{6} \tag{2.24}$$

2.3.2 Unentangled polymer dynamics

The Rouse model is the simplest model proposed to study polymer dynamics. The model was proposed in 1935 and it was based on the following assumptions:

1. The chain is schematized as a freely-jointed chain;

2. The chain is immersed in a viscous solvent;

3. Mass and friction are concentrated in N beads linked by (N-1) springs, which simulated the viscous and elastic viscous behavior of a polymer system, respectively.

Figure 2.9, depicts a scheme of the investigated system. Each spring has a length b with a spring constant $\frac{k_B T}{b^2}$.

If ζ is the friction coefficient of a single bead, the total Rouse chain

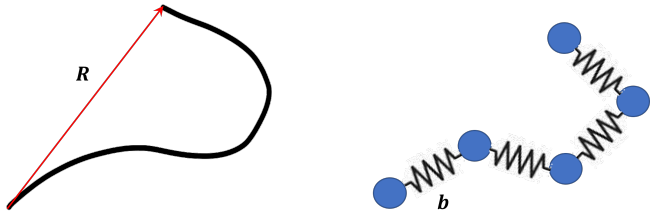

Figure 2.9. Schematization of the Rouse's chain

friction can be evaluated as:

$$\zeta_R = N\zeta \tag{2.25}$$

Combining Equation 2.25 with the Einstein relation ($\mathscr{D} = \frac{k_B T}{\zeta}$), it is possible to evaluate the diffusion coefficient of the whole Rouse chain:

$$\mathscr{D}_R = \frac{k_B T}{\zeta_R} \tag{2.26}$$

where k_B is the Boltzmann's constant and T is the absolute temperature. The time required to the Rouse chain to move a distance of order R is:

$$\lambda_R \approx \frac{R^2}{\mathscr{D}_R} = \frac{\zeta}{k_B T} R^2 N \tag{2.27}$$

A particular property of polymers is that they are fractal objects, that is, they are characterized by self-similar structures at different length scales. This fractal nature allows to extend the dynamics of portions of a chain to the whole system by appropriate scaling laws. Specifically, it is possible to relate the size of a polymer chain (R) to the total number of monomers in it (N) through Equation 2.28:

$$R \approx b N^{\nu} \tag{2.28}$$

and it can be demonstrated that for an ideal chain the fractal exponent ν is equal to 1/2 [55].

Equation 2.27 and 2.28 give the expression of the Rouse time for an ideal chain:

$$\lambda \approx \frac{\zeta b^2}{kT} N^2 \tag{2.29}$$

Rouse obtained the following result for the relaxation modulus of the chain:

$$G(t) = \frac{c_B k_B T}{N} \sum_{p=1}^{N} exp\left(-\frac{2t}{\lambda_p}\right) \tag{2.30}$$

where c_B is number of density of bonds [56]; λ_p is the spectrum of relaxation times. Note that the maximum value of λ_p is the longest relaxation time, also called Rouse time defined in Equation 2.29. The viscosity of the Rouse model is obtained from the integration of $G(t)$ between zero and infinity. Such integration yields the following expression:

$$\eta \approx \frac{\zeta}{b} N \phi \tag{2.31}$$

where ϕ is the volume fraction of polymer. Equation 2.31 indicates that the viscosity of the Rouse model is proportional to the number of chain monomers, that is, to the chain molecular weight.

2.3.3 Entangled polymer dynamics

The Rouse theory was conceived to predict the viscoleasticity of polymeric solutions. However, it proved to be valid for concentrated systems and for relatively low molecular weights. In this regime, it was observed that the viscosity increases linearly with molecular weight, M_w, in agreement with predictions. However, above a critical value, the viscosity scales with the power of 3.4 upon M_w (Figure 2.10a). At the same time, an elastic plateau (rubber-like behavior) appears in the frequency spectrum before reaching the terminal regime (Figure 2.10b).

In concentrated solutions or melts, the polymer chains are intertwined with each other. Subsequently, the motion of the single chain is prevented by the presence of topological obstacles provided by the other chains. These topological constraints are called *entanglements*.

The presence of entanglements dramatically changes the viscoelastic properties of polymers. These behave like elastic solids on short time

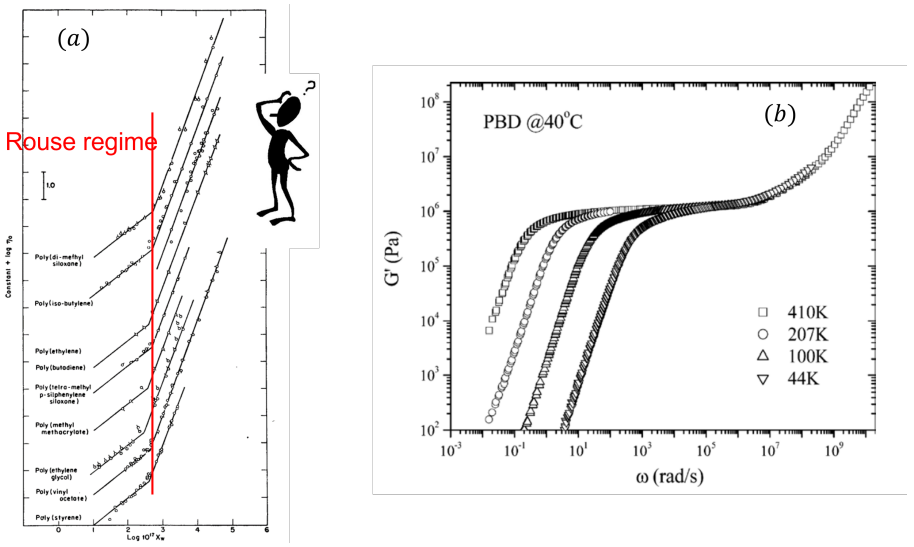

Figure 2.10. (a) Viscosity as function of the molecular weight. (b) The storage modulus from a dynamic frequency sweep test

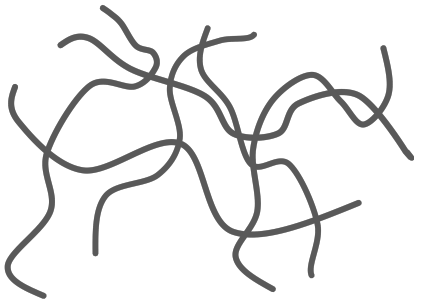

Figure 2.11. Illustration of an entangled system.

scales. However, for relatively long times, they can flow. The flow corresponds to the complete disengagement of the chain from the initial "*cage of entanglements*" by a snake-like motion, the so-called reptation.
The study of the dynamics of the system shown in Figure 2.11 is particularly complex because it encompasses the simultaneous motion of n-single chains interacting with each other. Such a problem is called a many-body problem.
In 1967, Edwards proposed a simplification to this problem by reducing the study of the complex system to that of a single chain confined by fixed obstacles (single-body problem) [57, 58], as shown in Figure 2.12.

Figure 2.12. A single chain hedged by the other chains represented by dots

The problem was re-proposed by de Gennes in 1971 [51]. He studied the motion of an extremely long chain within a fixed network. The chain was modelled as a freely-jointed chain consisting of N monomers. Moreover, its length was much greater than the distance between two points representing topological constraints. This assumption ensured that the chain was totally trapped within the network. The presence of entanglements limits the possible conformations a chain can assume by restricting it within a curvilinear tube-like region. Therefore, the chain itself was confined within a thin, permanent, undeformable tube. The chain could move through "defects" present along the chain. These defects could diffuse along the chain involving movement of the chain, similar to that of a snake so as to release portions of it from the tube.
Two characteristic times were identified by de Gennes. The first was re-

lated to the density of defects along the chain:

$$\tau_d = \pi^{-2}(Na)^2/\Delta \tag{2.32}$$

where N is the number of monomers, a is the distance between two successive monomers, Δ is the diffusion coefficient of the defects along the chain. The time τ_d is proportional to the square of the molecular weight. A time longer than τ_d is required in order to disengage the chain from the tube and renew its conformation. This characteristic time was named *reptation time* (τ_{rep}):

$$\tau_{rep} = \frac{(Na)^3}{\pi^2 b^2 \bar{\rho} \Delta} \tag{2.33}$$

where b is the length of a defect (assuming all defects have the same length) and $\bar{\rho}$ is the equilibrium value of the density of the defects. Equation 2.33 suggests that the reptation time is proportional to M_w^3. The incorporation of additional relaxation mechanisms, such as contour length fluctuations, could properly account for the experimental value of 3.4 found for the exponent.

2.3.4 The *tube-model* theory

The theory on the dynamics of a single chain by de Gennes was extended by Doi and Edwards in 1976 and applied to molten polymers and concentrated solutions. As proposed in 1971, also in this model the chain (test-chain) was confined due to the presence of the other chains inside an imaginary tube that allowed it its curvilinear axis, which is called the *"primitive path"*. The primitive path (or contour length) is defined as the shortest path connecting the ends of the chain and preserving the topology imposed by the entanglements. The chain can, therefore, be represented by its primitive path, that is, a Rouse chain characterized by consecutive statistic segments with a length equal to the distance between 2 entanglements. This dimension is assumed to be equal to the tube diameter. The primitive path can only move longitudinally back and forth with a curvilinear diffusion coefficient as defined in Equation 2.26. In fact, the motion of the whole chain can be assumed as the motion of the Rouse chain along the tube.

By introducing a curvilinear coordinate s, the survival probability of

the tube segment located at s at a time t, namely $\psi(s,t)$, can be calculated from the balance Equation 2.34:

$$\frac{\partial \psi(s,t)}{\partial t} = \mathscr{D}\frac{\partial^2 \psi(s,t)}{\partial s^2} \tag{2.34}$$

The equation states that the motion of the chain can be evaluated as a diffusive motion of tube segments along the chain. By solving the equation, the surviving fraction of the original tube segments can be evaluated. In terms of the relaxation modulus, it can be expressed as the product of the plateau elastic modulus and this fraction [59, 60], which decays to zero in a certain time. The main parameters to consider in order to describe the theory are: the elastic plateau modulus; the dimensions of the tube; the number of entanglements; relaxation times corresponding to different time scales. In the tube-model, these parameter come out to be correlated with one another.

Plateau Modulus

The elastic plateau modulus, strictly related to the elasticity of the entanglements density, is defined as follows

$$G_0^N = \frac{4}{5} N_m \frac{b^2}{a^2} k_B T \tag{2.35}$$

where b is the length of a statistical segment defined as Kuhn segment. Considering the relation between the number of monomers per unit volume and the monomer molecular weight, m_0 ($N_m = \frac{\rho N_A}{m_0}$, with N_A the Avogadro's number), Equation 2.35 can be re-written as:

$$G_0^N = \frac{4}{5} \frac{\rho RT}{m_0} \frac{b^2}{a^2} \tag{2.36}$$

This expression relates the elastic plateau modulus (G_0^N) to the diameter of the tube (a). Note the 4/5 constant proposed by Ferry [23] that was missing in Doi and Edwards' original theory [59] and in the work of Graessley [61]. According to the work of Doi and Edwards and the definitions

reported in [62], considering the number of tube segments (Z):

$$Za^2 = Nb^2 \tag{2.37}$$

the elastic plateau modulus results from Equation 2.36 and 2.37:

$$G_0^N = \frac{4}{5}\frac{\rho RT}{m_0}\frac{Z}{N} \tag{2.38}$$

Combining Equation 2.38 and 2.39, it is possible to derive the definition of Z which is also called *number of the entanglements per chain.* From Equation 2.38, the definition of the molecular weight between entanglements (M_e) can be obtained:

$$M_e = \frac{\rho RT}{G_0^N} \tag{2.39}$$

The theory leads to link the M_e to the dimension of the tube:

$$a^2 = \frac{4}{5}\frac{M_e}{m_0}b^2 \tag{2.40}$$

Relaxation times

In tube-model theory, all relaxation phenomena are controlled by the monomeric friction coefficient, as predicted in Rouse's model. The longest relaxation time of the chain, also known as reptation time ($\tau_r ep$), is defined as reported in Equation 2.41:

$$\tau_d = \frac{\zeta N^3 b^4}{\pi^2 k_B T a^2} \tag{2.41}$$

In addition, a limiting relaxation time can be identified, which occurs on length scales equal to the dimension of a single tube segment (or the distance between two entanglements). This time is called *equilibration time*, τ_e.

$$\tau_e = \frac{\zeta a^4}{3\pi^2 k_B T b^2} \tag{2.42}$$

The fast Rouse motions occurring within a single portion of the tube segment is called *Rouse rotational relaxation.* The complete relaxation of such

chain portions on this length scale corresponds to τ_e.

$$\tau_R = \frac{\zeta N^2 b^2}{3\pi^2 k_B T} \tag{2.43}$$

Considering the definition of the number of the entanglements per chain (Z) reported in Equation 2.37, the three relaxation times are related to each other as follows:

$$\tau_R = Z^2 \tau_e = (\frac{5}{4})^2 (\frac{M}{M_e})^2 \tau_e \tag{2.44}$$

$$\tau_d = 3Z^3 \tau_e \tag{2.45}$$

2.4 Entangled melts and concentrated solutions: scaling laws

The rheological characterization of polymer solutions is a crucial point of this work. Polymers are fractal objects, hence, the dynamics of a chain segment are self-similar with respect to those of the whole chain. The fractal nature of polymers allows to establish scaling laws between the properties of melts and solutions.

2.4.1 Solvent quality and concentration regimes

The volume spanned by a polymer coil in solution (pervaded volume) depends on temperature, solvent quality, and concentration. Based on polymer-solvent interactions, we can distinguish three types of solvents:

- *good solvent.* In good solvents, polymer-solvent interactions are favored with respect to polymer-polymer interactions. Therefore, at low concentrations, the polymer coils expands because of repulsion between monomers.
- *θ-solvent.* In θ conditions, polymer-polymer interactions and polymer-solvent interactions have the same probability. In this regime, ideal chain statistics apply.
- *poor solvent.* In poor solvent conditions, polymer-polymer interactions are favored with respect to polymer-solvent interactions, hence

the polymer chain is in a collapsed state because of monomeric attraction.

The volume occupied by the polymer is generally much smaller than the pervaded volume. The ratio of the effective polymer volume to the pervaded volume is referred to as overlap volume fraction, ϕ^*. The product of ϕ^* by the density of the solution yields the overlap concentration c^* . When the polymer concentration is smaller than c^*, the solution is called dilute, whereas, above c^*, the semi-dilute regime is approached. In the semi-dilute regime, the polymer coils start to overlap, therefore, both solvent and other chains can be found in the pervaded volume. The volume occupied by polymer is still very small compared to the pervaded volume. In semi-dilute solutions, the polymer conformation depends on the length scale considered. At intermediate length scales, excluded volume effects prevail, whereas they are screened at small length scales by thermal energy, and at large length scales by interactions with other chains. The length scale range in which excluded volume effects dominate decreases with concentration until it becomes zero at a particular value, c^{**}. At c^{**}, ideal statistics apply at all length scales. Such a concentration defines the onset of the concentrated regime. When the polymer coils start to overlap to a relevant extent, entanglements are also possible. As an example, Figure 2.13 reports the different concentration regimes for polystyrene in good solvent depending on concentration and chain dimensions.

2.4.2 Scaling laws of the rheological parameters in concentrated regime

In the last part of Subsection 2.3.4, the relationships between elastic plateau modulus and molecular weight between entanglements were introduced. From Equation 2.38, the elastic plateau modulus results independent on molecular weight. In fact, given $N \propto M_w$ and $Z = M_w/M_e$, the plateau modulus depends only on the molecular weight between entanglements. The latter depends on the concentration by the following equation:

$$M_e(\phi) = M_e(1)\phi^{-\alpha} \tag{2.46}$$

where $M_e(\phi)$ is the molecular weight between entanglements at a fixed

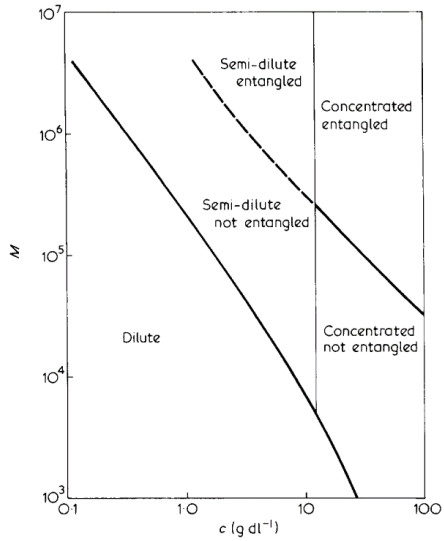

Figure 2.13. Concentration regimes for PS in good solvent, reprinted from [63].

concentration, $M_e(1)$ is the M_e in the melt state and α is the dilution exponent. Combining Equation 2.38 and 2.46, it is possible to derive the scaling law of the plateau modulus versus concentration.

$$G_N^0(\phi) = G_N^0(1)\phi^{1+\alpha} \tag{2.47}$$

Equation 2.47 includes the parameter α, which is defined as *dilution exponent*. In literature, it is well established that this value can vary between 1 and 4/3. Still today, there is no unambiguous definition that can define the numerical value of this parameter.
As shown in Figure 2.10, above a critical molecular weight, $\eta \propto \phi^{3.4}$. Assuming $\eta = G_N^0\tau_d$ and the dilution exponent $\alpha = 1$, where τ_d is the terminal relaxation time, the latter scales with $\phi^{1.4}$ [64]. Considering *contour lenght fluctuations (CLF)* relaxation (see Section 2.5) scales with ϕ^2, consequently, the reptation time scales with ϕ^1.

2.5 Effect of dispersity on rheology and mixing rules

As mentioned in Chapter 1, rheology is a useful tool to asses the distribution of molecular weights. It is much more sensitive to the presence of high molecular weight fractions than other techniques, such as GPC. In this section, the methodology for extrapolating the distribution of molecular weights from the viscoelastic behavior of a polymer through the "modulus model" is described. The first attempts to infer the MWD from viscoelasticity were based on empirical methods. Specifically, cumulative MWD was related to the viscoelastic data through the relationship reported in Equation 2.48:

$$W_U = \left(\frac{G'(\omega)}{G_N^0}\right)^{0.5} \tag{2.48}$$

where W_U is the weight fraction of unrelaxed chains. The reduced modulus reported in Equation 2.48 was fitted with a known equation [65]. The final MWD was derived from its cumulative distribution assuming the proportionality $1/\omega \propto M_w$.
With the development of molecular dynamics theories, the relationship between MWD and rheology was expressed in terms of the *"mixing rule"*. Equation 2.49 describes the correlation between MWD and relaxation modulus in the most general form [66, 67, 68].

$$G(t) = G_N^0 \left(\int_{\ln M_e}^{+\infty} F(t,M)^{\frac{1}{\beta}} w(M)\ dlnM\right)^{\beta} \tag{2.49}$$

where: G_N^0 is the elastic plateau modulus, M_e is the molecular weight between entanglements, w is the distribution of molecular weights, β is a constant and F is the relaxation function of a monodisperse polymer, generally referred to as kernel function. The relaxation modulus reflects multiple relaxation mechanisms, namely, whole-chain diffusion mechanisms, diffusion between entanglements and local motions in the high-frequency domain. Neglecting the relaxation mechanisms of the glassy region, the relaxation modulus is expressed by Equation 2.50.

$$G(t) = G_{Rouse}(t) + G_c(t) \tag{2.50}$$

where G_{Rouse} includes the Rouse relaxation at length scales smaller than that of entanglements and longitudinal Rouse modes along the tube. G_c includes the slowest relaxation phenomena describing the tube-renewal process.
The original tube-model theory, described in the previous section, predicts a viscosity scaling law: ($\eta \propto M^3$) against an exponent of 3.4, experimentally verified. Consequently, it is reasonable to assume that the simple reptation is not enough to describe the relaxation of the whole chain. In particular, Doi proposed the concept of CLF, which is a relaxation mechanism related to the ends of the chain [69]. An additional mechanism not included in the starting theory, but important to describe the dynamics of a polydisperse system, is the *constraint release (CR)*. The test chain is constrained in the tube due to the presence of other chains forming entanglement. Changing the point of view, a test chain also represents a constraint for the surrouding chains. As a result, when the test chain relaxes, the other chains are simultaneously released from the constraint. This phenomenon is modeled with the *double reptation (DR)* predicting a value of $\beta = 2$ in Equation 2.49. Furthermore, relaxed chains act as a solvent, enlarging the tube in which the test chain reptates, a phenomenon called *"dynamic tube dilation" (DTD)* . The test chain is dissolved by shorter chains that relax more quickly, expanding the tube diameter. Increasing β up to 2.3, as suggested in various research works [18, 16], is a simple method to take in account the DTD. The relaxation of the system is sped up by the occurrence of these phenomena.
The kernel function reported in Equation 2.49 is the function containing the relaxation mechanisms described above. Over the years, several possible models have been proposed in order to adopt an appropriate function which describes the dynamics of polymer systems.
In [70, 71], a comparison among five kernel different functions is proposed: step function [14, 15], single-exponential function [72, 73], *Doi* function [59], *des Cloizeaux* theoretical function [74] and the empirical *Baumgaertel–Schausberger–Winter (BSW)* function [75].
Equation 2.49 was used in different ways in literature. The simplest case is for direct problems. For polymers with a known macromolecolar distribution and architecture, if the kernel function is fixed, it is possible to obtain the rheological response with good agreement with experimental

data. Although the theories have been tested for monodisperse polymers, the use of a mixing rule combined with an appropriate kernel function, leads to obtain consistent results even for polydisperse systems.
The inverse problem consists of obtaining the MWD from rheological data. It is more complicated to solve and it is ill-posed. Several procedures have been proposed to obtain the MWD from the rheological experimental data. In the work of Thimm et al, the authors derive a direct expression of the MWD by solving the integral with simplifications [73]. Another possibility is to fix a functional form for w. Initially, the most commonly used functional was a log-normal distribution [76, 77]. Later, the use of a generalized exponential function (GEX) or a double generalized exponential function (D-GEX) was proposed [17]. This function turns out to be the most general possible by including other functions such as Flory, Schultz, Tung and Weibull distributions [78].

Chapter 3

Materials and Methods

The present study is part of the project *RHEOPOLAR* (RHEOlogical determination of POlyolefin ARchitectures, pr. #834) funded by the Dutch Polymer Institute (DPI). The first part of this chapter describes the tested materials, which were provided by different DPI partners. The second part deals with the equipment used to prepare the polyolefin solutions and for rheological measurements. Finally, the models used to obtain the MWD from rheology are described.

3.1 Materials

All materials described below were thermally stabilized by means of antioxidants. A mixture of antioxidants made of Irganox® 1010 (primary antioxidant, radical scavenger) and Irgafos® 168 (secondary antioxidant, peroxide decomposer) was added to the polymeric solutions or melts to improve their thermal stability [79]. The concentration of each antioxidant was 0.2% wt based on the total mass of the sample.

3.1.1 Polyethylene

High molecular weight polyethylene samples were kindly supplied by Sabic (Saudi Arabia). One polyethylene (henceforth coded as UH1) has a weight average-molecular weight of $7.1 \cdot 10^5$ g/mol and a polidispersity index of 11. We note that the sample UH1 cannot be strictly classified as

a UHMWPE as its M_w is lower than 10^6 g/mol. On the other hand, this allows to test the validity of the method to evaluate MWD of samples also slightly below the UHMW range. The other UHMWPE (henceforth coded as UH2) has a weight average-molecular weight of $3.2 \cdot 10^6$ g/mol and a polydispersity index of 9.7. The polydispersity index of both samples was measured by the supplier via GPC (see Figure 3.1).
Oligo-ethylene with an average molecular weight of 4000 g/mol and a polydispersity index of 2.35 was purchased from Merck (Germany).

3.1.2 Polypropylene

Two polypropylene samples were provided by Reliance (India). The first sample (coded as UHMWPPr) has an average molecular weight of $1.37 \cdot 10^6 g/mol$ and a polidispersity of 10.7, whereas the second sample (coded as RIL202PP) has an average molecular weight of $9.1 \cdot 10^5 g/mol$ and a polidispersity of 10.6. Both samples were synthesized according to the patented procedure described in [80]. The details of the macromolecolar distribution were obtained by means of a GPC analysis performed by the company. It is well known that, when the M_w is higher than 10^6, a polymer melt can be classified as ultra high molecular weight. According to the molecular distribution details provided by GPC, we can define UHMWPPr as ultra high molecular weight polymers and RIL202PP as a high molecular weight polypropylene.
In order to extract the MWD from rheology, the knowledge of some constants appearing in rheological models is needed. Three UHMW-iPPs with a narrow molecular weight distribution have been used as calibration standard. The materials are coded as *n19*, *n31* and *n70*. These samples are provided by the University of Munich and their properties are reported in Table 3.1. The synthesis of such samples were performed according to the procedure reported in [81, 82].

Sample	$M_{w,GPC}[g/mol]$	PDI
n19	$7.93 \cdot 10^5$	1.53
n31	$1.15 \cdot 10^6$	1.26
n70	$1.27 \cdot 10^6$	1.67

Table 3.1. Average molecular weight and polydispersity of iPPs from GPC

3.2 Methods

3.2.1 Evaluation of MWD via GPC

Sabic samples

For SEC analysis, two PL MIXED ALS columns are used, with pore size of 20 μm. The flow rate is $0.5ml/min$. Analysis are performed at 160°C. The detectors used are an IR5, infrared detector used as concentration and chemical composition detector, and a Wyatt EOS Helios multi angle light scattering detector, to obtain absolute M_w and radius of gyration. The samples are dissolved in trichlorobenzene (TCB) at 160°C. To avoid entanglement of the polymers, the concentration must be below the overlap concentration. To fullfill this condition, a rule of thumb is that the product $[\eta] \cdot c$ must be lower than 1.5, where c is the concentration and $[\eta]$ is the intrinsic viscosity.
In Figure 3.1, the MWDs of both polyethylenes provided by the company are shown.

University of Munich samples

In Figure 3.2a, the MWD of all isotactic polypropylenes provided by University of Munich are reported. Gel permeation chromatography (GPC) was performed with a PL-GPC 220 instrument equipped with 2× Olexis 300 mm× 7.5 mm columns and triple detection via a differential refractive index detector, a PL-BV 400 HT viscometer, and light scattering (Prescision Detectors Model 2040, 15 and 90°). Measurements were performed at 160°C using HPLC-grade 1,2,4-trichlorobenzene (TCB; 100 mgL^{-1} BHT)

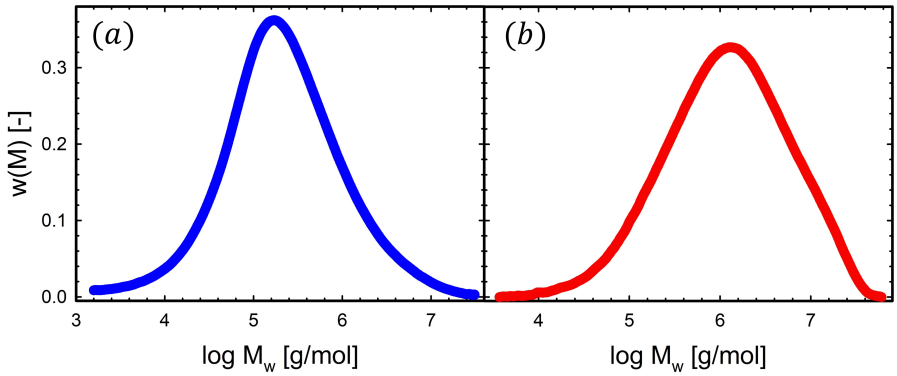

Figure 3.1. MWD for (a) UH1 and (b) UH2

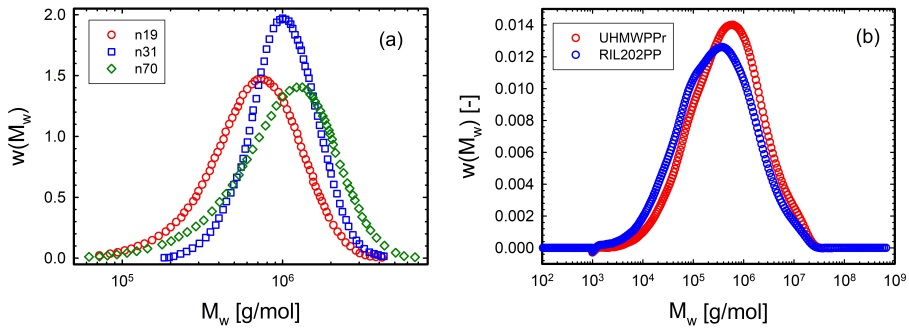

Figure 3.2. MWD of iPP provided by University of Munich (a) and Reliance (b)

from Sigma-Aldrich with a constant flow rate of 1 mL/min and a calibration set with narrow-MWD polyethylene (PE) and polystyrene (PS) standards for detector calibration. Samples were prepared by dissolving 0.5-0.7 mg of the polymer in 1.0 mL of stabilized TCB for 1 h at 140°C immediately before each measurement. The molecular mass was determined absolutely by using dn/dc=0.097 mLg^{-1} [83].

Reliance samples

In Figure 3.2b, the MWD of all isotactic polypropylenes provided by Reliance are reported. The molecular weight and MWD of RIL polypropylene samples was determined using a fully automated Polymer Char gel permeation chromatography instrument equipped with IR5 detector (GPC-IR) at 140°C temperature in 1,2,4-trichlorobenzene solvent.

3.2.2 Preparation of polymer solutions

Solution of PE and PP were prepared by means of two different methods.
For each UHMWPE, four polyethylene solutions with varying concentration were prepared according to the following protocol. Appropriate amounts of oligo-ethylene as solvent, UHMWPE and antioxidants were pre-mixed in a heated round flask with a magnetic stirrer under nitrogen atmosphere. The pre-mixed solution was then collected and fed to a co-rotating twin-screw micro-compounder (CPC Eindhoven, The Netherlands) [84, 29]. The mixing temperature was fixed at 220 °C. The solution was first mixed for 5 minutes at 80 rpm and then for 5 to 10 minutes at 100 rpm under nitrogen atmosphere. The extrudate was collected and molded in a hot press at 200 °C to obtain discoid specimens for rheological measurements. The weight concentrations of the four UH1 solutions were 20, 30, 40 and 50%, whereas those of the four UH2 solutions were 10, 15, 20, 30%.

As far as PP is concerned, in order to avoid the degradation of the pre-mixed solution, depending on the concentration, we prepared a dispersion of UHMWPPr, oligo-propylene and antioxidants in dichloromethane

(DCM). After the evaporation of DCM, the dispersion was then pressed in a hot press at 170°C. The resulting sheet was cut and fed to a co-rotating twin-screws DACA microcompounder (DACA Instruments, Goleta, CA, USA). The solutions were prepared at a mixing temperature of 210°C and 100 rpm for 10 minutes under nitrogen atmosphere. The collected extrudate was then molded at 190°C in order to prepare discs for the rheological measurements.

3.2.3 Differential scanning calorimetry measurements (DSC)

Calorimetric measurements were performed on a DSC 2500 (TA Instrument, USA). Each sample was subjected to two repeated heating/cooling cycles from 25 to 200°C at a heating rate of 5°C/min. The second cycle was used to evaluate the thermal properties of the samples.
The calorimetric data have been used to evaluate the final concentration in the extruded solution. This empirical method will be showed in the next chapter.

3.2.4 Rheological characterization

Rheological measurements were performed on a stress-controlled MCR702 rheometer (Anton Paar) with a parallel plate geometry. The diameter of the plates is 10 mm. Temperature control was ensured by a Peltier heating system PTD200 (Anton Paar). To reach temperatures higher than 170 °C, a convection oven (CTD600) was used. Depending on the DSC analysis, dynamic measurements were performed at 2 % strain, in the temperature range from 200 °C to 140 °C under nitrogen atmosphere. To test the thermal stability of the solutions, a dynamic time sweep test at the highest temperature was performed at 10 rad/s and 2 % strain. Creep tests were also performed at 200°C in order to obtain the terminal regime. It has been remarked by several authors that measurements, specially for PE, can be affected by wall-slip phenomena[85]. Furthermore, the presence of short chains may enhance the phenomenon due to fast disentanglement[86, 87]. To ensure that wall-slip did not affect the dynamic measurements at the different temperatures, we run experiments with varying gap heights. The tests were found reproducible irrespective of the gap height. The values

of stress and strain set for creep and dynamic tests are within the linear limit. The creep compliance was converted in dynamic moduli through the Schwarzl algorithm[41] implemented with a home-made Matlab® routine.

3.2.5 Mixing rule: Kernel functions

In this section, two approaches to express the kernel function (F_{sr} in Equation 2.49) for linear architectures are presented. The first approach used in the present work is based on the *time-dependent diffusion double reptation* model, whereas the second approach is based on the work of *Vega et al.* [88]. According to the model [89, 74, 90], the kernel function can be expressed as reported in Equation 3.1

$$F_{sr}\left(t, M\right) = \frac{8}{\pi^2} \sum_{i,odd} \frac{1}{i^2} \exp\left[-i^2 U(t, M)\right] \tag{3.1}$$

The constraint release effect is embedded in the definition of F through the parameter β:

$$F\left(t, M\right) = \left(F_{sr}(t, M)\right)^{\beta} \tag{3.2}$$

where F_{sr} is the simple reptation relaxation function. In Equation 3.2, the function $U(t, M)$ is the sum of two terms:

$$U\left(t, M\right) = \frac{t}{\tau_{rep}} + \frac{M^*}{M}\, g\left(\frac{Mt}{M^* \tau_{rep}}\right) \tag{3.3}$$

The first term in Equation 3.3 is used to model the reptation relaxation mechanism where $\tau_{rep} = k_{tdd} M^3$ for very long chains, it corresponds to what Doi and Edwards obtained with the original tube-model theory. The second term takes into account contour length fluctuations (CLF). The constants k_{tdd} and M^* are material parameters [18]. Concerning the function $g(x)$, we adopt the simplified form reported in [18], namely $g(x) = -x + x^{0.5}[x + (\pi x)^{0.5} + \pi]^{0.5}$.

Following the second approach reported in the work of *Vega et al.* [88],

the kernel function can be expressed as reported in Equation 3.4.

$$F_{sr}(t, M) = \frac{8}{\pi^2} \sum_{i,odd} \frac{1}{i^2} \exp\left[-\frac{i^2 t}{\tau_{rep}}\right] \tag{3.4}$$

the reptation time of a chain with mass M is calculated as follows:

$$\tau_{rep}(M) = 3\tau_e \left(\frac{M}{M_e}\right)^3 \left[1 - \kappa \left(\frac{M_e}{M}\right)^{0.5}\right]^2 \tag{3.5}$$

The constant κ is of order of unity. In particular, from simulations, it can be demonstrated that $\kappa = 1.69$ [88, 91] In Equation 3.5, the first term accounts for the reptation time and the second one for the contribution of CLF to the reptation. The expression for the Rouse time for an entanglement segment, τ_e is reported in Equation 3.6:

$$\tau_e = \frac{\zeta_0 \; M_e^2 \; \frac{\langle R^2 \rangle}{M}}{3 \; \pi^2 \; K_B \; T \; M_0} \tag{3.6}$$

where $\langle R^2 \rangle / M$ is the ratio end-to-end distance/molecular weight for an ideal equilibrium random coil, ζ_0 the monomeric friction coefficient, M_e the molecular weight between entanglements, M_0 the molecular weight of the repetitive unit and K_B Boltzmann's constant.
The approach of Des Cloizeaux needs two parameters for the Kernel function (k_{tdd} and M^*), whereas the approach of Vega needs one (τ_e). If the parameters are known, the mixing rule can be used in both direct and inverse problems.

3.2.6 Mathematical methods to solve the inverse problem

When the GPC results are available, a numerical approach can be used to solve the direct problem to predict the rheological response from MWD, without any assumption on the analytical form of MWD. Regarding the inverse problem, an analytical form of the MWD is needed. In the work of [15, 17], the authors used a generalized exponential function. In order to avoid the use of functions, Park et al. applied Tikhonov regularization

method to invert the integral in Equation 2.49.

GEX approach

Besides the analitical expression of $F(t, M)$, an analytical form of the MWD function must be also hypothesized for evaluating the integral in Equation 2.49. Along the same lines of reference [18, 15], the *generalized exponential function (GEX)* was used:

$$w_{\mathrm{GEX}}(M) = \left(\frac{M}{M_0}\right)^{a+1} exp\left(-\left(\frac{M}{M_0}\right)^{b}\right) \tag{3.7}$$

where M_0, a, b are the parameters of the GEX function. a and b are linked to the polydispersity, whereas M_0 is associated to the average numeric molecular weight. In fact, the larger the values for a and b the narrower is the distribution around M_0. In the case of a bimodal distribution, Equation 3.7 is unreliable due to the impossibility to fit another peak. This issue can be bridged by using a *double-GEX (DGEX)* distribution with five parameters:

$$\begin{aligned} w_{\mathrm{DGEX}}(M) = p\left(\left(\frac{M}{M_{01}}\right)^{a+1} exp\left(-\left(\frac{M}{M_{01}}\right)^{b}\right)\right) + \\ + (1-p)\left(\left(\frac{M}{M_{02}}\right)^{a+1} exp\left(-\left(\frac{M}{M_{02}}\right)^{b}\right)\right) \end{aligned} \tag{3.8}$$

With respect to Equation 3.7, there are two additive parameters in Equation 3.8. M_{02} and p.
Whatever equation for the MWD is used, the determination of all parameters is made by the χ^2 procedure using objective functions:

$$\chi^2 = \frac{1}{2n_{\mathrm{exp}}} \sum_{i=1}^{n_{\mathrm{exp}}} \frac{(G'_{\mathrm{exp}} - G'_{\mathrm{model}})^2}{(G'_{\mathrm{exp}})^2} + \sum_{i=1}^{n_{\mathrm{exp}}} \frac{(G''_{\mathrm{exp}} - G''_{\mathrm{model}})^2}{(G''_{\mathrm{exp}})^2} \tag{3.9}$$

where n_{exp} is the number of experimental points in G' and G'' spectra. The transformation of the relaxation modulus in dynamic moduli to min-

imize χ^2 is made with the Schwarzl algorithm [41]. The evaluation of the (D-)GEX parameters is made with the Nelder-Mead algorithm [92], implemented in Matlab with the command *fminsearch*. However, this command has no boundary condition for the parameters evaluation, so we used a modified algorithm to avoid negative values of the parameters [93, 94].

Tikhonov regularization

In this paragraph, an alternative mathematical method to evaluate the MWD from linear rheological behavior is presented. In matrix form, Equation 2.49 can be written as:

$$\underline{g} = \underline{\underline{F}} \cdot \underline{W} \tag{3.10}$$

where the vector $\underline{g} = \left(\frac{G}{G_N^0}\right)^{1/\beta}$ is the reduced relaxation modulus. The matrix $\underline{\underline{F}}$ is the kernel function and the vector $\underline{W}$ is the unknown MWD. Equation 3.10 is the matricial expression of the Fredholm integral of the first kind. The ill-conditioning of the matrix $\underline{\underline{F}}$ (conditioning number much higher than 1) leads to an impossibility to invert the matrix and evaluating the MWD. In Tikhonov regularization, the minimization function becomes a penalized least-squares procedure expressed by Equation 3.11:

$$\underline{J}(\lambda,\ W) = \|\underline{\underline{F}} \cdot \underline{W} - \underline{g}_{rheo}\|^2 + \lambda\|\underline{\underline{L}} \cdot \underline{W}\|^2 \tag{3.11}$$

where $\underline{g}_{rheo}$ is the reduced relaxation modulus obtained from rheological measurements, $\lambda > 0$ is the Tikhonov regularization parameter and $\underline{\underline{L}}$ is the identity matrix. Solving Equation 3.11 and setting $\frac{\partial J}{\partial M} = 0$, we obtain an expression to evaluate the vector $\underline{W}$:

$$\underline{W} = (\underline{\underline{P}}^T\ \underline{\underline{P}} + \lambda\underline{\underline{L}})^{-1}\underline{\underline{P}}^T\ \underline{g}_{rheo} \tag{3.12}$$

Equation 3.12 is valid if $F \in \mathbb{R}^{mxn}$ with $m = n$. In the case $m > n$, W can be evaluated from the singular value decomposition of the matrix $\underline{\underline{F}}$ as reported in work of [95]. In order to apply Equation 3.12, in this work the matrix $\underline{\underline{F}}$ is built such that is squared ($m = n$). With this approach, the quality of the result is strongly affected by the noise in the experimental data. However, as suggested in [96], the parameter λ can

be useful to moderate the final result. In fact, the lower the value of λ the more accurate is the final solution, but with a large statistical error on the evaluation of the vector W_i [40, 95]. On the contrary, the larger the value of λ the smoother the solutions are, but the accuracy is strongly reduced. Different procedures have been introduced to evaluate the best value of λ. In [97] the author adjusted the value of the Tikhonov parameter step-by-step in order to eliminate any modes with negative weights. A systematic regularization procedure was introduced by Weese [98] with the *self-consistent method* to evaluate the best Tikhonov parameter. In this work, we selected the Tikhonov parameter with a Matlab® routine based on the $L-curve$ analysis [99].

Chapter 4

Determination of the Molecular Weight Distribution of Ultra-High Molecular Weight Polyethylene from Solution Rheology

In this chapter, the linear rheology of ultra-high molecular weight polyethylene (UHMWPE) solutions is reported with the aim of determining the molecular weight distribution of the polymer. The UHMWPE is dissolved in oligo-ethylene in order to avoid issues related to unfavourable interactions with the solvent. To prepare the solutions, UHMWPE, solvent and a fixed amount of antioxidants are mixed by means of a co-rotating twin-screw micro-compounder. All prepared solutions are within the concentrated regime, as confirmed by the scaling laws of the main rheological parameters (plateau modulus, relaxation time, zero-shear viscosity) with concentration. Based on the viscoelastic response of the solutions, we adopt a heuristic approach to extrapolate the linear viscoelastic behaviour of the melt, according to a time-concentration superposition principle. Such a technique allows to span many decades of angular frequency, eventually attaining the terminal relaxation regime. The latter is difficult to achieve by direct measurements in the molten state because of

experimental issues such as extremely long experimental times and thermal limits. The viscoelastic spectrum of the melt is used to obtain the molecular weight distribution (MWD) according to the time-dependent diffusion/double reptation model. The MWD of two UHMWPE evaluated by using this approach agrees well with data obtained from gel permeation chromatography.

4.1 Introduction

Ultrahigh molecular weight polyethylene is a tough material used in many industrial and biomedical applications due to its high abrasion resistance, tensile strength, durability and biocompatibility [100, 101]. The ultra high molecular weight ($M_w > 10^6 \ \ g/mol$) improves the mechanical properties and the wear resistance but makes its processing more difficult due to the very large melt viscosity. In general, the mechanical properties of UHMWPE depend on both molecular weight and molecular weight distribution (MWD). The determination of MWD of UHMWPE is not an easy task. For example, standard MWD measurements via gel permeation chromatography (GPC) are prone to errors due to the lack of solubility of UHWMPE in common solvents at low temperature, and to long elution times [102].

Rheology is a sensitive tool to extrapolate the MWD of UHMWPE. MWD can be inferred from linear viscoelastic data based on either the flow curve or the relaxation modulus. However, both measurements and calculations have limitations. UHMWPE has a large number of entanglements per chain and a high elastic plateau modulus ($2.2MPa$) [6].This may represent a limit during the viscoelastic measurements. For example, a large number of entanglements implies a very long relaxation time, difficult to be probed experimentally. Furthermore, the very large polydispersity and the low molecular weight fraction of chains may enhance wall-slip phenomena [85, 86, 87]. From the modelling perspective, the evaluation of MWD from rheological data is an ill-posed problem [103, 11] whose accuracy depend on the available relaxation data [104]. In particular, the accuracy improves if the viscoelastic relaxation spectrum includes the relaxation times of the longest components of the distribution, that is, if terminal flow behaviour

is experimentally observed. As mentioned above, this requires very long measurements on the melt. The issue can be partially circumvented by invoking superposition principles. The simplest one is time-temperature superposition (TTS) [105]. Above the melting temperature, UHMWPE is a thermorheologically simple material. However, in this range, the horizontal shift factor follows an Arrhenius dependence due to the large distance from the glass transition. Hence, the effect of temperature on viscosity and relaxation times is rather limited. In order to extend the frequency range, Talebi et al. proposed a time-molecular weight superposition principle [16]. They shifted the mastercurves of different polyethylene samples with different molecular weight in order to build master curves of the viscoelastic moduli. However, such a technique entails the rheological characterization of different polyethylene melts with, at least, similar polidispersity.
An alternative to broaden the measured viscoelastic spectrum of UHMWPE consists of measuring rheology of solutions. According to the theory, [106] within the concentrated regime, the linear viscoelastic response does not change as the solvent quality varies, which was confirmed experimentally [106, 29].
Several solvents are reported in literature for dissolving UHMWPE, including: decalin, tetralin, xylene, toluene, and tri-chloro benzene. However, most of them are toxic [28]. Vegetable oils such as orange oil and olive oil were also used as solvents for UHMWPE. [84, 29, 107]. Nevertheless, these are rather ill-defined systems, whose composition might depend on the batch or source, with consequent reproducibility issues. In the work of [108], a paraffin oil is preferred as solvent for UHMWPE, due to its low volatility and the fact that the chemistry is the same as that of UHMWPE. However, paraffin may contain more volatile components that can evaporate at the test temperature (120 - 200 °C), reducing the thermal stability of the solution during long time rheological measurements. Alternative methods have been proposed to decrease the viscosity of UHMWPE to values of the order of 10^4 to 10^5 $Pa \cdot s$. They involve the preparation of blends with lower molecular weight polyethylene [109, 110, 111, 112, 113]. From a thermodynamic point of view, solvent and solute with the same chemistry form a homogeneous mixture at equilibrium. However, there are kinetic limits due to the high viscosity ratio between high molecular weight polyethylene and low molecular weight polyethylene and long diffu-

sion times of the matrix chains in the UHMWPE. In order to overcome the latter problem, an alternative could be the use of disentangled UHMWPE (a metastable state with a lower viscosity than entangled UHMWPE). [114, 115, 116, 117]. Disentangled UHMWPE has lower melt viscosity and larger diffusion coefficient with respect to entangled UHMWPE, therefore, the dissolution process should be enhanced. Recently, disentangled UHMWPE was used to decrease the diffusion time of chains during blending of HDPE and UHMWPE [112].

In a recent work [118], the UHMWPE was dissolved in very low molecular weight polyethylene wax, in order to improve mechanical properties of drawn UHMWPE avoiding volatile solvents and extraction procedures.

Regarding the preparation of the solutions, one must first consider that large polydispersity and molecular weight strongly affect the dissolution process [119]. Several techniques are introduced in the literature to dissolve UHMWPE in solvents. [109] compare different preparation techniques, including mixing in a single screw extruder and the solvent blending method using decalin. In the work of [120], a blend of UHMWPE and liquid paraffin was prepared in the mixing chamber of a rheometer (HAAKE HBI System 90). The most established technique is the extrusion using a co-rotating twin screw micro-compounder [84, 29, 121]. During the preparation of these blends, a fixed amount of antioxidants is added. An optimization of the amount of antioxidants in polyethylene is carried out by means of rheological tests [79].

Different methods for the evaluation of the molecular weight distribution from rheological measurements are available in literature. Some techniques are based on empirical correlations between rheological quantities, such as plateau modulus and zero shear viscosity, and MWD [14]. Polydispersity also correlates with the shape of Van Gurp-Palmen plots [13]. Other methods are based on molecular models [12, 15, 16, 18, 17, 19]. These are divided in two general models referred to as viscosity model and modulus model [12, 16]. In the viscosity model, it is assumed that the viscosity of the polydisperse melt depends on the viscosity and mass fraction of the single components according to a nonlinear mixing rule [20, 21]. The MWD can be determined from viscosity data combining both differential and integral approaches [22]. In the modulus model, the molecular weight distribution is related to the relaxation modulus of the melt. The modu-

lus model is more sensitive to low concentration of high molecular weight fractions [23, 12].
In this work, we present a method to evaluate the molecular weight distribution of UHMWPE through solution rheology. To avoid issues related to solvent quality, we use oligoethylene as a solvent. Two UHMWPE grades are used to prepare solutions at different volume fractions. Master curves of the solutions are obtained using the time-temperature superposition principle. Measurements at low frequency are extended by running creep experiments and converting the creep compliance into dynamic moduli. The master curves of the solutions were used to extrapolate the linear rheological behavior of the pure melts according to a time-concentration superposition principle. Then, according to Chapter 3, calculations based on a recent version of the modulus model are used to evaluate the molecular distribution of the melt. The method is validated by comparing the MWD of two UHMWPEs against data obtained from gel permeation chromatography.

4.2 Results and discussion

4.2.1 Evaluation of polymer concentration through DSC analysis

Differential scanning calorimetry was performed to assess the actual polymer concentration of the solutions. Figure 4.1a and 4.1b show heating/cooling cycles for the melt UH2 and the solution at 15% wt, respectively. As expected, the DSC data of the melt feature a single peak whereas two peaks can be observed for the solution. The higher peak is attributed to the crystallization/melting of the UHMWPE whereas the smaller peak is associated with crystallization/melting of the oligomer. The presence of two distinct peaks suggests that the two components fully phase-separate below the melting temperature of the UHMWPE. The area below the narrow peak is proportional to the enthalpy of crystallization/melting of UHMWPE in solution, hence to its concentration.

As a consequence, by plotting the enthalpy of UHMWPE in solution as a function of the polymer concentration, a linear plot should be obtained. Figure 4.2 depicts the peak enthalpy as a function of concentration.

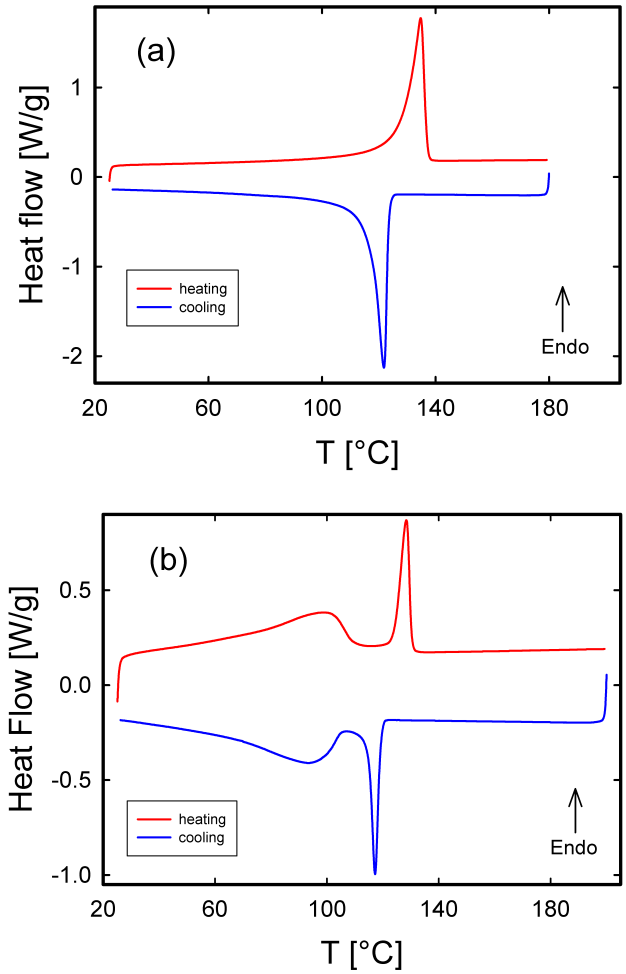

Figure 4.1. DSC analysis on (a) the melt UH2 and (b) a solution at 15 % wt.

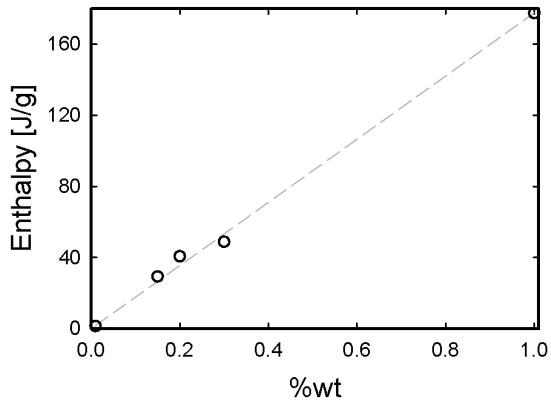

Figure 4.2. Cristallyzation/melting enthalpy vs concentration diagram related to the melt UH2. The dashed line is a linear regression through the data.

The data in Figure 4.2 follow a linear trend confirming the validity of the protocol used to prepare the solutions.

4.2.2 Linear Viscoelasticity

As mentioned above, we tried to extend dynamic measurements for the melts over the largest possible frequency range. To this end, we prepared solutions of UHMWPE with oligomer and extrapolated the linear viscoelastic (LVE) response of the melts from that of the corresponding solutions.
We first checked the thermal stability of the solutions by performing time sweep tests at the highest experimental temperature (200°C) for at least three hours. The sample were found to be stable within this time period as the drop of the viscoelastic moduli was lower than 3%. After ensuring thermal stability, we measured the dynamic moduli of each solution as function of frequency at different temperatures. Hence, we applied the time-temperature superposition principle to build master curves for each solution.
In order to properly determine the rheo-MWD, it is highly important that

during the experiments wall slip does not take place.

Wall slip

A macroscopic signature of wall-slip is that rheological quantities become geometry-dependent. To rule out wall slip, we have performed tests by changing geometry and checked the reproducibility of the results. As an example, in Figure 4.3a, we report two dynamic frequency sweep tests performed at the same gap with different diameters on the solution with UH2 at 20%, at 170°C. Furthermore, we report measurements at 170°C and different gap heights for the melts UH1 and UH2 (Figure 4.3b and 4.3c, respectively) . The data demonstrate that reproducibility is independent on the geometry used, thus excluding wall-slip.

In Figure 4.3a and 4.3c, measurements on the sample coded UH2, whereas Figure 4.3b on the sample UH1 are reported. Furthermore, in [122], solutions at 5, 10, 20 $\%_{wt}$ were prepared and no wall slip effects have been reported. Concerning melts, the effect of wall slip on similar samples was also investigated in [123], in which measurements at different gaps are performed on UHMWPE solutions. No evidence of wall slip was found.

Creep measurements

If the terminal relaxation time of the UHMWPEs was short enough, a creep or stress relaxation experiment would be an effective way to attain terminal relaxation behaviour. However, this is a tricky procedure for the two samples investigated here. From the master curves of Figure 4.12a and 4.12b, which are at a reference temperature of 170°C, it can be extrapolated that the terminal relaxation of UH2 is achieved at approximately 10^{-6} rad/s, whereas that of UH1 is achieved at approximately 10^{-5} rad/s. This means that experimental times of 12 days for UH2 and 1 day for UH1 are needed to attain terminal relaxation, in either a creep or a stress relaxation test at the same temperature. By performing the experiments at 200°C, the experimental times become almost the half than those at 170°C, yet they are quite long. When keeping the samples at high temperature for such long times, thermal degradation cannot be excluded. Therefore, working

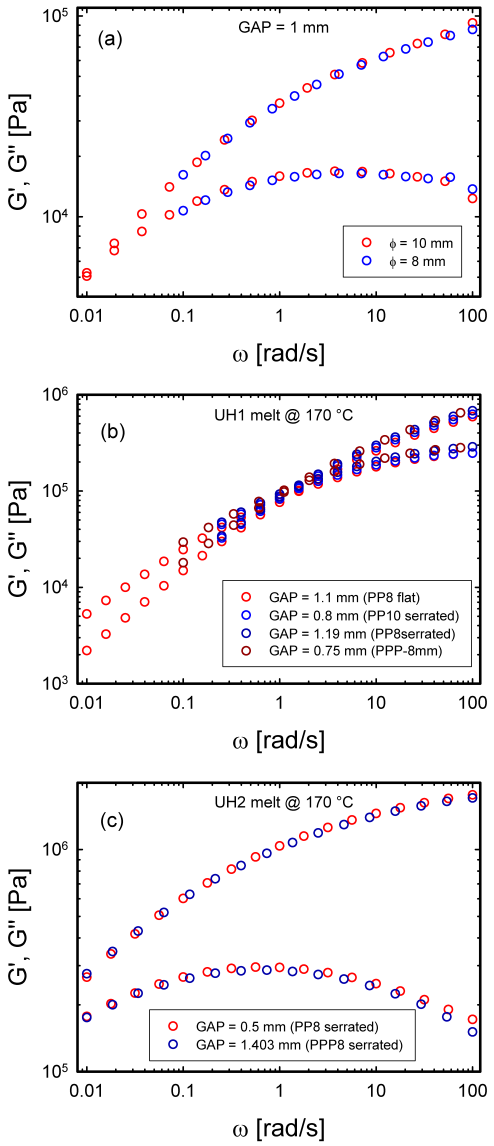

Figure 4.3. dynamic frequency sweep tests on different samples by varying geometry (see legend).

in solution represents a valid alternative, especially for the highest M_w sample. Not only it avoids thermal degradation but it can be less time consuming as the creep should be repeated at least twice at two different values of stress in order to verify linearity at all time-scales.
As an example, we report a 6 hr creep performed on the sample UH1 at 170°C in Figure 4.4a. It can be seen that, in such an experimental time, the steady state of the creep viscosity is far from the plateau (Figure 4.4b).

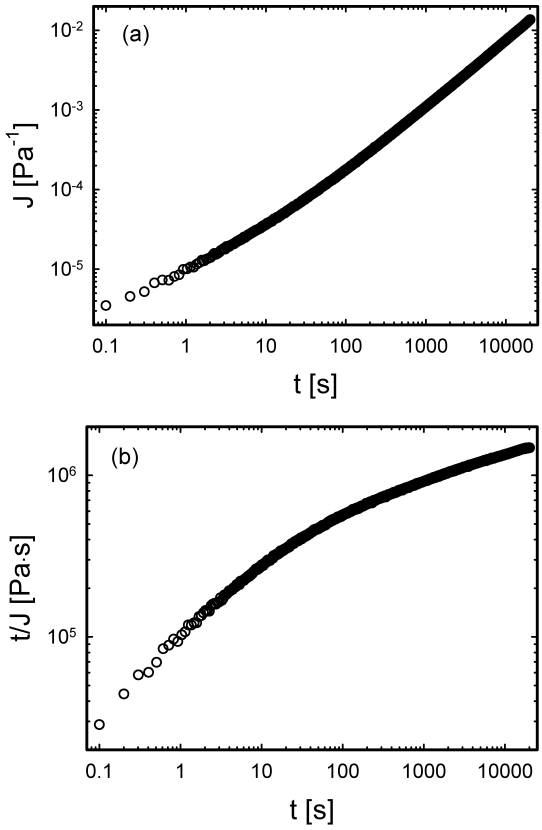

Figure 4.4. Creep experiment on UH1 at 170°C. (a) Creep compliance vs time and (b) Creep viscosity vs time.

time-Temperature Superposition

The master curves of the different solutions prepared from UH2 are reported in Figure 4.5. For each solution, data at low frequency were extended by performing a creep test at the highest possible temperature before thermal degradation. We observe that, for the most diluted solution, terminal flow behaviour is attained.

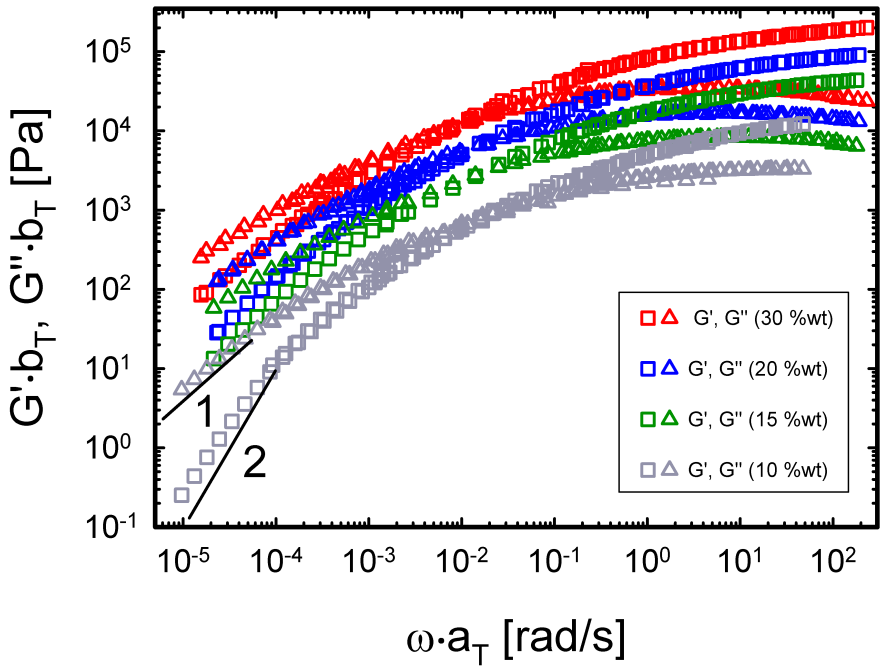

Figure 4.5. Master curves for solutions of UH2 at a reference temperature of 170 °C. The black lines indicate the terminal relaxation regime

The horizontal shift factors used to build the master curves of the different solutions are reported in Figure 4.6 for both UHMWPEs. As expected, they follow a linear dependence upon the inverse of temperature, indicating Arrhenius-like behaviour. Vertical shift factors were found close to unity. From the horizontal shift factors, the flow activation energy was calculated. The results are reported in the inset of Figure 4.6. The average

value is consistent with literature data [124, 125].

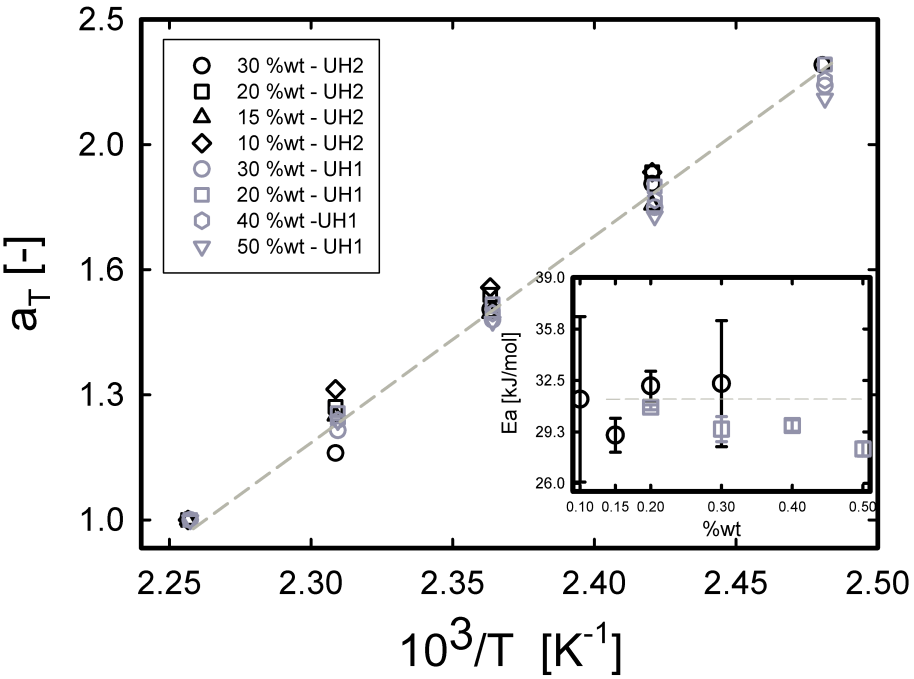

Figure 4.6. Horizontal shift factors used to build the master curves of the different solutions. The dashed line is used to guide the eyes. The activation energy evaluated from the shift factors is reported in the inset. Error bars are given by the standard deviation of the residuals.

An issue associated with time-temperature superposition is the possible breakdown of such a principle at temperatures close to the crystallization temperature of polyethylene. We verified the consistency of the master curves through Van Gurp-Palmen plots of the data [126]. An example is shown in Figure 4.7 for the solution of UH2 at 15 % wt. The good overlap of the data at different temperatures indicates that the TTS principle is valid in the measured temperature range.

The homogeneity of the solutions can be verified through a phase angle vs $\omega\phi$ plot [122]. As an example, such a plot for UH2 solutions is reported in Figure 4.8.

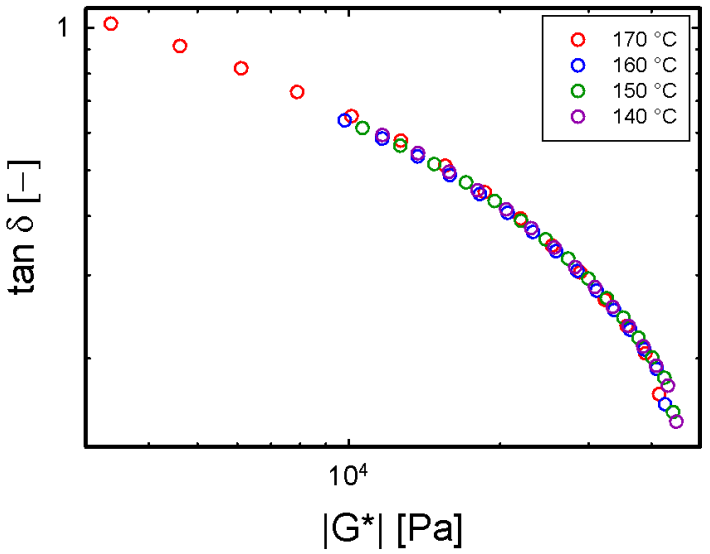

Figure 4.7. Van Gurp-Palmen plot for a solution at 15 % wt of UHMWPE in the temperature range of 170 °C down to 140 °C

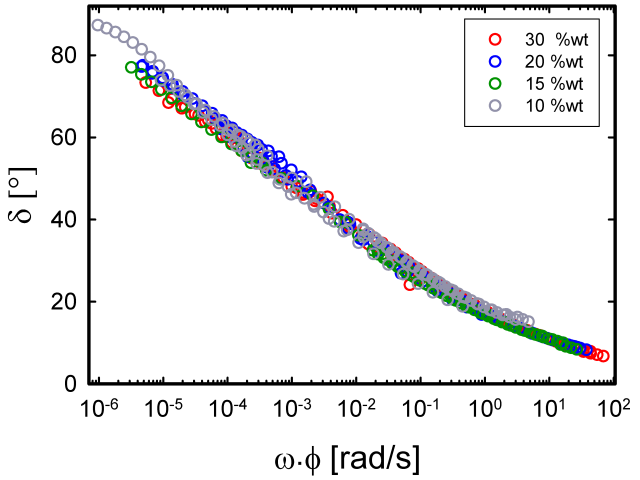

Figure 4.8. phase angle as a function of $\omega\phi$ for the different solutions of UH2 in oligo-ethylene.

Since the oligomer and UHMWPE have approximately the same density ($0.97 g/cm^3$), we assumed that the volume and weight fraction of UHMWPE in solution are approximately the same. The good overlap of the data at the different concentrations is indicative of homogeneity of the solutions.

Evaluation of rheological parameters

As a futher confirmation of consistency, we verified the scaling laws of the main rheological parameters of polymer melts and concentrated solutions, that is, the crossover time, zero-shear viscosity and plateau modulus. The crossover time is evaluated as the inverse of the crossover frequency between the storage and loss moduli. As zero-shear viscosity is not attained at all concentrations, an estimation was made by fitting the LVE spectra with Maxwell modes. The zero shear viscosity was then evaluated as [7]:

$$\eta_0 = \lim_{\omega \to 0} \frac{G''(\omega)}{\omega} \tag{4.1}$$

The plateau modulus was evaluated by applying the integral method to polydisperse polymers [6]:

$$G_N^0 = \frac{4}{\pi} \int_{-\infty}^{\omega_{\max}} G''(\omega) d ln \omega \tag{4.2}$$

Equation 4.2 is based on the idea that the curve of G'' vs ω is symmetric. As pointed out in reference [6], such a method yields values of G_N^0 which are systematically smaller than the experimental ones. However, given the lack of data at high frequency, it is a reasonable method to obtain an estimate of the plateau modulus. In Figure 4.9, the scaling laws of the crossover time, plateau modulus and zero-shear viscosity upon concentration are reported for both UH1 and UH2 solutions. The data were normalized by the characteristic parameters of the solutions at 30% wt.

Assuming that oligomer and UHMWPE have approximately the same density, the polymer volume fraction ϕ can be identified with the weight percentage $\% \, wt$. In Figure 4.9a, we observe that the crossover time scales with $\phi^{1.1}$. The exponent is very similar to that of the scaling law of the

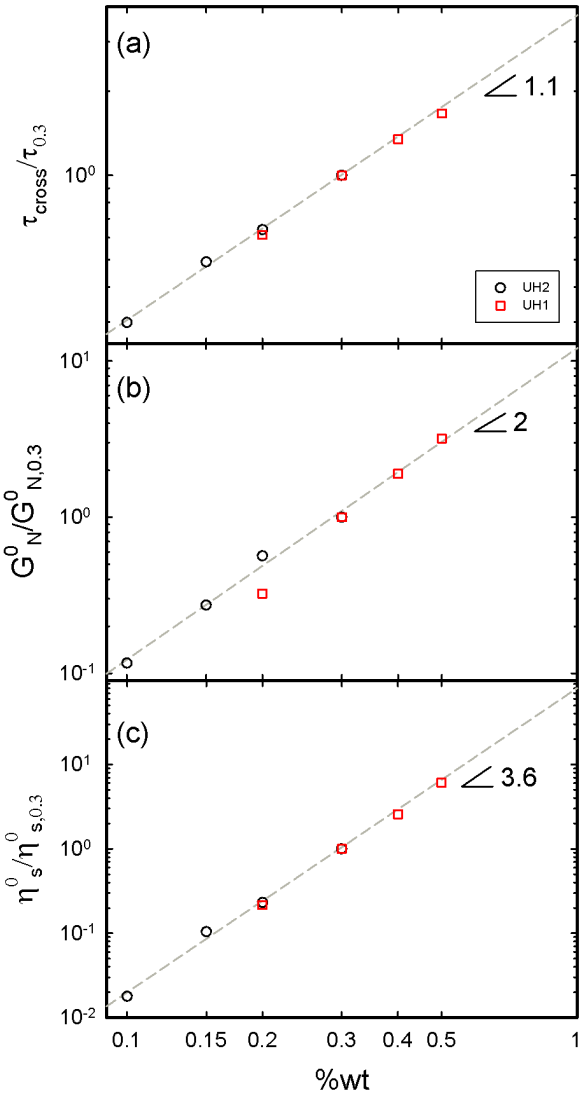

Figure 4.9. Scaling laws of the crossover time (a), plateau modulus (b) and zero-shear viscosity (c) upon concentration for UH1 (red symbols) and UH2 (black symbols). The data are normalized by the parameters of the solutions at 30%.

reptation time upon volume fraction, $\tau_{rep} \propto \phi^{\alpha}$ as relaxation by countour length fluctuations is expected to play a minor role here due to the large number of entanglements per chain [64]. Concerning the dependence of the plateau modulus with the concentration (see Figure 4.9b), the data also follow the expected scaling law [127]:

$$G_N^0(\phi) = G_N^0(1)\phi^{1+\alpha} \tag{4.3}$$

where $G_N^0(\phi)$ is the plateau modulus of the solution, $G_N^0(1)$ is the plateau modulus of the melt and α is the dilution exponent [128], assumed to be equal to unity. Finally, in Figure 4.9(c) the dependence of zero-shear viscosity on the concentration is reported. From Figure 4.5, the terminal regime can be reached only for the solution at 10 %wt. The slope of 3.6 in log-log plot is in agreement with the theoretical scaling law reported in literature [129, 130] and the value extrapolated for the melt is in agreement with the empirical correlation proposed by [131]. However, this procedure to evaluate the zero-shear viscosity may overestimate the real value. Consequently, the actual slope in Figure 4.9c could be lower.

4.2.3 Time-Concentration Superposition

As mentioned above, the LVE data of the solutions were used to extrapolate the master curves of the melt over the largest possible frequency range. In order to extract a reliable MWD, the master curves of the melt should ideally span in frequency from the terminal regime to the elastic plateau region. To this end, the master curves of the solutions in Figure 4.5 were horizontally and vertically shifted to obtain the master curves of Figure 4.10. A single frequency sweep of the melt, measured at the reference temperature of the solutions (170°C), was also included in the shifting procedure, for comparison.

In Figure 4.10 the master curves of the solution at 30% were used as a reference. The relevant rheological parameters for both systems are reported in Table 4.1, together with the vertical and horizontal shift factors.

A superposition approach was used by [16] to obtain the mastercurve of UHMWPE by measuring the rheology of a series of lower M_w polyethylene melts. In this case, the superposition works if the polydyspersity of

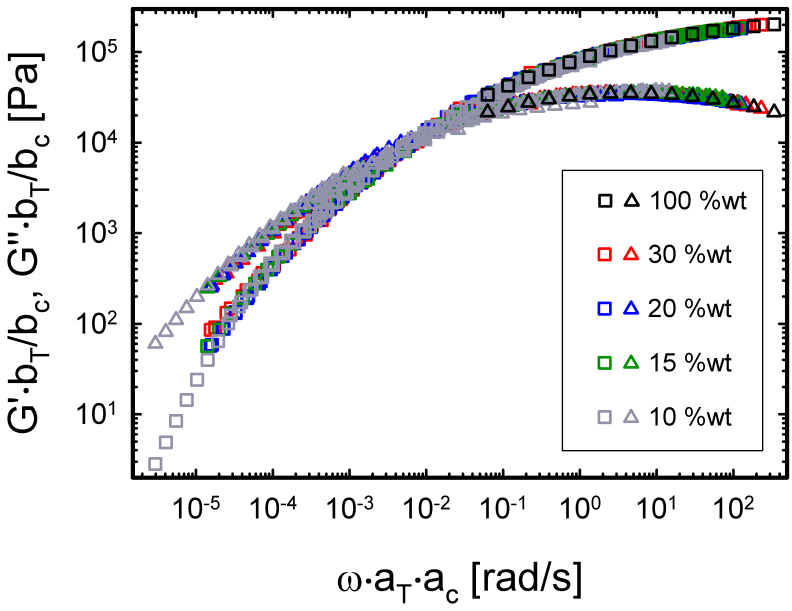

Figure 4.10. Superposition of master curves of solutions of UH2 in Figure 4.5 at different concentrations at a reference concentration of 30 % wt.

		$\tau_{cross}(\phi)$ [s]	$G_N^0(\phi)$ [Pa]	$\eta_s^0(\phi)$ $[Pa \cdot s]$	a_c	b_c
UH1	20 $\%_{wt}$	0.12	$4.38 \cdot 10^4$	$7.35 \cdot 10^3$	0.23	2.35
UH1	30 $\%_{wt}$	0.19	$1.35 \cdot 10^5$	$3.40 \cdot 10^4$	1	1
UH1	40 $\%_{wt}$	0.26	$2.56 \cdot 10^5$	$8.76 \cdot 10^4$	1.74	0.67
UH1	50 $\%_{wt}$	0.32	$4.32 \cdot 10^5$	$2.08 \cdot 10^5$	2.79	0.49
UH2	10 $\%_{wt}$	37.31	$2.37 \cdot 10^4$	$5.16 \cdot 10^5$	0.31	11.1
UH2	15 $\%_{wt}$	61.35	$5.57 \cdot 10^4$	$3.01 \cdot 10^6$	0.66	4.22
UH2	20 $\%_{wt}$	80	$1.15 \cdot 10^5$	$6.68 \cdot 10^6$	0.67	2
UH2	30 $\%_{wt}$	125	$2.04 \cdot 10^5$	$2.88 \cdot 10^7$	1	1

Table 4.1. Rheological parameters and concentration shift factors of the different solutions.

the different samples is similar. The advantage of our approach is that we use only a single melt, namely the UHMWPE of our interest.
We note that both superposition principles are empirical and work only in a limited frequency range. Concerning the time-concentration superposition principle, the ratio between the terminal relaxation time and the entanglement time τ_D/τ_e, decreases upon dilution [132], as $\tau_D/\tau_e \propto Z(1)^{3.4}\phi^{3.4\alpha}$, where $Z(1)$ is the number of entanglements of the melt. Hence, by changing the polymer volume fraction, the master curves of the melt and of the different solutions should not overlap over the whole frequency range. However, the master curves here are limited to the range from the terminal regime to the plateau region. In addition, given the very high number of entanglements of the melt $Z(1)$, the effect of dilution upon the ratio τ_D/τ_e becomes minimal as the two time-scales are very different. In Figure 4.10, the curves of G' at the different concentrations do not perfectly superimpose at low frequencies. This could be attributed to the effect of CLF. If the latter is non negligible, the validity of the concentration-superposition procedure can be questioned. To assess the relevance of CLF, one can estimate the weight fraction of chains with less than 10 entanglements. If this fraction is very small, CLF can be assumed negligible and the procedure can be applied. Considering Equation 2.46 and assuming $M_e(1)$ equal to 1640 g/mol, Table 4.2 reports the above mentioned evaluation for both samples.

		$M_e(\phi)$ [g/mol]	$M_e(\phi) \cdot 10$ $[g/mol]$	%Area MWD
UH1	20 $\%_{wt}$	8200.65	82006.48	25.69
UH1	30 $\%_{wt}$	5467.1	54670.98	17.47
UH1	40 $\%_{wt}$	4100.323	41003.23	12.94
UH1	50 $\%_{wt}$	3280.26	32802.59	10.13
UH2	10 $\%_{wt}$	16401.29	164012.96	9.79
UH2	15 $\%_{wt}$	10934.2	109341.97	6.45
UH2	20 $\%_{wt}$	8200.65	82006.48	4.73
UH2	30 $\%_{wt}$	5467.1	54670.98	3.02

Table 4.2. Evaluation of the contribution of short chains to the total MWD.

The parameter % Area MWD reported in Table 4.2 is defined in Equation 4.4.

$$\frac{\int_0^{M_e(\phi)\cdot 10} \frac{w(M)}{M} dM}{\int_0^{+\infty} \frac{w(M)}{M} dM} \tag{4.4}$$

The parameter defined in Equation 4.4 results lower than 10 % for UH2 and 25 % for UH1. This suggests that the CLF effect is small for the UHMWPE. Regarding UH1, the effect of CLF becomes relevant and may affect the extrapolation of the longest relaxation time of the pure melt. Another critical aspect worth of note is the effect of the dynamic tube dilation (DTD), reported in Chapter 2. Many experimental works show that the shorter chains of the sample can also play the role of solvent for the reptation of the longer chains and therefore, reduce their reptation time [133, 128, 134, 135]. The double reptation model ignores this fact if the parameter β is fixed to 2 in the Equation 2.49. The validity of the time-concentration superposition principle is also corroborated by the dependence of the shift factors upon volume fraction. The horizontal (a_c) and vertical (b_c) shift factors used to build the master curves of Figure 4.10 are reported in Figure 4.11.

In order to obtain the best superposition, the master curves of the solutions and the dynamic data of the melt in Figure 4.10 are freely shifted. However, we find that the horizontal shift factor follows almost the same dependence of the crossover time (Figure 4.9a) and the vertical shift factors follows nearly the same dependence of the plateau modulus (Figure 4.9b). Dashed lines in Figure 4.11 are best fit through the data. The fact that horizontal and vertical shift of the master curves follow the theoretical scaling laws of the relevant rheological parameters supports the applicability of the time-concentration principle in the explored frequency range. By using the master curves of Figure 4.10 and the shift factors of Figure 4.11, the master curve of the corresponding melt at the same reference temperature ($T_{ref} = 170$°C) can be obtained. The master curves of the two melts obtained with the method described above are depicted in Figure 4.12a and 4.12b.

The validity of the applied method can be also proved by comparing the data obtained with the solution method and the creep conversion (obtained with the software NLReg) into dynamic moduli (see Figure 4.13).

The fact that we do not attain terminal relaxation in the creep exper-

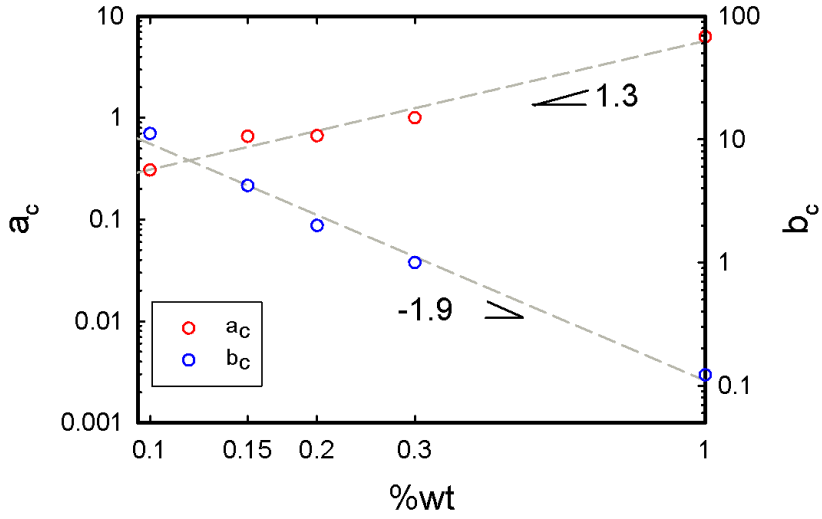

Figure 4.11. Shift factor used to obtain the master curves of Figure 4.10.

iment makes the result of the conversion unreliable at low frequency. The creep transformation shows the tendency to recover an elastic shoulder of G', which is not observed from the master curves of the solutions.

4.2.4 Evaluation of the MWD of the melts

Once the master curves of the melts are obtained, we can apply the modulus method described in Chapter 3 to obtain the molecular weight distributions. The results of MWD evaluation of UH2 and UH1 are depicted in Figure 4.12c and 4.12d, respectively. In Table 4.3 we report the values of the constants used in Equation 3.3 and the results from the χ^2 minimization procedure defined in Equation 3.9.

The same values of the model parameters were used for both samples. They are consistent with those reported in the works of [18] and [136]. In Equation 2.49, the value of the elastic plateau modulus was assumed equal to $2.2MPa$. In literature, the value of G_N^0 of polyethylene is in the range $[2, 3.5]MPa$ [88, 6, 137, 138, 139]. We adopted the most frequent value

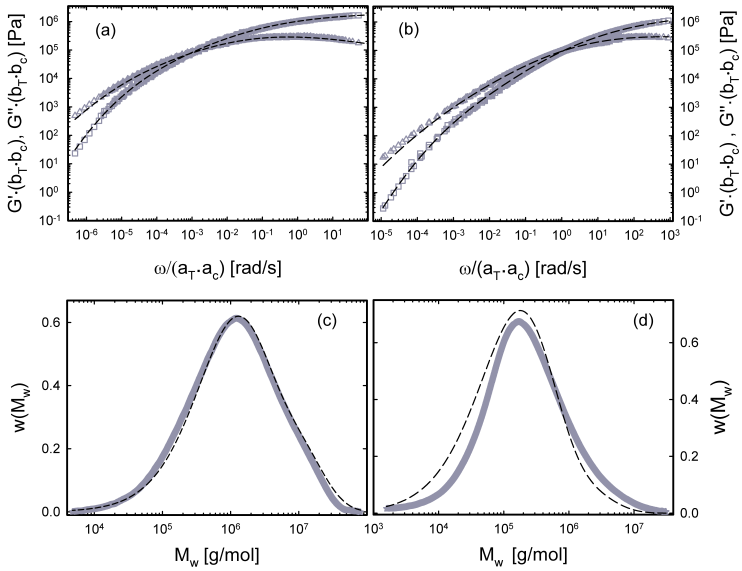

Figure 4.12. Master curves of (a) UH2 and (b) UH1. Gray squares and gray triangles indicate elastic and viscous moduli, respectively. MWD of (c) UH2 and (d) UH1. Gray stars are experimental data from GPC measurements. Black dashed lines in all panels indicate calculations based on the model described in Subsection 2.4.2.

Sample	$k_{\mathrm{tdd}} 10^{-17}$ [s/((g/mol)^3)]	M^* [g/mol]	χ^2
UH1	1.4	20000	2.41
UH2	1.4	20000	0.98

Table 4.3. Material parameters used to evaluate the MWD for both UHMWPE.

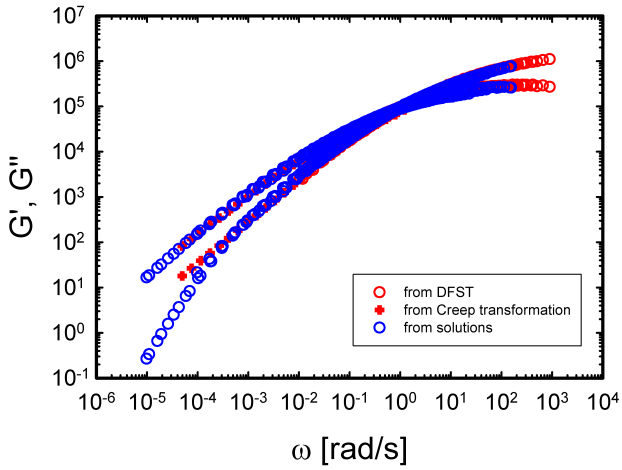

Figure 4.13. Comparison of the creep and solution method to obtain the master curves of the melt UH1.

of $2.2MPa$ [6]. The resulting MWDs obtained from the model (dashed black lines) are compared with gel permeation cromatography data (grey symbols). From Figure 4.12, we observe that excellent agreement between model predictions and GPC data is observed for UH2. The agreement between rheology and GPC data of UH1 is not as good as for UH2, yet satisfactory. The discrepancy could attributed to the fact that UH1 is a smaller molecular weight, hence rheological measurements cannot unveil a sufficient part of the high frequency spectrum, in the elastic plateau range. As mentioned above, this is necessary to obtain reliable predictions of the MWD. Another possibility for the mismatch is that the values of the model parameters are optimized over a relatively small range of samples and molecular weights. On the other hand, the overall agreement between GPC and predictions confirms the validity of the method described here and offers an appealing route for the determination of the molecular weight of UHMWPE samples from rheology.
As further confirmation of this procedure, we also solved Equation 2.49 by applying the Tikhonov regularization described in Chapter 3. Figure 4.14 reports the results of the inversion for both samples.

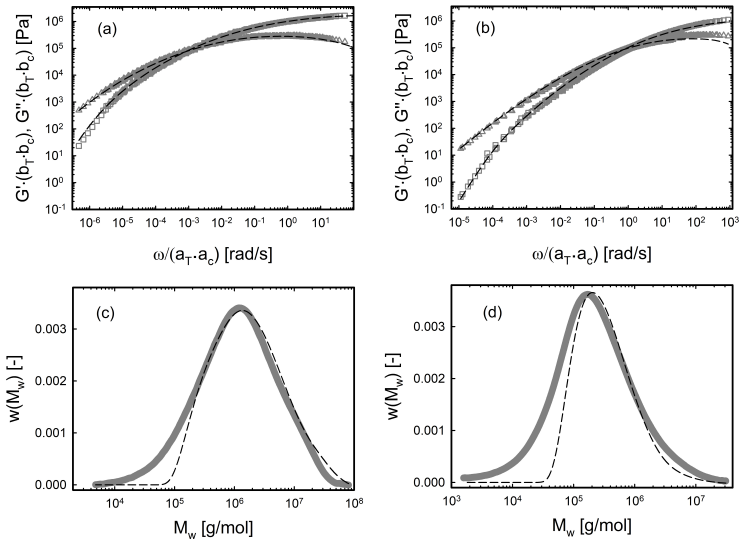

Figure 4.14. Master curves of (a) UH2 and (b) UH1. Gray squares and gray triangles indicate elastic and viscous moduli, respectively. MWD of (c) UH2 and (d) UH1. Gray stars are experimental data from GPC measurements. Black dashed lines in all panels indicate calculations based on the model.

The results confirm the agreement found by means of the previous method. However, this procedure may be unreliable to evaluate the first part of the molecular weight distribution.

4.3 Conclusions

This work aimed at evaluating the molecular weight distribution of ultra-high molecular weight polyethylene samples from solution rheology. To this end, two ultra-high molecular weight samples kindly provided by Sabic were dissolved in oligomeric polyethylene to prepare polymer solutions at different concentrations. The choice of the oligomer as a solvent is dictated by the necessity to avoid unfavorable interaction between polymer and solvent during sample preparation. Blending of the polymer with oligomer was achieved by means of a micro-compounder. The selected values of concentration are such that the different solutions fall within the concentrated regime. This is necessary to achieve consistent scaling laws. A complete rheological characterization of the solutions in linear regime was made over the largest possible frequency range by applying time-temperature superposition. The temperature range was limited by crystallization at low temperature and by polymer degradation at high temperature. Once the master curves of the solutions were obtained, we applied a time-concentration superposition principle in order to extrapolate the master curves of the corresponding melt. The validity of the principle in the explored frequency and concentration range is corroborated by the agreement between the horizontal and vertical shift factors and the scaling of the relevant rheological parameters, that is, the crossover time and the elastic modulus. The time-concentration superposition principle allowed to obtain master curves of UHMWPE samples from the terminal relaxation up to the elastic plateau region. The rheological data were used to extract the molecular weight distributions of the two melts according to a double-reptation/diffusion based model. A satisfactory agreement was found between the MWDs extracted from the model and those obtained via GPC analysis, indicating that the followed method represents an effective and simple way to obtain molecular weight distributions of UHMWPE samples from rheological measurements. The advantage of the proposed method with respect to creep or stress relaxation experiments consists in

avoiding long experiments at high temperature, where degradation may easily occur. As far as creep is concerned, it also avoids further complications related to creep conversion into dynamic moduli. On the other hand, the solution method described here relies on obtaining homogeneous solutions, which might be a limit for samples with M_n above one million as they would be extremely difficult to dissolve in oligomers.

Chapter 5

Evaluating the Molecular Weight Distribution of UltraHigh Molecular Weight Polyproprylene through rheology

The methodology developed in Chapter 4 for PE is applied here to ultrahigh molecular weight polypropylene (PP). We obtained three isotactic polypropylene (iPP) samples with relatively narrow MWD, synthesized by prof. Rieger's group at the Technical University of Munchen (Germany). Furthermore, two commercial PP samples with broad MWD were provided by Reliance Industries (India). The linear viscoelastic (LVE) properties of the samples are evaluated over the largest possible range of time-scales, from the terminal relaxation to the elastic plateau region. To this end, a combination of dynamic measurements at different temperatures and creep measurements is used. Regarding the sample with the largest molecular weight, it is diluted in oligo-propylene to make two solutions at 30% and 40%. The rheology of the solutions is then measured, and a time-temperature-concentration superposition principle is applied to extract the mastercurve of the pure melt. Once the LVE spectra of the samples are established, we validate a mixing rule approach to extract the molecular

weight distribution of UHMWPP via rheology. As literature studies on UHMWPP are rather scarce, the three iPPs are used as a benchmark to obtain the necessary material parameters to apply the mixing rule. Then, based on such parameters, the MWD of the two commercial UHMWPPs is assessed.

5.1 Introduction

Polyolefins are one of the most widespread class of polymers, with many applications ranging from construction to electronics. Among them, polyethylene (PE) and polypropylene (PP) are the most produced ones. The possibility to achieve ultrahigh molecular weight (UHMW) polyolefins favored the design of tough materials, with high impact strength, tensile strength, and resistance to corrosion.

A major challenge regarding the characterization of UHMW polyolefins is the determination of their molecular weight distribution (MWD). As the latter is closely related to their mechanical properties, its evaluation is of primary importance for processing and applications.

Modern analysis routinely employs chromatographic techniques in the liquid state to ascertain the MWD or possible heterogeneities based on chain length, tacticity, and chemical composition [140]. Gel-permeation chromatography (GPC), is a technique for separating molecules based on their size. In particular, polymer molecules of different dimensions can be fractionated due to a pore-size distribution of the stationary phase in the packing column [141]. The pore distribution affects the elution time of molecules of different size.

Liquid chromatographic methods can be considered reliable up to molecular weight of 10^6 g/mol. Beyond this threshold, the determination of the elution volume can be affected by relevant error [142, 143, 144, 145].

In the last decades, chromatographic techniques underwent several refinements. In particular, it is possible to couple the standard SEC with other techniques, e.g. optical methods (IR, mass spectrometry) to better characterize the architecture of polymer systems. However, a standard procedure to measure the MWD of ultra high molecular weight polymers is currently missing.

Rheology is a useful tool to improve the characterization of macromolecular

distribution of UHMW polymers, as the rheological behavior of polymeric systems is strongly influenced by their macromolecular structure. For example, the linear viscoelastic response is more sensitive to the presence of high molecular weight chains than GPC [7]. Several approaches were proposed to find the link between rheology and MWD, either based on the viscosity or the relaxation modulus, $G(t)$ [146, 11]. Concerning the latter, the dependence of molecular distribution on rheological properties can be expressed in terms of a relation between the MWD and $G(t)$. A linear mixing rule was proposed in [59], whereas a quadratic one was adopted in [89, 72]. The presence of a quadratic relationship between the relaxation modulus and the MWD stems from a constraint release effect, referred to as double reptation [89, 147, 148].

The mixing rule implies that each molecular weight fraction, $w(M)$, of the distribution contributes to the relaxation modulus of the polydisperse polymer through the Kernel function, namely the relaxation function of a monodisperse polymer of mass M. The Kernel function depends on the specific chemistry and chain architecture. Different approaches were adopted to define the Kernel function of linear polymers,involving either two parameters [89] or a single parameter [88].

When the MWD of a polymer is known a priori, the mixing rule can be used to predict the $G(t)$ of a polymer. Conversely, if the MWD is unknown, then $G(t)$ can be used to extract MWD. However, the latter is an ill-posed problem as more than one distribution $w(M)$ can satisfy the mixing rule. In this case, assumptions need to be made about $w(M)$, and the different mathematical approaches used for its evaluation can lead to different results. In both cases, an estimate of the material parameters to define the Kernel function is required.

The relaxation modulus was largely used to evaluate the MWD of UHMWPE [146, 149]. For this material, it is difficult to measure the dynamic linear viscoelastic properties in a large interval of frequencies, therefore superposition methods were proposed to extend the range of probed time scales [146, 149]. The material properties of UHMWPP are less explored, with only few studies available about the effect of a UHMW tail on the rheology and mechanical properties [150]. Furthermore, the evaluation of MWD of UHMWPP from rheology is a virtually uncharted territory as the material parameters required for the Kernel function are yet to be estimated.

In this chapter we investigate the possibility to extract the MWD of UHMWPP from rheological properties. To obtain the linear viscoelastic response of UHMWPP over the largest frequency range, we use a time-concentration superposition principle successfully adopted for UHMWPE in Chapter 4 [149]. We adopt the mixing rule for evaluating the MWD from the relaxation modulus. First, we obtain an estimate of the material parameters of PP from a set of three lab-made isotactic samples with relatively narrow molecular weight distribution. Then, we use such values to validate the mixing rule approach for commercial UHMWPPs with broad MWD. We also discuss the possibility to use rheology to detect artifacts from GPC measurements.

5.2 Summary of the materials

Table 5.1 summarizes the MWD parameters of the five PP samples used in this work.

Code	Source	M_w [g/mol]	PDI
UHMWPPr	Reliance Ind.	$1.37 \cdot 10^6$	10.7
RIL202PP	Reliance Ind.	$9.1 \cdot 10^5$	10.6
n19	Rieger's Lab	$7.93 \cdot 10^5$	1.53
n31	Rieger's Lab	$1.15 \cdot 10^6$	1.26
n70	Rieger's Lab	$1.27 \cdot 10^6$	1.67

Table 5.1. Summary of the samples used in this chapter.

5.3 Results and Discussion

5.3.1 Linear Viscoelasticity

Applying the method reported in Chapter 4, the LVE spectrum of the UHMWPPr sample was obtained from time-temperature-concentration superposition. To this end, two solutions were prepared by dissolving a proper amount of UHMWPPr in PP12k at a weight concentration of 30%

and 40%. The master curves of the two solutions were obtained by applying TTS (Figure 5.1a) and, then, they were superimposed to the LVE data of the UHMWPPr melt (Figure 5.1b).

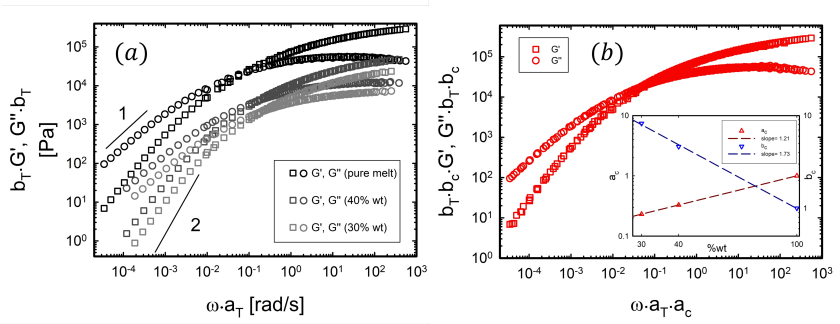

Figure 5.1. (a) Mastercurves of solutions and melt of UHMWPPr dissolved in iPP12k at T_{ref} = 200°C; (b) extrapolated behavior of UHMWPPr from solutions

The insert in Figure 5.1b reports the horizontal and vertical shift factors resulting from the superposition procedure.
The linear viscoelastic spectra of n19, n31, n70 and RIL202PP were measured directly in the pure melt state. Figure 5.2a depicts the mastercurves of the samples with the narrow MWD whereas Figure 5.2b reports those of UHMWPPr and RIL202PP. All mastercurves are at a reference temperature of 200 °C. The horizontal shift factors to build the mastercurves of the melts follow an Arrhenius-like dependence on the inverse of temperature and the flow activation energy is 45 kJ/mol. The value of the flow activation energy is consistent with the values reported in literature for polypropylene [151, 152]. For all melts, we measured the terminal relaxation by performing a creep test at the highest temperature (200°C) and converting the creep compliance to the dynamic moduli.
Measurements below 130 °C were forbidden by incipient crystallization. For this reason, the high frequency data do not allow to detect the minimum of the loss modulus, from which the plateau modulus, G_N^0, could be extrapolated [7, 6]. Therefore, we applied the integral method reported in [6] to obtain G_N^0. This method allows to extrapolate the value of plateau

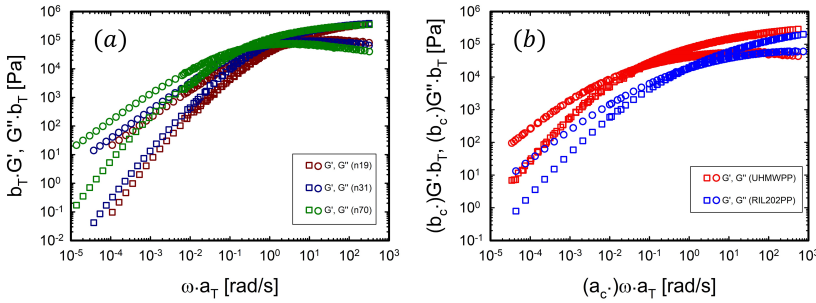

Figure 5.2. (a) Mastercurves of n19 (dark red symbols), n31 (dark blue symbols), n70 (dark green symbols); (b) Mastercurves of RIL202PP (blue symbols) and UHMWPPr (red symbols). All mastercurves are reported at $T_{ref} = 200°C$.

modulus from the maximum of G'' (see Equation 5.1).

$$G_N^0 = \frac{4}{\pi} \int_{-\infty}^{\omega_{\max}} G''(\omega) dln\omega \tag{5.1}$$

The extrapolated average value of the plateau modulus is $5 \cdot 10^5 Pa$, in agreement with values reported in literature [152, 153, 154]. According to Equation 2.39, the value of the plateau modulus leads to the evaluation of the molecular weight between entanglement (M_e) for iPP. Such value results to be 6200 g/mol.

5.3.2 Evaluation of material parameters

In order to apply the rheological models to extrapolate MWD from linear rheology, it is necessary to know the values of the material constants k_{tdd}, M^*, and τ_e for PP (see Chapter 3). To this aim, the known MWDs of n19, n31, n70 obtained from GPC are discretized, and Equation 2.49 is solved directly to obtain the LVE spectra. The parameters of the Kernel function are optimized to achieve the best simultaneous fit of the LVE spectra. First we use the Kernel function with two parameters [17, 18] and then the one with a single parameter [88]. The results of the fitting procedure are reported in Figure 5.3.

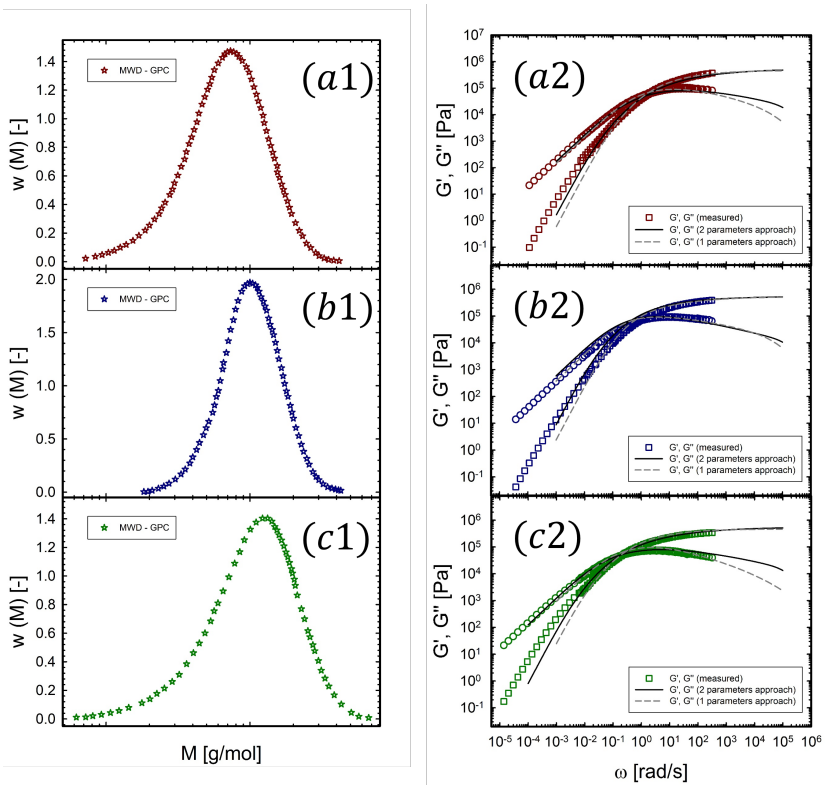

Figure 5.3. On the left, the MWD from GPC of n19 (a1), n31 (b1) and n70 (c1). On the right, comparison between the measured linear rheology and the solution of the direct problem of the mixing rule with 2 parameters approach (solid line) and 1 parameter approach (dashed line)

Overall, the agreement between experimental and predicted rheological data can be considered satisfactory. We note that the two-parameters Kernel function provides a better fit with respect to the single-parameter one. However, in both cases, the predicted G' deviates from the experimental value at low frequencies, especially for the samples n19 and n70. More precisely, the predictions indicate a faster relaxation compared to the experimental data. We attribute this discrepancy to the presence of a small fraction of sparsely long branched chains, which delay the onset of the terminal regime.
Based on the work of Trinkle at al. [155], we compared the phase angle (δ) as a function of the reduced complex modulus ($|G^*|/G_N^0$) for the three samples.

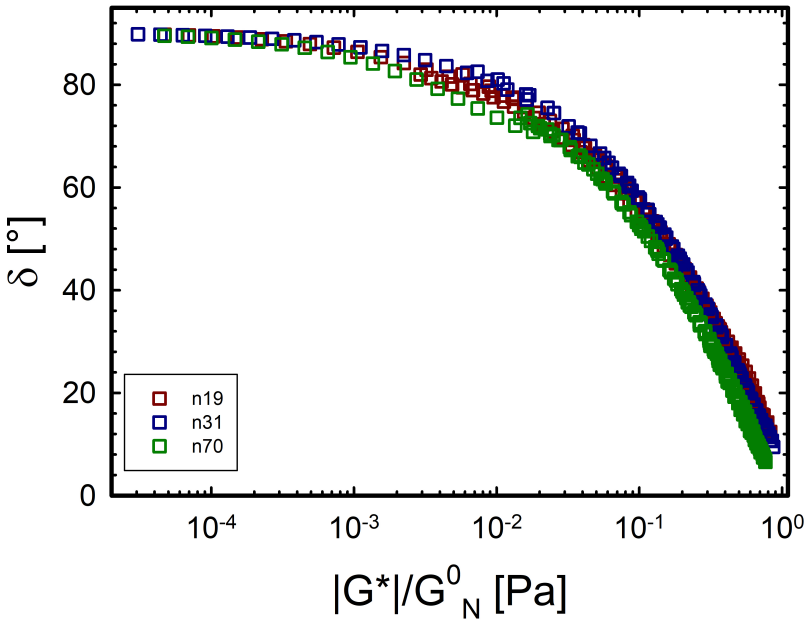

Figure 5.4. Reduced van Gurp-Palmen plot for the three nearly monodisperse UHMWPP.

The presence of LCB should result in a bump at higher values of the reduced modulus, as proposed in [155]. Such a bump does not clearly

appear in the curves of Figure 5.4, suggesting that, if branches are present, they are most likely sparse. The optimization of the fitting procedure allowed to estimate the values of the material parameters for PP. Such values are reported in Table 5.2.

$k_{\text{tdd}} \times 10^{21}$ [s/((g/mol)^3)]	$M^* \times 10^{-5}$ [g/mol]	$\tau_e \cdot 10^8$ [sl]
3.5	3-8	1.23

Table 5.2. Material parameters used in both models

Regarding the parameter M^*, we observed that a variation within the range $[3 \cdot 10^5, \quad 8 \cdot 10^5]$ does not affect the final results. Furthermore, for both approaches, we used the experimental exponent to describe the reptation mechanism. In both kernel functions, the longest relaxation time scales with respect to the molecular weight with an exponent of 3.6 instead of 3.0. As reported in Chapter 2, the theory predicts an exponent of 3.4.

5.3.3 Determination of the MWD of the commercial UHMW-PPs

Once the constants have been estimated, the direct problem of obtaining the viscoleastic moduli from the MWD could be solved for the broadly disperse commerical samples UHMWPPr and RIL202PP. To this end, the GPC curves were discretized and Equation 2.49 was solved numerically to obtain the LVE spectra. The comparison between the calculated and experimental LVE spectra is reported in Figure 5.5.

The predictions obtained with the two-parameters approach are vertically shifted toward lower values with respect to the measured spectrum. This issue can be solved by decreasing the value of M^*. The M^* parameter is associated with relaxation via CLF. As reported in [60], the CLF mechanism depends on M_w. In this study, we estimated the material constants from samples with a narrow MWD to investigate samples with high polydispersity. Therefore, the value of M^* could be overestimated. A similar trend is observed in literature for PE, where M^* results higher for narrow MWD polyethylenes with respect to broad MWD ones [18, 136]. For this reason, we lowered the value of M^* by one order of magnitude. The effect

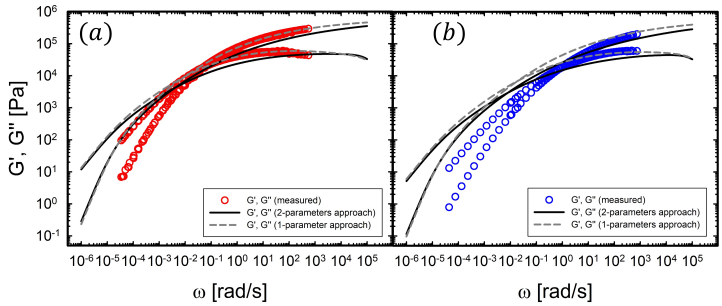

Figure 5.5. Comparison between the measured dynamic moduli and the response obtained from GPC by applying 2-parameters model (black solid line) and 1-parameter model (dark gray dashed line)

of M^* is reported in subsubsection 5.3.3. This sufficed to obtain reasonable predictions in the high frequency range also with the two-parameters approach, as shown in Figure 5.6,

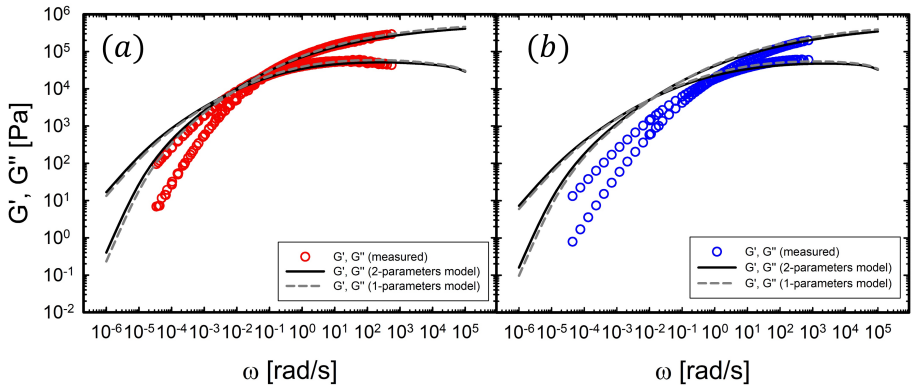

Figure 5.6. Comparison between the measured dynamic moduli and the response obtained from GPC by applying 2-parameters model (black solid line) and 1-parameter model (dark gray dashed line)

However, a large deviation around the cross-over between predicted and experimental LVE moduli remains.
The large discrepancy between data and predictions in Figure 5.6 raises questions about the reliability of the GPC results. We remark the fact

that we solved for the viscoelastic response by discretizing GPC results, hence no artifacts due to ill-posed problems arise. The measured LVE spectra of both samples indicate a much faster relaxation compared to the predictions, suggesting that the high molecular weight tail of the MWD curves might be questionable. To exclude such a part of the curve, we fitted both GPC results with a GEX function. The results of the fitting procedure are reported in Figure 5.7.

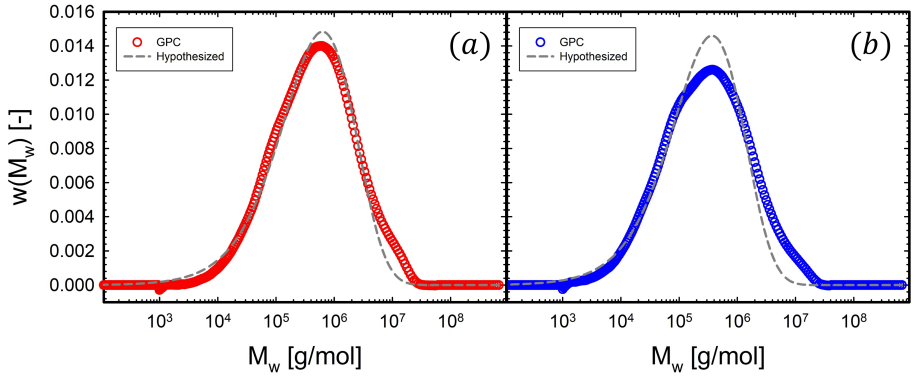

Figure 5.7. Hypothesized distributions for UHMWPPr and RIL202PP

The GEX fit excludes the high molecular weight tail of the distribution for both samples. By inverting the distributions reported in Figure 5.7 in dark gray dashed lines, we obtain the results of Figure 5.8.

The agreement between the model and the measured rheological behavior in Figure 5.8 indicates that the shoulder of the distribution is most likely a GPC artifact.

Effect of M^*

The use of the time-dependent diffusion double reptation model to estimate F_{sr} requires the values of the parameters k_{tdd} and M^*, which depend on the longest relaxation time and contour length fluctuations, respectively. By optimizing the mixing rule in Equation 2.49 for UHMWiPPs with narrow and broad dispersity, we found that the value of k_{tdd} does not change whereas M^* needs to be reduced. This discrepancy is related the effect of polydispersity on the contour length fluctuations.

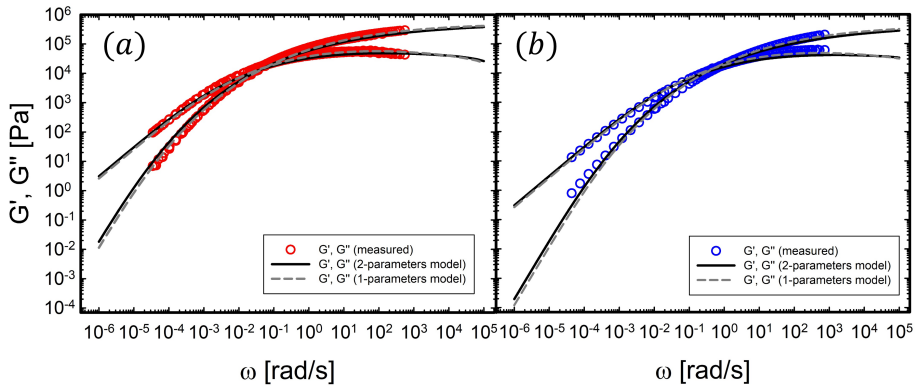

Figure 5.8. Comparison betwwen the measured dynamic moduli and the response obtained by hypothesizing different MWD for UHMWPPr and RIL202PP

The optimization of M^* for the broad polypropylene is reported in Figure 5.9.

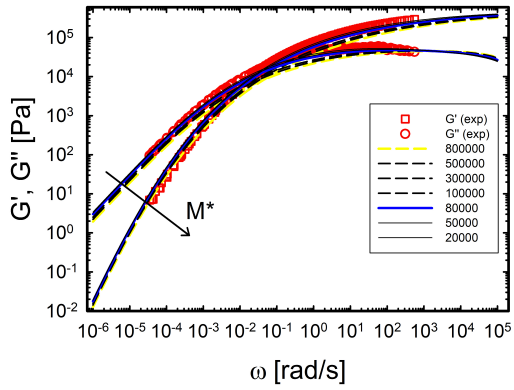

Figure 5.9. Comparison between experimental rheology of UHMWPPr (red symbols) and theoretical response (lines). The plot is parametric in M^*.

Decreasing the value of M^* from $8 \cdot 10^5$ to $8 \cdot 10^4$, the experimental and theoretical G' and G'' are matched. The plot also demonstrates that variations of M^* within the same order of magnitude are negligible.

If we use the best M^* found for broad polypropylenes to model the rheological response of the narrow ones, the agreement reported in the main text in Figure 5.3 is lost, as reported in Figure 5.10.

5.3.4 Inverse Problem

We have demonstrated how to optimize the material parameters for PP in order to establish the link between rheological properties and MWD, and highlighted possible artifacts from GPC measurements. In both cases, we employed the mixing rule in the direct way, that is, we calculated the rheological quantities from the MWD. On the other hand, practical problems deal with the inverse situation: the viscoelastic properties are measured with the aim of inferring the unknown MWD. As mentioned above, this task implies the solution of an ill-posed problem. In this section, we analyze this possibility for the commercial UHMWPPs, addressing drawbacks and caveats associated with the inverse routine.

GEX approach

To solve the inverse problem, the functional form of the unknown MWD must be hypothesized. We fixed the functional form of $w(M)$ to a generalized exponential function (GEX, see Equation 3.7).
Another problem related to the inversion of Equation 2.49 is the choice of the starting values of the parameters of the GEX function, namely a, b, and M_0. Depending on the initial values, the algorithm may converge to different stable solutions. We underline that the aim of this work is not to investigate the stability of Equation 2.49 but to provide a method to find the most likely MWD. To this end, the choice of the starting values in this work is based on empirical correlations from rheology. In particular, we used the empirical scaling law (see Equation 5.2) reported in [156] to extimate an average molecular weight from the zero shear viscosity, whereas Equation 5.3 reported in [154, 157, 158, 159] was used to estimate the polidispersity index from the value of the crossover modulus, G_{cross}:

$$\log \eta_s^0 = -15.2 + 3.47 \cdot \log M_w \tag{5.2}$$

$$PDI = \frac{10^5}{G_{cross}} \tag{5.3}$$

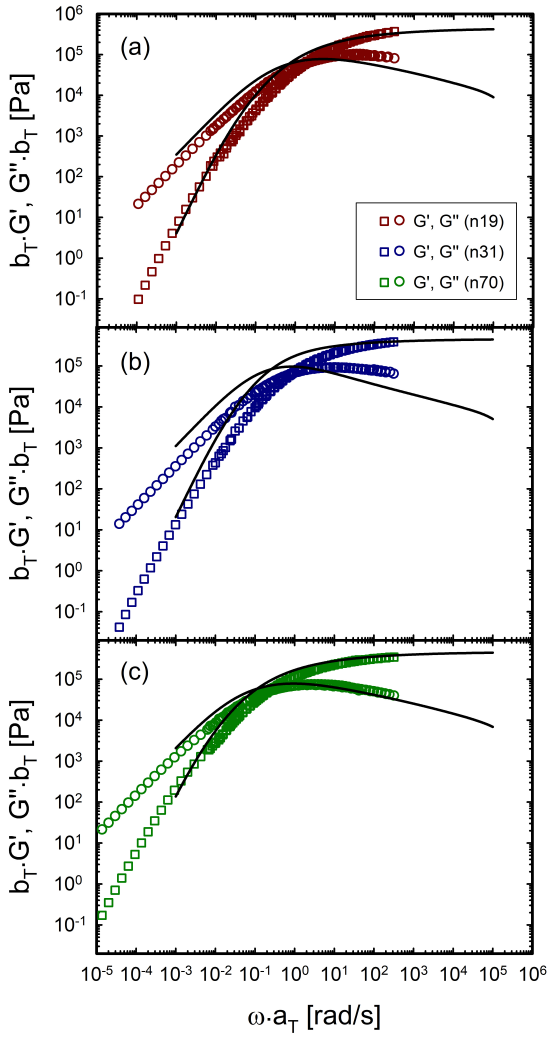

Figure 5.10. comparison between the measured linear rheology and the solution of the direct problem of the mixing rule with 2 parameters approach by using the material parameters for UHMWPPr and RIL202PP for n19 (a), n31 (b) and n70 (c)

Once M_w and PDI are known, M_n is also determined. The relations between the GEX-parameters, M_n and M_w are reported below [17, 18, 160]:

$$M_n = M_0\Gamma\left(\frac{a+1}{b}\right)/\Gamma\left(\frac{a}{b}\right) \tag{5.4}$$

$$M_w = M_0\Gamma\left(\frac{a+2}{b}\right)/\Gamma\left(\frac{a+1}{b}\right) \tag{5.5}$$

Based on Equation 5.4 and 5.5, we fixed the starting values to invert the integral in Equation 2.49, by considering $M_0 \approx M_n$. The evaluation of GEX-parameters is based on the objective function to minimize χ^2 defined in Equation 3.9.
Figure 5.11 shows the comparison between the experimental and calculated LVE and GPC data. We used both *two parameters approach* and *one parameter approach* for the kernel function.

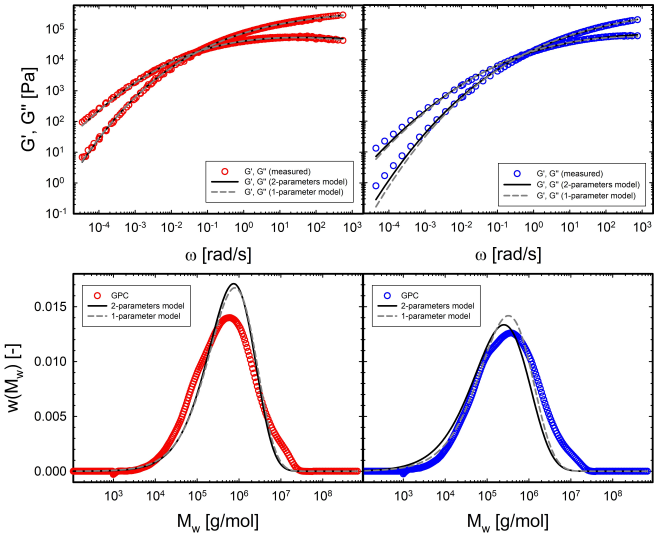

Figure 5.11. Inverse problem for UHMWPPr (red symbols) and RIL202PP (blue symbols) with 2-parameters model (solid black line) and 1-parameter model (dashed dark gray line)

The agreement between the experimental GPC and the calculated one is satisfactory, albeit worse with respect to the direct problem where the

GEX parameters were evaluated by direct fitting of the experimental GPC curve. This gives confidence in using the inverse approach with the estimated material parameters for PP in order to evaluate the MWD of UHMW commercial samples with high polydispersity.

Tikhonov regularization

In this paragraph, we examine an alternative mathematical method to evaluate the MWD from linear rheological behavior without any assumption about the functional form of the GPC curve. This method is based on the *Tikhonov regularization*. The mathematical details of the method are reported in Chapter 3. The material parameters used for applying Tikhonov regularization are the same as those estimated in the previous section. The results of the inversion from rheology to MWD are reported in Figure 5.12.

The results are very similar, irrespective of the type of kernel function used. It is clear that, although no hyphothesis on the functional form of the MWD is needed, this methodology does not guarantee reliable results like the GEX approach. Furthermore, the MWD of both samples features a low M_w cut-off. This issue can be also appreciated in [91] and can be associated to a mere machine accuracy issue.

5.4 Conclusions

The aim of this work was to evaluate the molecular weight distribution of ultra-high molecular weight polypropylene samples from rheology. A first challenge associated with this task was to estimate the values of the material parameters needed to implement a mixing rule based on the relaxation modulus. To this end, we tested three nearly monodisperse lab-made

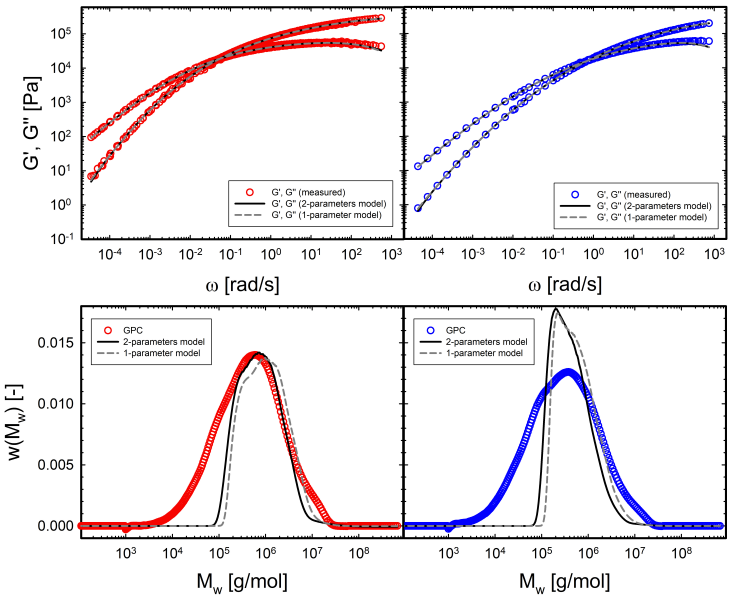

Figure 5.12. From rheology to MWD by using the Tikhonov regularization method for UHMPPr (red symbols) and RIL202PP (blue symbols)

UHMWPP samples with a well-known MWD from GPC. Once the values of the parameters were established, we demonstrated the applicability of the proposed methodology to UHMWiPPs with broad polydispersity. Our work supports the reliability of the rheological method to extract the MWD of UHMWiPPs, and provides a robust estimate of the values of the material parameters reported in the two used approaches to implement the mixing rule. Another results is the evaluation of the entanglement relaxation time (τ_e) for isotactic polypropylene which experimentally unattainable due to the occurrence of crystallization at higher temperatures (140 °C). From an experimental standpoint, we also demonstrated the possibility to adopt a time-temperature-concentration superposition approach for UHMWPP, where experimental issues limit the frequency range of the mastercurves of the melt. Finally, the results suggest that rheology can be used as a tool to detect possible experimental artefacts of MWD obtained via GPC.

Chapter 6

Conclusions and Outlook

This thesis work was motivated by the necessity to control the macroscopic properties of ultrahigh molecular weight polyolefins, which highly depend on molecular weight and polydispersity. In the last few decades, rheology has emerged as a powerful tool to evaluate the MWD of polymeric systems, as it can link the macroscopic viscoelastic response of polymer systems to the molecular architecture. Furthermore, it is particularly sensitive to the presence of long chains with high molecular weights. This represents an advantage over standard techniques such as gel permeation chromatography to evaluate the molecular weight distribution.
The study of macromolecular dynamics is often based on model systems, with reduced polydispersity and relatively low molecular weight. This makes the work of experimentalists relatively easy. On the other hand, industry is interested in polymer melts with broad molecular weight distributions and complex structures, which are hard to handle because of their large viscosity and elasticity. A valid alternative to circumvent the above difficulties is to work with concentrated polymer solutions. The addition of a solvent may have several beneficial effects. It serves as a plasticizer, lowering the levels of viscoelasticity, speeding up the dynamics and avoiding or delaying elastic instabilities. Furthermore, it allows working at lower temperatures, thus minimizing thermal degradation. A polymer solution would also be less prone to crystallization, thus allowing for a wider temperature range of viscoelastic characterization.
The rheological characterization of polymer solutions instead of melts has

many advantages. However, the choice of appropriate solvents can be problematic because, as reported in literature, most polyolefin solvents are toxic, flammable, and difficult to handle [28]. In recent years, the correlation between melts and solutions has been studied by dissolving a pure melt in oligomers of the same chemical nature. In particular, in [161, 162, 163, 64] polystyrenes with different molecular weights are dissolved in oligo-styrenes with molecular weights lower than the molecular weight between entanglements.

The use of an oligomeric solvent represents an advantage. Indeed, it avoids the use of organic solvents which may evaporate leading to thermal stability problems during long-time measurements. In this work, polyolefin-based materials such as ultra high molecular weight polyethylene and polypropylene with a broad macromolecular dispersity have been used. All samples were kindly provided by Dutch Polymer Institute partners such as Sabic, Reliance, Borealis and the University of Munich. Depending on the chemical nature, the corresponding oligomer was used as a solvent. Due to the same chemical nature it represents a θ-solvent for the pure melt within the temperature range in which the system can be investigated. Once the solutions have been characterized, it is necessary to select an appropriate rheological model in order to describe the relaxation dynamics of the system. Polymer architecture determines the model to use. Chapter 4 presents the procedure used to characterize from a rheological point of view UHMWPE kindly provided by Sabic. Specifically, pure melt was dissolved in an oligoethylene at different concentrations. By measuring the linear viscoelastic properties of the solutions, the rheological response of pure melt can be extrapolated by applying the time-Termperature-concentration superposition. At this point, a molecular model was used to extrapolate the distribution function of molecular weights. The function was, then, compared with the GPC measurement. The results confirmed the GPC measurements provided by the company, validating our rheological approach to obtain the MWD of UHMW polymers

Because of the high viscoelasticity of polyethylene, a comparison between direct measurement on the melt and the extrapolated behavior from solutions is not possible in the frequency range from the elastic plateau modulus down to the terminal regime. Due to the lower viscoelasticity, Polypropylene can be used for this purpose, as it is possible to measure

the pure melt. Consequently, a comparison between the linear viscoelastic response of the pure melt with that obtained by extrapolation is possible. In Chapter 5, the methodology used for polyethylenes was applied to two industrial polypropylenes kindly supplied by Reliance. The aim of the work is to rheologically verify the consistency of the molecular weight distributions obtained via GPC. In order to apply the rheological models which link the rheological behavior to the molecular weight distribution, the knowledge of some constants linked to the chemical nature of the polymer is necessary. Conversely to UHMWPE, ultra high molecular weight polypropylene received less attention from a scientific point of view. For example, the material parameters of PP were not available in literature. Therefore, three UHMW-iPPs provided by the University of Munich were used to evaluate the constants for the models related to polypropylene. Then, the approach proposed for PE, was successfully applied to PP. This confirmed that the proposed approach is a valid route to obtain the MWD of UHMW polymers.

However, it is important to emphasize that the models used can be applied only to polymers with linear architecture and a wide relaxation spectrum is needed. As reported in the previous chapters, linear viscoelastic properties are very sensitive to micro-structural details of a polymer system. The investigation requires the description of a wide relaxation spectrum, which covers the relaxation of the longest chain in the low frequencies domain to the local phenomena in the high frequencies domain. From an experimental point of view, the typical approach is the time-temperature superposition to obtain a relaxation spectrum in widest time-domain. However, the occurring of crystallization hinders information in the high frequencies range and alternative methods are required to extend the range. In this work, we extended the frequencies domain by applying the time-concentration superposition. The applicability of such methods can be limited in some cases as reported in Chapter 4. In order to extend the frequency range from the tTs, other techniques have been proposed in literature. The use of torsional resonators, diffusive wave spectroscopy (DWS), and Brillouin light scattering lead to investigate the shear rheology in the frequency range of GHz [164, 165, 166, 167]. Another approach is the use of a piezo-rheometer which allows to investigate the shear properties in the frequency range up to kHz [164, 168, 167].

While the original reptation theory was devised for linear chains only, it was later proven that more complex structures relax in peculiar ways. For example, reptation in star polymers is hindered, and they can only relax via arm retraction [169]. As a more general result, the linear viscoelastic response of linear polymers is markedly different from that of branched-like architectures [170]. The rheological response, therefore, can be seen as a fingerprint of the molecular architecture. Besides the more "exotic" star architecture, the family of branched systems involves many other topologies. Comb polymers, for example, are made of linear chains with loosely-grafted short branches. Their viscoelastic response is characterized by two main relaxation modes, due to branch withdrawal and backbone relaxation, respectively [171, 172]. The rheological fingerprint of other complex architectures such as bottlebrush, wedge and dendronized polymers is the absence of an entanglement plateau in the intermediate frequency range, and the onset of a low-frequency elastic plateau of the order of $1kPa$ [173, 174, 175, 176, 177].
More complex dynamics, especially related to branched architectures, were not examined in the previous chapters. In this case, the relaxation dynamics involves the backbone and the arms via a hierarchical mechanism. On short time scales (or high frequencies) the arms relax via CLF. Subsequently, the central backbone relaxes via retraction of the arms and reptation on longer time scales (or low frequencies). This mechanism leads to an increase in the longer relaxation time compared to the linear counterpart. In Chapter 5, it is emphasized how the presence of few arms can affect the rheological response compared to a linear architecture.
The presence of arms has a large effect on the viscosity. In particular, above the molecular weight between entanglements, it can be observed experimentally that increasing the molecular weight, viscosity follows an exponential dependence on the molecular weight, losing the typical power-law dependence. Figure 6.1 shows that the higher molecular weight of the arms the larger effect on the deviation from linear behavior occurs.

As reported in the previous chapter, rheology is very sensitive to different types of branching. Figure 6.2 shows the linear viscoelastic responses of different architectures.

From an industrial point of view, however, a branched system is characterized by a variety of branched structures with a specific distribution.

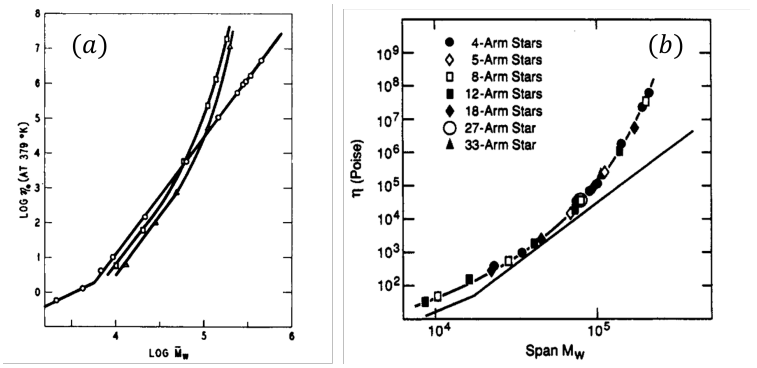

Figure 6.1. Scaling of the zero-shear viscosity with the molecular weight of a star system (a) [178] and the molecular weight of an arm (b) [179]

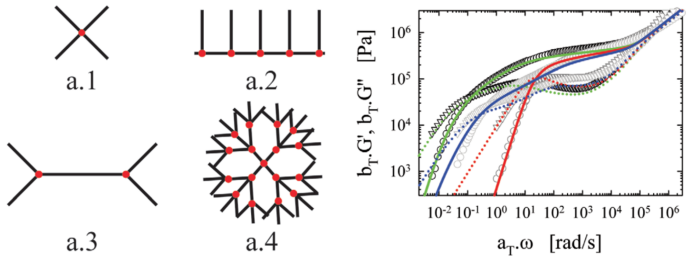

Figure 6.2. Rheological fingerprint of different macromolecular architectures [180]

The presence of a distribution of architectures makes the macromolecular characterization more complicated. In addition, depending on the mode of synthesis, operating conditions, reactor used, a variety of products with different characteristics can be obtained. The variety of products can also differ among the batches. From a rheological point of view, on the other hand, the presence of a branching distribution leads to a broader molecular weight distribution. Consequently, the effect of branching on the rheological response can be hindered by the polydispersity effect.
From a modeling point of view, a starting point can be the model proposed by *Milner and McLeish* [181]. In this case, the description of molecular dynamics can be unified for branching and linear chains, considering the latter as 2-arms star. Based on energetic considerations, *van Ruymbeke* proposed a different approach of solving the mixing rule that included all relaxation mechanisms [182, 183]. The resolution of the problem was based on the so-called *"Time Marching Algorithm" (TMA)*. The advantage of TMA is represented by the possibility to treat all relaxation mechanisms simultaneously without separating time scales. The proposed mixing rule is reported in Equation 6.1:

$$G(t) = G_N^0 \left(\sum_i \varphi_i \int_0^1 \left(p_{rept}(x_i, t)\ p_{CLF}\ (x_i, t)\ p_{CR}\ (x_i, t) \right) dx_i \right) \quad (6.1)$$

where $p(x_i, t)$ is the survival probability of a molecular segment which can relax by reptation, contour length fluctuations and constraint release. In the case of branched system, Equation 6.1 must take into account the survival probabilities of the arms to relax via CLF and CR and the backbone via reptation, CLF, CR and DTD.

The next step in the advanced rheological characterization of the MWD of polyolefins is to work on long-chain branched architectures. The method adopted for linear architectures has been tested for branched polymers with encouraging results. In this part, preliminary results on a LCB-iPP provided by Borealis are reported. In the previous chapters, the theoretical scaling laws for polymeric solutions were verified with the main rheological parameters. Since the architectures investigated are linear, the scaling laws follow power laws (linear in a log-log plot). In the case of branched

polymers, however, solution rheology could be useful to discriminate different architectures that follow predominantly exponential scaling laws.
In this perspective, Borealis provided a LCB-iPP (coded HMS) with an average molecular weight of $6.32 \cdot 10^5$ and a polydispersity of 13.7. The latter was, first, measured in the melt state and later dissolved in a 12k oligopropylene following the same procedure as reported in Chapter 3. Regarding the pure melt, the linear viscoelastic behavior was measured and the terminal regime has been reached by performing a creep test.

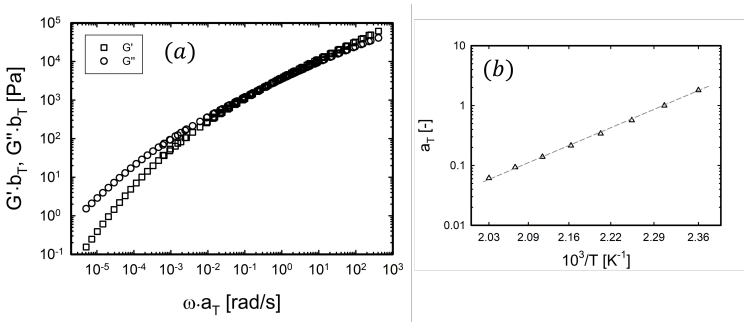

Figure 6.3. (a) Mastercurve of HMS at a reference temperature of 160 °C. (b) the horizontal shift factors used to superimpose the dynamic response at different temperatures.

The horizontal shift factors reported in Figure 6.3b were fitted with an Arrhenius-like equation. The flow activation energy estimated from the fit is $88kJ/mol$, which is consistent with the typical values reported for branched polypropylene in literature [151]. In addition, stress relaxations were performed at the lowest investigated temperature to attempt extending the viscoelastic behavior at higher frequencies.

In Figure 6.4a, the relaxation modulus is obtained for an applied strain of 15%. The reduced signal torque during the relaxtion, hinder the possibility to reach the terminal regime with a stress relaxation test. In Figure 6.4b, the stress relaxation test is useless to extend the behavior at higher frequency.
So far, we only dealt with linear rheology. However, nonlinear rheology could be a valid characterization tool for determining the degree of branching of industrial samples. In particular, branching strongly affects the extensional rheological respose of polymers.

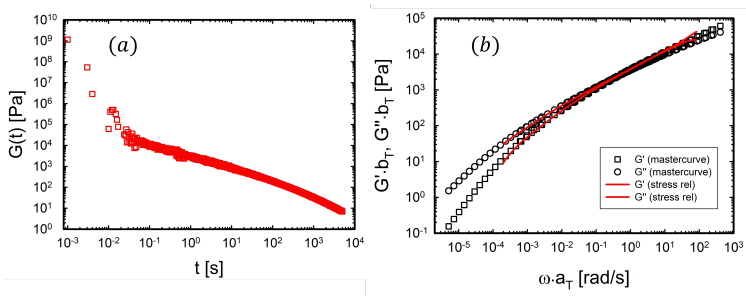

Figure 6.4. (a) Stress relaxation test at T=160 °C. (b) Comparison between the dynamic response and the moduli obtained from a stress relaxation transformation

To provide an example, once the characterization in the linear viscoelastic regime of the melt is completed, the extensional behavior was also measured. Tests were performed on an Ares rotational rheometer with Senmanat's kit. This kit allows to measure the uniaxal extensional viscosity by means of a rotational rheometer. Measurements in the extensional regime at a temperature of 150 °C are shown in Figure 6.5.

In Figure 6.5, the linear viscoelastic envelope (LVE) was obtained from the shear tests at the same temperature. From the same figure, the rheological fingerprint of branched polymers can be observed, which show the typical *Strain Hardening* phenomenon. This phenomenon can be discriminated from the *flow-induced crystallization* phenomenon by introducing the dimensionless Weissenberg number mentioned in Chapter 2. In this case, the characteristic time of the test is much less than the characteristic time of the material (the longest relaxation time, $\tau_d \approx 2.4 \cdot 10^4$). Consequently, $Wi >> 1$ implies that the phenomenon observed is related to nonlinear properties of the polymer, ruling out the flow-induced crystallization.

Following the approach reported for linear architecture discussed in Chapter 4 and 5, solutions of HMS were prepared in the concentrated regime and measured. In Figure 6.6 the mastercurves at a reference temperature of 160 °C from a concentration of 30%$_{wt}$ up to the pure melt are reported.

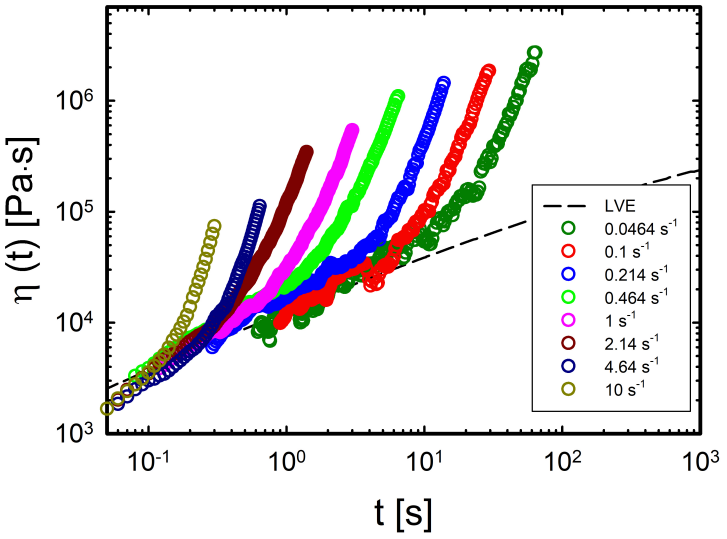

Figure 6.5. Elongational viscosity measured at 150 °C

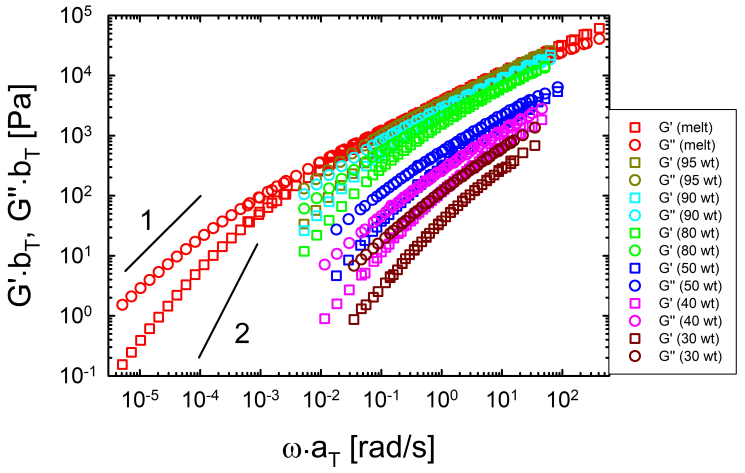

Figure 6.6. Mastercurves of the pure HMS and all prepared solutions in olygo-propylene 12k at a reference temperature of 160 °C

By applying the time-T-concentration superposition principle, the final mastercurve is obtained. From an empirical point of view, it can be observed that, by shifting horizontally and vertically the curves, they perfectly follow the behavior of the measured pure melt.

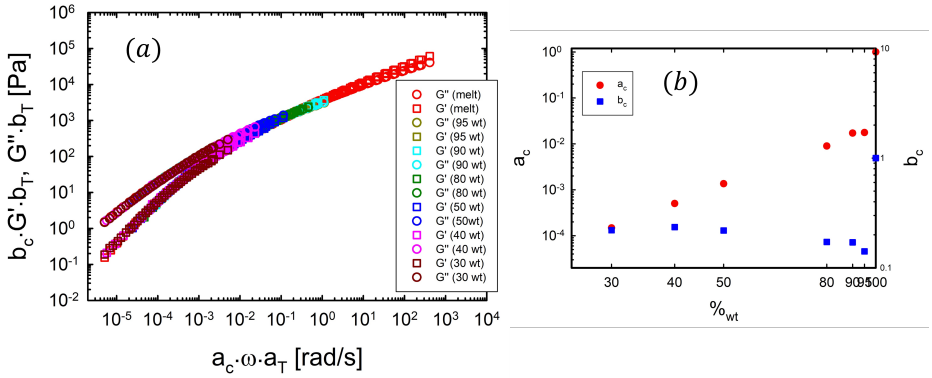

Figure 6.7. (a) Superposition of all concentrations on the pure melt. (b) Shift factors to apply the concentration superposition

Moreover, considering the shift factors obtained, the horizontal shift factors scale with an exponential with respect to the concentration. However, the "quasi-randomic" dependence of vertical shifts needs to be investigated more deeply.

Regarding the modeling, a first proposed attempt was made in collaboration with Prof. van Ruymbeke. The followed approach was proposed in [184]. The goal is to determine a possible composition of branched structures in the system. To this aim, the knowledge of MWD obtained via GPC is necessary. The problem can be simplified by decomposing the starting MWD as a sum of *n-lognormal distributions*. Following this approach, the problem turns out to be ill-posed, since there are infinite combinations that decompose the curve. One possible decomposition is shown in Figure 6.8.

Table 6.1 reports the properties of each log-normal distribution depicted in Figure 6.8.

The choice of the gray distribution in Table 6.1 can be rationalized

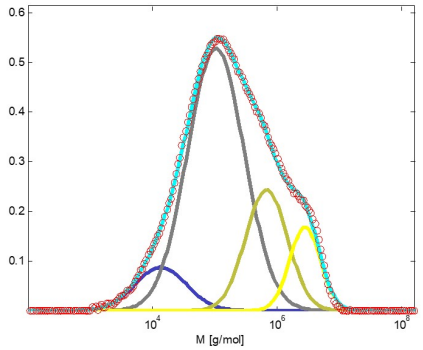

Figure 6.8. A possible decomposition of the MWD provided by the company

MWD	$Composition$ [%]	M_w [kg/mol]	PDI
blue	9	21	2.5
gray	60	185	3
dark yellow	20	920	1.8
yellow	11	3300	1.4

Table 6.1. Properties of the MWDs reported in Figure 6.8

considering that, in order to capture the sample relaxation at high frequencies, we need to hypothesize a M_w around 190 kg/mol. Each curve can be associated to a specific macromolecular architecture. The mixing rule in Equation 6.1 can be solved in a direct way for each architecture by considering the relaxation mechanisms that distinguish the different architectures. The sum of all rheological responses can be compared with the measured one. In Figure 6.9, two possible distributions of architectures in the polymer system are reported based on the assumptions of decomposition and architectures in the system.

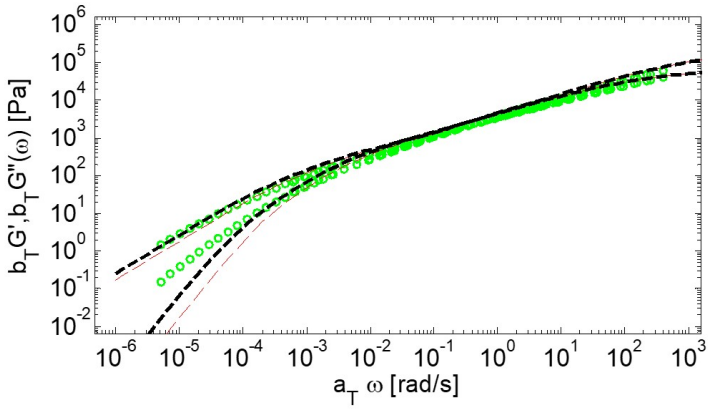

Figure 6.9. Possible architecture distributions in the system. The green symbols refer to the experimental results

The effect of branches leads to an increase in the relaxation time according to the hierarchical relaxation mechanism. Based on this, we considered architectures which retard the relaxation of the whole polymer system. The composition of possible architectures are summarized below:

- the dynamic moduli in red dashed line come from the presence of: 9 % of short linear chains (M_w=21 kg/mol), 60 % of linear chains (M_w=185 kg/mol and PDI=3) and 31 % of dangling arms (M_w=185 kg/mol and PDI=3). The resulting rheological behavior is reported with red dashed lines in Figure 6.9;

- the dynamic moduli in black dashed line come from the presence of:

9 % of short linear chains (M_w=21 kg/mol), 60 % of linear chains (M_w=185 kg/mol and PDI=3), 30.8 % of dangling arms (M_w=185 kg/mol and PDI=3) and 0.2 % of very slow relaxing molecules, stars-like with a $M_a = 1250 kg/mol$ (black dashed lines in Figure 6.9).

As mentioned above, the investigation of this sample represents only a starting point. A combination of linear and nonlinear rheology, the optimization of the algorithm and information from chemical synthesis may be useful to improve the quality of the assumptions made about decomposition and refine the rheological method to extract relevant information about the molecular distribution of branched industrial samples.

Bibliography

[1] Dorel Feldman. Polymer history. *Designed Monomers and Polymers*, 11(1):1–15, 2008.

[2] Polyethylene and polypropylene production capacity worldwide from 2017 to 2023 (in million metric tons). https://www.statista.com/statistics/1118115/global-polyethylene-polypropylene-capacity/. Accessed: 10-01-2023.

[3] Best Available Technologies for Production of Polymers. https://eippcb.jrc.ec.europa.eu/reference/production-polymers, 2007.

[4] Access ropes. https://www.accessropes.com/product-category/uhmwpe-rope/. Accessed: 16-01-2023.

[5] Dario Nichetti and Ica Manas-Zloczower. Viscosity model for polydisperse polymer melts. *Journal of rheology*, 42(4):951–969, 1998.

[6] Chenyang Liu, Jiasong He, Evelyne Van Ruymbeke, Roland Keunings, and Christian Bailly. Evaluation of different methods for the determination of the plateau modulus and the entanglement molecular weight. *Polymer*, 47(13):4461–4479, 2006.

[7] John M. Dealy, Daniel J. Read, and Ronald G. Larson. *Structure and rheology of molten polymers: from structure to flow behavior and back again*. Carl Hanser Verlag GmbH Co KG, 2018.

[8] W.R. Moore. Viscosities of dilute polymer solutions. *Progress in polymer science*, 1:1–43, 1967.

[9] Piero Manaresi, Andrea Munari, Francesco Pilati, and Elisabetta Marianucci. A general intrinsic viscosity-molecular weights relationship for polydisperse polymers. *European polymer journal*, 24(6):575–578, 1988.

[10] B.A. Whitehouse. Gel permeation chromatograph calbration. intrinsic viscosity-polydispersity effect. *Macromolecules*, 4(4):463–466, 1971.

[11] Markus Gahleitner. Melt rheology of polyolefins. *Progress in polymer science*, 26(6):895–944, 2001.

[12] William H. Tuminello. Determining molecular weight distributions from rheological properties of polymer melts. *Rheology Bulletin*, 69(2), 2000.

[13] Stefan Trinkle and Christian Friedrich. Van gurp-palmen-plot: a way to characterize polydispersity of linear polymers. *Rheologica Acta*, 40(4):322–328, Jul 2001.

[14] William H. Tuminello. Molecular weight and molecular weight distribution from dynamic measurements of polymer melts. *Polymer Engineering & Science*, 26(19):1339–1347, 1986.

[15] Maria Rossella Nobile and Franco Cocchini. Evaluation of molecular weight distribution from dynamic moduli. *Rheologica acta*, 40(2):111–119, 2001.

[16] Saeid Talebi, Rob Duchateau, Sanjay Rastogi, Joachim Kaschta, Gerrit W. M. Peters, and Piet J. Lemstra. Molar mass and molecular weight distribution determination of uhmwpe synthesized using a living homogeneous catalyst. *Macromolecules*, 43(6):2780–2788, 2010.

[17] Evelyne Van Ruymbeke, Roland Keunings, and Christian Bailly. Determination of the molecular weight distribution of entangled linear polymers from linear viscoelasticity data. *Journal of non-newtonian fluid mechanics*, 105(2-3):153–175, 2002.

[18] Evelyne Van Ruymbeke, Roland Keunings, Vincent Stéphenne, A. Hagenaars, and Christian Bailly. Evaluation of reptation models for predicting the linear viscoelastic properties of entangled linear polymers. *Macromolecules*, 35(7):2689–2699, 2002.

[19] Xiangnan Ye and Tam Sridhar. Effects of the polydispersity on rheological properties of entangled polystyrene solutions. *Macromolecules*, 38(8):3442–3449, 2005.

[20] Bruce H. Bersted and J. D. Slee. A relationship between steady-state shear melt viscosity and molecular weight distribution in polystyrene. *Journal of Applied Polymer Science*, 21(10):2631–2644, 1977.

[21] Alexander Ya. Malkin and Albert E. Teishev. Flow curve–molecular weight distribution: Is the solution of the inverse problem possible? *Polymer Engineering & Science*, 31(22):1590–1596, 1991.

[22] Yongming Liu, Montgomery T. Shaw, and William H. Tuminello. Obtaining molecular-weight distribution information from the viscosity data of linear polymer melts. *Journal of Rheology*, 42(3):453–476, 1998.

[23] John D. Ferry. *Viscoelastic properties of polymers*. John Wiley & Sons, 1980.

[24] Sanjay Rastogi, Lada Kurelec, Juul Cuijpers, Dirk Lippits, Markus Wimmer, and Piet J Lemstra. Disentangled state in polymer melts; a route to ultimate physical and mechanical properties. *Macromolecular Materials and Engineering*, 288(12):964–970, 2003.

[25] Anurag Pandey, Yohan Champouret, and Sanjay Rastogi. Heterogeneity in the distribution of entanglement density during polymerization in disentangled ultrahigh molecular weight polyethylene. *Macromolecules*, 44(12):4952–4960, 2011.

[26] Paul Smith and Piet J. Lemstra. Ultra-drawing of high molecular weight polyethylene cast from solution. *Colloid and Polymer Science*, 258(7):891–894, 1980.

[27] Paul Smith, Piet J. Lemstra, and Henk C. Booij. Ultradrawing of high-molecular-weight polyethylene cast from solution. ii. influence of initial polymer concentration. *Journal of Polymer Science: Polymer Physics Edition*, 19(5):877–888, 1981.

[28] Cornelis W. M. Bastiaansen and Joseph A.P.M. . Solution of ultra-high molecular weight polyethylene, 1995.

[29] André Brem, Olivier Lhost, and Theo A. Tervoort. Influence of solvent quality and crystallization conditions on the drawability of ultra-high molecular weight polyethylene cast from solution. *Macromolecules*, 53(14):5957–5970, 2020.

[30] Magnus Kristiansen, Theo A. Tervoort, and Paul Smith. Synergistic gelation of solutions of isotactic polypropylene and bis-(3, 4-dimethyl benzylidene) sorbitol and its use in gel-processing. *Polymer*, 44(19):5885–5891, 2003.

[31] Theo A. Tervoort, Jeroen Visjager, and Paul Smith. On abrasive wear of polyethylene. *Macromolecules*, 35(22):8467–8471, 2002.

[32] Sameer R. Paital and Narendra B. Dahotre. Review of laser based biomimetic and bioactive ca–p coatings. *Materials Science and Technology*, 24(9):1144–1161, 2008.

[33] Steven M. Kurtz. *UHMWPE biomaterials handbook: ultra high molecular weight polyethylene in total joint replacement and medical devices*. Academic Press, 2009.

[34] Eugene C. Bingham. Rheology. i. the nature of fluid flow. *Journal of chemical education*, 6(6):1113, 1929.

[35] Eugene C. Bingham. Rheology. ii. the nature of plastic flow and its relation to fluid flow. *Journal of Chemical Education*, 6(8):1206, 1929.

[36] Isaac Newton. *Philosophiae naturalis principia mathematica*. W. Dawson, 1687.

[37] Robert J. Hooke. *De potentia restitutuva, Or of Spring Explaining the Power of Springing Bodies*. John Martyn Printer to the Royal Society, London, 1678.

[38] Thomson William. On the elasticity and viscosity of metals. *Proceedings of the Royal Society of London*, 142:289–297, 1865.

[39] Maxwell James Clerk. Iv. on the dynamical theory of gases. *Philosophical Transactions of the Royal Society*, 157:49–88, 1867.

[40] Josef Honerkamp and Jürgen Weese. Determination of the relaxation spectrum by a regularization method. *Macromolecules*, 22(11):4372–4377, 1989.

[41] F.R. Schwarzl. Numerical calculation of storage and loss modulus from stress relaxation data for linear viscoelastic materials. *Rheologica Acta*, 10(2):165–173, 1971.

[42] K.H. Meyer, G. Susich, and E. Valko. Die elastischen eigenschaften der organischen hochpolymeren und ihre kinetische deutung. *Kolloid-Zeitschrift*, 59(2):208–216, 1932.

[43] Albert Einstein. Zur theorie der brownschen bewegung. *Annalen der physik*, 324(2):371–381, 1906.

[44] Marian Smoluchowski. The kinetic theory of brownian molecular motion and suspensions. *Annalen der Physik*, 21:756–780, 1906.

[45] Eugen Guth and Hermann Mark. Zur innermolekularen, statistik, insbesondere bei kettenmolekiilen i. *Monatshefte für Chemie und verwandte Teile anderer Wissenschaften*, 65(1):93–121, 1934.

[46] Werner Kuhn. Über die gestalt fadenförmiger moleküle in lösungen. *Kolloid-Zeitschrift*, 68(1):2–15, 1934.

[47] Melvin Mooney. A theory of large elastic deformation. *Journal of applied physics*, 11(9):582–592, 1940.

[48] Leslie Ronald George Treolar. *The Physics of Rubber Elasticity*. Clarendon Press, 1949.

[49] Prince E. Rouse Jr. A theory of the linear viscoelastic properties of dilute solutions of coiling polymers. *The Journal of Chemical Physics*, 21(7):1272–1280, 1953.

[50] Bruno H. Zimm. Dynamics of polymer molecules in dilute solution: viscoelasticity, flow birefringence and dielectric loss. *The journal of chemical physics*, 24(2):269–278, 1956.

[51] Pierre-Gilles de Gennes. Reptation of a polymer chain in the presence of fixed obstacles. *The Journal of Chemical Physics*, 55(2):572–579, 1971.

[52] Masao Doi and Samuel F. Edwards. Dynamics of concentrated polymer systems. part 1.—brownian motion in the equilibrium state. *Journal of the Chemical Society, Faraday Transactions 2*, 74:1789–1801, 1978.

[53] Masao Doi and Samuel F. Edwards. Dynamics of concentrated polymer systems. part 2.—molecular motion under flow. *J. Chem. Soc., Faraday Trans. 2*, 74:1802–1817, 1978.

[54] Masao Doi and Samuel F. Edwards. Dynamics of concentrated polymer systems. part 3.—the constitutive equation. *Journal of the Chemical Society, Faraday Transactions 2*, 74:1818–1832, 1978.

[55] Michael Rubinstein and Ralph H. Colby. *Polymer physics*, volume 23. Oxford university press New York, 2003.

[56] A.E. Likhtman. 1.06 - viscoelasticity and molecular rheology. In Krzysztof Matyjaszewski and Martin Möller, editors, *Polymer Science: A Comprehensive Reference*, pages 133–179. Elsevier, Amsterdam, 2012.

[57] Samuel F. Edwards. The statistical mechanics of polymerized material. *Proceedings of the Physical Society (1958-1967)*, 92(1):9, 1967.

[58] Samuel F. Edwards. Statistical mechanics with topological constraints: I. *Proceedings of the Physical Society (1958-1967)*, 91(3):513, 1967.

[59] Masao Doi and Samuel F. Edwards. *The theory of polymer dynamics*, volume 73. oxford university press, 1988.

[60] Evelyne Van Ruymbeke, Chen-Yang Liu, and Christian Bailly. Quantitative tube model predictions for the linear viscoelasticity of linear polymers. *Rheology Reviews*, 39:53–134, 2007.

[61] William W. Graessley. Some phenomenological consequences of the doi–edwards theory of viscoelasticity. *Journal of Polymer Science: Polymer Physics Edition*, 18(1):27–34, 1980.

[62] R.G. Larson, Tamarapu Sridhar, L.G. Leal, Gareth Huw McKinley, A.E. Likhtman, and T.C.B. McLeish. Definitions of entanglement spacing and time constants in the tube model. *Journal of Rheology*, 47(3):809–818, 2003.

[63] William W. Graessley. Polymer chain dimensions and the dependence of viscoelastic properties on concentration, molecular weight and solvent power. *Polymer*, 21(3):258–262, 1980.

[64] Alexis André, Taisir Shahid, Filip Oosterlinck, Christian Clasen, and Evelyne Van Ruymbeke. Investigating the transition between polymer melts and solutions in nonlinear elongational flow. *Macromolecules*, 54(6):2797–2810, 2021.

[65] William H. Tuminello, T.A. Treat, and A.D. English. Poly (tetrafluoroethylene): molecular weight distributions and chain stiffness. *Macromolecules*, 21(8):2606–2610, 1988.

[66] DW Mead. Determination of molecular weight distributions of linear flexible polymers from linear viscoelastic material functions. *Journal of Rheology*, 38(6):1797–1827, 1994.

[67] Frederic Leonardi, Jean-Charles Majeste, Ahmed Allal, and Gerard Marin. Rheological models based on the double reptation mixing rule: the effects of a polydisperse environment. *Journal of Rheology*, 44(4):675–692, 2000.

[68] Maria Rossella Nobile and Franco Cocchini. A generalized relation between mwd and relaxation time spectrum. *Rheologica acta*, 47:509–519, 2008.

[69] Masao Doi. Explanation for the 3.4-power law for viscosity of polymeric liquids on the basis of the tube model. *Journal of Polymer Science: Polymer Physics Edition*, 21(5):667–684, 1983.

[70] S.H. Wasserman and W.W. Graessley. Effects of polydispersity on linear viscoelasticity in entangled polymer melts. *Journal of Rheology*, 36(4):543–572, 1992.

[71] D. Maier, A. Eckstein, C. Friedrich, and J. Honerkamp. Evaluation of models combining rheological data with the molecular weight distribution. *Journal of Rheology*, 42(5):1153–1173, 1998.

[72] Christos Tsenoglou. Molecular weight polydispersity effects on the viscoelasticity of entangled linear polymers. *Macromolecules*, 24(8):1762–1767, 1991.

[73] Wolfgang Thimm, Christian Friedrich, Michael Marth, and Josef Honerkamp. An analytical relation between relaxation time spectrum and molecular weight distribution. *Journal of Rheology*, 43(6):1663–1672, 1999.

[74] J. Des Cloizeaux. Relaxation of entangled polymers in melts. *Macromolecules*, 23(17):3992–4006, 1990.

[75] M. Baumgaertel, A. Schausberger, and H.H. Winter. The relaxation of polymers with linear flexible chains of uniform length. *Rheologica Acta*, 29(5):400–408, 1990.

[76] Christian Carrot and Jacques Guillet. From dynamic moduli to molecular weight distribution: A study of various polydisperse linear polymers. *Journal of Rheology*, 41(5):1203–1220, 1997.

[77] Cattaleeya Pattamaprom, Ronald G. Larson, and Anuvat Sirivat. Determining polymer molecular weight distributions from rheological properties using the dual-constraint model. *Rheologica acta*, 47:689–700, 2008.

[78] Johannes Brandrup, Edmund H. Immergut, Eric A. Grulke, Akihiro Abe, and Daniel R. Bloch. *Polymer handbook*, volume 89. Wiley New York, 1999.

[79] A.K. Dordinejad, F. Sharif, M. Ebrahimi, and R. Rashedi. Time-sweep rheometry for evaluating polyethylene degradation behavior: Effect of formulation and process conditions. *Polymer Testing*, 70:39–46, 2018.

[80] Virendrakumar Gupta, Saurabh Singh, Jomichan Joseph, Kamlesh J Singala, and Bhavesh K Desai. Attrition resistant catalyst system for manufacture of polyolefins, March 28 2017. US Patent 9,605,089.

[81] Alexander Schöbel, Eberhardt Herdtweck, Matthew Parkinson, and Bernhard Rieger. Ultra-rigid metallocenes for highly iso-and regiospecific polymerization of propene: The search for the perfect polypropylene helix. *Chemistry–A European Journal*, 18(14):4174–4178, 2012.

[82] Lucas Stieglitz, Tim M Lenz, Andreas Saurwein, and Bernhard Rieger. Perfectly isotactic polypropylene upon in situ activation of ultrarigid meso hafnocenes. *Angewandte Chemie International Edition*, 61(46):e202210797, 2022.

[83] Baudilio Coto, José María Escola, Inmaculada Suárez, and M Joaquina Caballero. Determination of dn/dc values for ethylene–propylene copolymers. *Polymer testing*, 26(5):568–575, 2007.

[84] Raphael Schaller, Kirill Feldman, Paul Smith, and Theo A. Tervoort. High-performance polyethylene fibers "al dente": improved gel-spinning of ultra-high molecular weight polyethylene using vegetable oils. *Macromolecules*, 48(24):8877–8884, 2015.

[85] Savvas G. Hatzikiriakos. Wall slip of molten polymers. *Progress in Polymer Science*, 37(4):624–643, 2012. Topical Issue on Polymer Physics.

[86] Mahmoud Ansari, Yong W. Inn, Ashish M. Sukhadia, Paul J. DesLauriers, and Savvas G. Hatzikiriakos. Wall slip of hdpes: Molecular weight and molecular weight distribution effects. *Journal of Rheology*, 57(3):927–948, 2013.

[87] Mohammadali Sattari, Yongwoo Inn, and Paula M. Wood-Adams. Wall slip of bimodal polyethylene. *Macromolecules*, 55(11):4568–4577, 2022.

[88] J.F. Vega, S. Rastogi, G.W.M. Peters, and H.E.H. Meijer. Rheology and reptation of linear polymers. ultrahigh molecular weight chain dynamics in the melt. *Journal of Rheology*, 48(3):663–678, 2004.

[89] J. Des Cloizeaux. Double reptation vs. simple reptation in polymer melts. *EPL (Europhysics Letters)*, 5(5):437, 1988.

[90] J. Des Cloizeaux. Relaxation of entangled and partially entangled polymers in melts: time-dependent reptation. *Macromolecules*, 25(2):835–841, 1992.

[91] Jae Woo Park, Jinhwan Yoon, Jaehyug Cha, and Heon Sang Lee. Determination of molecular weight distribution and composition dependence of monomeric friction factors from the stress relaxation of ultrahigh molecular weight polyethylene gels. *Journal of Rheology*, 59(5):1173–1189, 2015.

[92] John A. Nelder and Roger Mead. A simplex method for function minimization. *The computer journal*, 7(4):308–313, 1965.

[93] John D'Errico. fminsearchbnd, fminsearchcon–file exchange–matlab central, 2012.

[94] John D'Errico. Bound constrained optimization using fminsearch. *Matlab R Central, available for download at http://www. mathworks. com/matlabcentral/fileexchange. Résumé*, 2012.

[95] Josef Honerkamp and Jürgen Weese. Tikhonovs regularization method for ill-posed problems. *Continuum Mechanics and Thermodynamics*, 2(1):17–30, 1990.

[96] R. Muralidhar and D. Ramkrishna. Inverse problems of agglomeration kinetics: Ii. binary clustering coefficients from self-preserving spectra. *Journal of colloid and interface science*, 131(2):503–513, 1989.

[97] Scott H. Wasserman. Calculating the molecular weight distribution from linear viscoelastic response of polymer melts. *Journal of Rheology*, 39(3):601–625, 1995.

[98] Jürgen Weese. A reliable and fast method for the solution of fredhol integral equations of the first kind based on tikhonov regularization. *Computer physics communications*, 69(1):99–111, 1992.

[99] Per Christian Hansen. Regularization tools: A matlab package for analysis and solution of discrete ill-posed problems. *Numerical algorithms*, 6(1):1–35, 1994.

[100] John M. Kelly. Ultra-high molecular weight polyethylene*. *Journal of Macromolecular Science, Part C*, 42(3):355–371, 2002.

[101] S. Li and A.H. Burstein. Ultra-high molecular weight polyethylene. the material and its use in total joint implants. *The Journal of Bone and Joint Surgery*, 76(7), 1994.

[102] Young-jun Shin, He-xin Zhang, Keun-Byoung Yoon, and Dong-ho Lee. Preparation of ultra high molecular weight polyethylene with MgCl2/TiCl4 catalysts: Effect of temperature and pressure. *Macromolecular Research*, 18(10):951–955, Oct 2010.

[103] R.S. Anderssen. The pragmatics of solving industrial (real-world) inverse problems with exemplification based on the molecular weight distribution problem. *Inverse Problems*, 15(2):R1–R40, jan 1999.

[104] Christian Carrot and Jacques Guillet. From dynamic moduli to molecular weight distribution: A study of various polydisperse linear polymers. *Journal of Rheology*, 41(5):1203–1220, 1997.

[105] John M. Dealy and Donald Plazek. Time-temperature superposition-a users guide. *Rheology Bulletin*, 78:16–31, 01 2009.

[106] Ralph H Colby, Lewis J Fetters, Walter G Funk, and William W. Graessley. Effects of concentration and thermodynamic interaction on the viscoelastic properties of polymer solutions. *Macromolecules*, 24(13):3873–3882, 1991.

[107] Abdul W. Rajput, Anwar ul Aleem, Farooq A. Arain, et al. An environmentally friendly process for the preparation of uhmwpe as-spun fibres. *International Journal of Polymer Science*, 2014, 2014.

[108] Sara L. Wingstrand, Nicolas J. Alvarez, Qian Huang, and Ole Hassager. Linear and nonlinear universality in the rheology of polymer melts and solutions. *Physical review letters*, 115(7):078302, 2015.

[109] Parimal Vadhar and Thein Kyu. Effects of mixing on morphology, rheology, and mechanical properties of blends of ultra-high molecular weight polyethylene with linear low-density polyethylene. *Polymer Engineering & Science*, 27(3):202–210, 1987.

[110] H. van Laak, J. Berzen J.and Ehlers, and M. Gusik. Solution of ultra-high molecular weight polyethylene, 1997.

[111] Hongwang Shen, Lei He, Chunhua Fan, Banghu Xie, Wei Yang, and Mingbo Yang. Effective dissolution of uhmwpe in hdpe improved by high temperature melting and subsequent shear. *Polymer Engineering & Science*, 55(2):270–276, 2015.

[112] Krishnaroop Chaudhuri, Suparna Poddar, Harshawardhan Pol, Ashish Lele, Ajit Mathur, Gandham S. Srinivasa Rao, and Rakshavir Jasra. The effect of processing conditions on the rheological properties of blends of ultra high molecular weight polyethylene with high-density polyethylene. *Polymer Engineering & Science*, 59(4):821–829, 2019.

[113] Yuezhen Bin, Lin Ma, Reiko Adachi, Hiromichi Kurosu, and Masaru Matsuo. Ultra-drawing of low molecular weight polyethylene—ultra-high molecular weight polyethylene blend films prepared by gelation/crystallization from semi-dilute solutions. *Polymer*, 42(19):8125–8135, 2001.

[114] Sanjay Rastogi, Dirk R. Lippits, Gerrit W.M. Peters, Robert Graf, Yefeng Yao, and Hans W. Spiess. Heterogeneity in polymer melts from melting of polymer crystals. *Nature Materials*, 4(8):635–641, Aug 2005.

[115] Sanjay Rastogi, Dirk R. Lippits, Günther W. H. Höhne, Brahim Mezari, and Pieter C.M.M. Magusin. The role of the amorphous phase in melting of linear UHMW-PE: implications for chain dynamics. *Journal of Physics: Condensed Matter*, 19(20):205122, apr 2007.

[116] Dario Romano, Niek Tops, Efren Andablo-Reyes, Sara Ronca, and Sanjay Rastogi. Influence of polymerization conditions on melting kinetics of low entangled uhmwpe and its implications on mechanical properties. *Macromolecules*, 47(14):4750–4760, 2014.

[117] Laurence G.D. Hawke, Dario Romano, and Sanjay Rastogi. Nonequilibrium melt state of ultra-high-molecular-weight polyethylene: A theoretical approach on the equilibrium process. *Macromolecules*, 52(22):8849–8866, 2019.

[118] Lihua Shen, John Severn, and Cees W.M. Bastiaansen. Drawing behavior and mechanical properties of ultra-high molecular weight polyethylene blends with a linear polyethylene wax. *Polymer*, 153:354–361, 2018.

[119] Beth A. Miller-Chou and Jack L. Koenig. A review of polymer dissolution. *Progress in Polymer Science*, 28(8):1223–1270, 2003.

[120] Chun-Fang Zhang, Yun-Xiang Bai, Jin Gu, and Yu-Ping Sun. Crystallization kinetics of ultra high-molecular weight polyethylene in liquid paraffin during solid–liquid thermally induced phase separation process. *Journal of Applied Polymer Science*, 122(4):2442–2448, 2011.

[121] Levente Szántó, Yukang Feng, Fan Zhong, Timo Hees, Evelyne van Ruymbeke, Rolf Mülhaupt, and Christian Friedrich. Ultra-broad molecular weight distribution effects on viscoelastic properties of linear multimodal pe. *Journal of Rheology*, 63(5):773–784, 2019.

[122] Sara L. Wingstrand, Luna Imperiali, Roman Stepanyan, and Ole Hassager. Extension induced phase separation and crystallization in semidilute solutions of ultra high molecular weight polyethylene. *Polymer*, 136:215–223, 2018.

[123] André Brem. *Solutions for Fiber Spinning. The role of solvent quality in gel-spinning of ultra-high-molecular-weight polyethylene*. PhD thesis, ETH Zurich, Zurich, 2019.

[124] X. Wei, J.R. Collier, and S. Petrovan. Shear and elongational rheology of polyethylenes with different molecular characteristics. ii. elongational rheology. *Journal of Applied Polymer Science*, 104(2):1184–1194, 2007.

[125] André Brem, Olivier Lhost, and Theo A. Tervoort. Influence of solvent quality and crystallization conditions on the drawability of ultra-high molecular weight polyethylene cast from solution. *Macromolecules*, 53(14):5957–5970, 2020.

[126] Marnix Van Gurp and Jo Palmen. Time-temperature superposition for polymeric blends. *Rheology Bulletin*, 67(1):5–8, 1998.

[127] Alois Schausberger and Iris V. Ahrer. On the time-concentration superposition of the linear viscoelastic properties of plasticized polystyrene melts using the free volume concept. *Macromolecular Chemistry and Physics*, 196(7):2161–2172, 1995.

[128] Taisir Shahid, Qian Huang, Filip Oosterlinck, Christian Clasen, and Evelyne Van Ruymbeke. Dynamic dilution exponent in monodisperse entangled polymer solutions. *Soft Matter*, 13(1):269–282, 2017.

[129] Pierre-Gilles De Gennes. Brownian motions of flexible polymer chains. *Nature*, 282(5737):367–370, 1979.

[130] M. Adam and M. Delsanti. Viscosity and longest relaxation time of semi-dilute polymer solutions. i. good solvent. *Journal de Physique*, 44(10):1185–1193, 1983.

[131] Florian J. Stadler, Christian Piel, Joachim Kaschta, Sascha Rulhoff, Walter Kaminsky, and Helmut Münstedt. Dependence of the zero shear-rate viscosity and the viscosity function of linear high-density polyethylenes on the mass-average molar mass and polydispersity. *Rheologica Acta*, 45(5):755–764, 2006.

[132] Qian Huang, Olga Mednova, Henrik K. Rasmussen, Nicolas J. Alvarez, Anne L. Skov, Kristoffer Almdal, and Ole Hassager. Concentrated polymer solutions are different from melts: Role of entanglement molecular weight. *Macromolecules*, 46(12):5026–5035, 2013.

[133] Evelyne Van Ruymbeke, V Shchetnikava, Y Matsumiya, and H Watanabe. Dynamic dilution effect in binary blends of linear polymers with well-separated molecular weights. *Macromolecules*, 47(21):7653–7665, 2014.

[134] Takatoshi Yaoita, Takeharu Isaki, Yuichi Masubuchi, Hiroshi Watanabe, Giovanni Ianniruberto, Francesco Greco, and Giuseppe Marrucci. Highly entangled polymer primitive chain network simulations based on dynamic tube dilation. *The Journal of chemical physics*, 121(24):12650–12654, 2004.

[135] Hiroshi Watanabe, Satoshi Ishida, Yumi Matsumiya, and Tadashi Inoue. Viscoelastic and dielectric behavior of entangled blends of linear polyisoprenes having widely separated molecular weights: Test of tube dilation picture. *Macromolecules*, 37(5):1937–1951, 2004.

[136] Krishnaroop Chaudhuri and Ashish K. Lele. Rheological quantification of the extent of dissolution of ultrahigh molecular weight polyethylene in melt-compounded blends with high density polyethylene. *Journal of Rheology*, 64(1):1–12, 2020.

[137] Zhongde Xu, Nikolaos Hadjichristidis, L.J. Fetters, and J.W. Mays. Structure/chain-flexibility relationships of polymers. In *Physical Properties of Polymers*, pages 1–50. Springer, 1995.

[138] James E. Mark. *Physical properties of polymers handbook*, volume 1076. Springer, 2007.

[139] Kirti Garkhail Sharma. *Easily processable ultra high molecular weight polyethylene with narrow molecular weight distribution*. PhD thesis, Chemical Engineering and Chemistry, 2005.

[140] Wolfgang Radke. Polymer separations by liquid interaction chromatography: principles–prospects–limitations. *Journal of Chromatography A*, 1335:62–79, 2014.

[141] André M. Striegel, Wallace W. Yau, Joseph J. Kirkland, and Donald D. Bly. *Modern Size-Exclusion Liquid Chromatography*. John Wiley & Sons, Inc., 2009.

[142] Michael Al Samman, Wolfgang Radke, Anna Khalyavina, and Albena Lederer. Retention behavior of linear, branched, and hyperbranched polyesters in interaction liquid chromatography. *Macromolecules*, 43(7):3215–3220, 2010.

[143] E.N. Viktorova, A.A. Korolev, V.A. Orekhov, A. Yu Kanat'eva, and A.A. Kurganov. Separating ultra-high molecular weight polymers on monolithic capillary columns. *Russian Journal of Physical Chemistry A*, 87(2):308–313, 2013.

[144] Elena Uliyanchenko, Peter J. Schoenmakers, and Sjoerd Van der Wal. Fast and efficient size-based separations of polymers using ultra-high-pressure liquid chromatography. *Journal of Chromatography A*, 1218(11):1509–1518, 2011.

[145] Elena Uliyanchenko, Sjoerd van der Wal, and Peter J. Schoenmakers. Challenges in polymer analysis by liquid chromatography. *Polymer Chemistry*, 3(9):2313–2335, 2012.

[146] Saeid Talebi, Rob Duchateau, Sanjay Rastogi, Joachim Kaschta, Gerrit W.M. Peters, and Piet J. Lemstra. Molar mass and molecular weight distribution determination of uhmwpe synthesized using a living homogeneous catalyst. *Macromolecules*, 43(6):2780 – 2788, 2010.

[147] Christos Tsenoglou. Viscoelasticity of binary homopolymer blends. volume 28, pages 185–186, 08 1987.

[148] Scott T. Milner. Relating the shear-thinning curve to the molecular weight distribution in linear polymer melts. *Journal of Rheology*, 40(2):303–315, 1996.

[149] Vincenzo Ianniello, Salvatore Costanzo, Rossana Pasquino, Giovanni Ianniruberto, Enrico Troisi, Theo A Tervoort, and Nino Grizzuti. Determination of the molecular weight distribution of ultrahigh molecular weight polyethylene from solution rheology. *Journal of Rheology*, 66(5):1079–1088, 2022.

[150] Takumitsu Kida, Takeyoshi Kimura, Ayaka Eno, Khunanya Janchai, Masayuki Yamaguchi, Yasuhiko Otsuki, Tokutaro Kimura, Tomoaki Mizukawa, Tomoya Murakami, Kazuki Hato, and Tomoya Okawa. Effect of ultra-high-molecular-weight molecular chains on the morphology, crystallization, and mechanical properties of polypropylene. *Polymers*, 13(23), 2021.

[151] Bernadette Duscher and Alois Schausberger. Influence of processing on the flow properties of long-chain branched polypropylene. *Polymer Engineering & Science*, 58(9):1596–1603, 2018.

[152] Hui Niu, Yuanjie Wang, Xiaoyan Liu, Yanshai Wang, and Yang Li. Determination of plateau moduli and entanglement molecular weights of ultra-high molecular weight isotactic polypropylene synthesized by ziegler-natta catalyst. *Polymer Testing*, 60:260–265, 2017.

[153] A. Eckstein, J. Suhm, C. Friedrich, R.D. Maier, J. Sassmannshausen, M. Bochmann, and R. Mülhaupt. Determination of plateau moduli and entanglement molecular weights of isotactic, syndiotactic, and atactic polypropylenes synthesized with metallocene catalysts. *Macromolecules*, 31(4):1335–1340, 1998.

[154] Naveed Ahmad, Rocco Di Girolamo, Finizia Auriemma, Claudio De Rosa, and Nino Grizzuti. Relations between stereoregularity and melt viscoelasticity of syndiotactic polypropylene. *Macromolecules*, 46(19):7940–7946, 2013.

[155] Stefan Trinkle, Philipp Walter, and Christian Friedrich. Van gurp-palmen plot ii–classification of long chain branched polymers by their topology. *Rheologica Acta*, 41(1):103–113, 2002.

[156] R. Hingmann and B.L. Marczinke. Shear and elongational flow properties of polypropylene meltsa. *Journal of Rheology*, 38(3):573–587, 1994.

[157] Souheng Wu. Chain structure and entanglement. *Journal of Polymer Science Part B: Polymer Physics*, 27(4):723–741, 1989.

[158] Sudhir S. Bafna. Is the cross-over modulus a reliable measure of polymeric polydispersity? *Journal of applied polymer science*, 63(1):111–113, 1997.

[159] R. Shroff and H. Mavridis. New measures of polydispersity from rheological data on polymer melts. *Journal of applied polymer science*, 57(13):1605–1626, 1995.

[160] Maria Rosella Nobile and Franco Cocchini. Predictions of linear viscoelastic properties for polydisperse entangled polymers. *Rheologica acta*, 39(2):152–162, 2000.

[161] Qian Huang, Olga Mednova, Henrik K. Rasmussen, Nicolas J. Alvarez, Anne L. Skov, Kristoffer Almdal, and Ole Hassager. Concentrated polymer solutions are different from melts: Role of entanglement molecular weight. *Macromolecules*, 46(12):5026–5035, 2013.

[162] Qian Huang, Ludovica Hengeller, Nicolas J. Alvarez, and Ole Hassager. Bridging the gap between polymer melts and solutions in extensional rheology. *Macromolecules*, 48(12):4158–4163, 2015.

[163] Salvatore Costanzo, Qian Huang, Giovanni Ianniruberto, Giuseppe Marrucci, Ole Hassager, and Dimitris Vlassopoulos. Shear and extensional rheology of polystyrene melts and solutions with the same number of entanglements. *Macromolecules*, 49(10):3925–3935, 2016.

[164] N Willenbacher, C Oelschlaeger, M Schopferer, P Fischer, Frédéric Cardinaux, and Frank Scheffold. Broad bandwidth optical and mechanical rheometry of wormlike micelle solutions. *Physical Review Letters*, 99(6):068302, 2007.

[165] J Bergenholtz, N Willenbacher, NJ Wagner, B Morrison, D Van den Ende, and J Mellema. Colloidal charge determination in concentrated liquid dispersions using torsional resonance oscillation. *Journal of colloid and interface science*, 202(2):430–440, 1998.

[166] Tobias Brack, Sreenath Bolisetty, and Jurg Dual. Simultaneous and continuous measurement of shear elasticity and viscosity of liquids at multiple discrete frequencies. *Rheologica Acta*, 57:415–428, 2018.

[167] Thanasis Athanasiou, Gunter K Auernhammer, Dimitris Vlassopoulos, and George Petekidis. A high-frequency piezoelectric rheometer with validation of the loss angle measuring loop: application to polymer melts and colloidal glasses. *Rheologica Acta*, 58:619–637, 2019.

[168] Bram Schroyen, James W Swan, Peter Van Puyvelde, and Jan Vermant. Quantifying the dispersion quality of partially aggregated colloidal dispersions by high frequency rheology. *Soft Matter*, 13(43):7897–7906, 2017.

[169] Scott T. Milner and Tom C.B. McLeish. Parameter-free theory for stress relaxation in star polymer melts. *Macromolecules*, 30(7):2159–2166, 1997.

[170] Tadeusz Pakula, Dimitris Vlassopoulos, George Fytas, and Jacques Roovers. Structure and dynamics of melts of multiarm polymer stars. *Macromolecules*, 31(25):8931–8940, 1998.

[171] Frank Snijkers, Dimitris Vlassopoulos, Hyojoon Lee, Jinseok Yang, Taihyun Chang, Paraskevi Driva, and Nikos Hadjichristidis. Start-up and relaxation of well-characterized comb polymers in simple shear. *Journal of Rheology*, 57(4):1079–1100, 2013.

[172] Frank Snijkers, Kathlyn M. Kirkwood, Dimitris Vlassopoulos, L Gary Leal, Anastasia Nikopoulou, Nikolaos Hadjichristidis, and Salvatore Coppola.

Viscoelasticity and nonlinear simple shear flow behavior of an entangled asymmetric exact comb polymer solution. *Journal of Rheology*, 60(3):451–463, 2016.

[173] William FM Daniel, Joanna Burdyńska, Mohammad Vatankhah-Varnoosfaderani, Krzysztof Matyjaszewski, Jarosław Paturej, Michael Rubinstein, Andrey V Dobrynin, and Sergei S Sheiko. Solvent-free, supersoft and superelastic bottlebrush melts and networks. *Nature materials*, 15(2):183–189, 2016.

[174] Christos Grigoriadis, Alper Nese, Krzysztof Matyjaszewski, Tadeusz Pakula, Hans-Jürgen Butt, and George Floudas. Dynamic homogeneity by architectural design–bottlebrush polymers. *Macromolecular Chemistry and Physics*, 213(13):1311–1320, 2012.

[175] Salvatore Costanzo, Leon F Scherz, Thomas Schweizer, Martin Kröger, George Floudas, A Dieter Schlüter, and Dimitris Vlassopoulos. Rheology and packing of dendronized polymers. *Macromolecules*, 49(18):7054–7068, 2016.

[176] Miao Hu, Yan Xia, Christopher S. Daeffler, Jinhua Wang, Gregory B. McKenna, Julia A. Kornfield, and Robert H. Grubbs. The linear rheological responses of wedge-type polymers. *Journal of Polymer Science Part B: Polymer Physics*, 53(13):899–906, 2015.

[177] Rossana Pasquino, Baozhong Zhang, Reinhard Sigel, H. Yu, Marcel Ottiger, Oscar Bertran, Carlos Aleman, A.Dieter Schlüter, and Dimitris Vlassopoulos. Linear viscoelastic response of dendronized polymers. *Macromolecules*, 45(21):8813–8823, 2012.

[178] Gerard Kraus and J.T. Gruver. Rheological properties of multichain polybutadienes. *Journal of Polymer Science Part A: General Papers*, 3(1):105–122, 1965.

[179] Lewis J. Fetters, Andrea D. Kiss, Dale S. Pearson, Gunther F. Quack, and F. Jerome Vitus. Rheological behavior of star-shaped polymers. *Macromolecules*, 26(4):647–654, 1993.

[180] Frank Snijkers, Rossana Pasquino, Peter D. Olmsted, and Dimitris Vlassopoulos. Perspectives on the viscoelasticity and flow behavior of entangled linear and branched polymers. *Journal of Physics: Condensed Matter*, 27(47):473002, 2015.

[181] S.T. Milner and T.C.B. McLeish. Reptation and contour-length fluctuations in melts of linear polymers. *Physical Review Letters*, 81(3):725, 1998.

[182] Evelyne Van Ruymbeke, Roland Keunings, and Christian Bailly. Prediction of linear viscoelastic properties for polydisperse mixtures of entangled star and linear polymers: Modified tube-based model and comparison with experimental results. *Journal of non-newtonian fluid mechanics*, 128(1):7–22, 2005.

[183] Evelyne Van Ruymbeke, Christian Bailly, Roland Keunings, and D Vlassopoulos. A general methodology to predict the linear rheology of branched polymers. *Macromolecules*, 39(18):6248–6259, 2006.

[184] Frank Snijkers, Evelyne Van Ruymbeke, Paul Kim, Hyojoon Lee, Anastasia Nikopoulou, Taihyun Chang, Nikos Hadjichristidis, Jai Pathak, and Dimitris Vlassopoulos. Architectural dispersity in model branched polymers: Analysis and rheological consequences. *Macromolecules*, 44(21):8631–8643, 2011.

List of Figures

List of Tables

Author's Publications

- Vincenzo Ianniello and Salvatore Costanzo. Linear and nonlinear shear rheology of nearly unentangled h-polymer melts and solutions. Rheologica Acta, 61(10):667–679, 2022.
- Vincenzo Ianniello, Salvatore Costanzo, Rossana Pasquino, Giovanni Ianniruberto, Enrico Troisi, Theo A Tervoort, and Nino Grizzuti. Determination of the molecular weight distribution of ultrahigh molecular weight polyethylene from solution rheology. Journal of Rheology, 66(5):1079–1088, 2022.
- Salvatore Costanzo, Vincenzo Ianniello, Rossana Pasquino, Nino Grizzuti, Giovanni Ianniruberto, and Giuseppe Marrucci. Strain hardening of unentangled polystyrene solutions in fast shear flows. Macromolecules, 55(20):9206–9219, 2022.
- Rossana Pasquino, Pietro Renato Avallone, Salvatore Costanzo, Ionita Inbal, Dganit Danino, Vincenzo Ianniello, Giovanni Ianniruberto, Giuseppe Marrucci, and Nino Grizzuti. On the startup behavior of wormlike micellar networks: The effect of different salts bound to the same surfactant molecule. Journal of Rheology, 67(2):353–364, 2023.